

**Epigenetic reprogramming involving histone H3
variants, histone modifications and DNA
methylation in mouse zygotes**

Dissertation
zur Erlangung des Grades
des Doktors der Naturwissenschaften
der Naturwissenschaftlich-Technischen Fakultät III
Chemie, Pharmazie, Bio- und Werkstoffwissenschaften
der Universität des Saarlandes

Von

Jie Lan

Saarbrücken

September, 2015

Tag des Kolloquiums: Am Dienstag, dem 19. Januar 2016
.....

Dekan: Prof. Dr.-Ing. Dirk Bähre
.....

Berichterstatter: Prof. Dr. Jörn Walter
.....

Prof. Dr. Uli Müller
.....

Vorsitz: Prof. Dr. Manfred J. Schmitt
.....

Akad. Mitarbeiter: Dr. Sonja Kessler
.....

My Motto of life

Do not aim for success if you want it. Just do what you love and believe in, and it will come naturally.

Acknowledgement

First and above all, I would like to express my special appreciation to my Doktorvater, Prof. Dr. Jörn Walter, for giving me the opportunity to complete my PhD thesis in his lab. I also want to thank him for great encouragement, invaluable guidance as well as several profound discussions. As an excellent and outstanding scientist, he could always hit the key points and come up with brilliant ideas in an incredibly fast way, which gives me a very deep impression. For this, I would like to give him a nickname “Blitzdenker”. What I learned from all his good qualities is really beneficial to both my life and work in the future.

As my second supervisor, Prof. Dr. Uli Müller, he really deserves great thanks from me for the full support including both the experimental questions and devices. Also, an unforgettable discussion with him about the regulation of TDG by acetylation benefited me a lot, for example, how to design the experiment in a well-organized way and avoid neglecting any small but critical points.

I want to give special thanks to Prof. Dr. Fugaku Aoki, Prof. Dr. Makoto Tachibana, Prof. Dr. Marjorie Brand, Prof. Dr. Michael R. Stallcup, Prof. Dr. Richard M. Schultz, Prof. Dr. Yoichi Shinkai for providing the cDNA constructs of histone H3.1, H3.2, G9a and HDAC2.

For Prof. Dr. Wolfgang Fischle, I want to extend a sincere thanks to him for the helpful suggestions and the sharing of the experimental materials (peptides).

For Prof. Dr. Robert.Schneider, I am really grateful to him for generously sharing his expertise concerning the histone variants and their deposition pathways into the chromatin.

For Prof. Dr. Gert-Wieland Kohring, I offer my sincere gratitude to him for the permission to the use of the machines like French press and centrifuges.

A special thanks is given to my supervising tutor, Dr. Konstantin Lepikhov (Kostya) for his great help with friendly kindness and endless patience from the beginning to the end of my PhD study covering the guidance of the hands-on experiments, the explanation of the principles, the suggestions of the solutions, the correction of the writing. He is very erudite and always the first one I ask for any suggestion or help. Besides work, I am very thankful to him in the daily life. It is never forgettable that he spent his precious time in helping me deal with my private things.

Mrs. Nicole Jundel, to whom I am deeply indebted, is always giving me the most help as she could. Especially for the preparation of the bureaucratic materials and documents, it took her lots of time, sometimes even much more because of my mistakes. In the daily life, she is like a mother to me, always encouraging me and assisting me in solving the problems. For all the things she has done, my heart is overflowed with gratitude.

Throughout my PhD work, Sarah Fuchs and Pascal Giehr, I owe them a lot for helping the performance of the experiments, analysis of the data, discussion of the results and so on. Apart from that, we spent a lot of wonderful time together, talking about many topics including movies, politics and so on, sharing the funny stories about football, traveling, festivals, etc. Especially Sarah, she is more than a friend to me. She is like my blood sister.

Dr. Sascha Tierling, my best friend, to whom I can not find words to express my gratitude, is always offering his help both in my experiments and in my daily life. There are

so many wonderful moments to remember, such as the visiting of the saarschleifer, the canoe day, the trip in the “Museumszug”, the relaxing time in the hiking tours, the Silvester-Parties with all his family members and so on, of which the Champion League Match between Bayern münchen and Schachtar Donezk is the most impressive. We are much alike in many aspects, from the hobby, the world views, philosophy to value. For me, he is also more than a friend. He is like my blood brother.

I also want to express my warm thanks to Dr. Nicole Souren, Pavlo Lutsik and my alumni Priv. Doz. Dr. Martina Paulsen, Dr. Julia Arand and Dr. Mark Wossidlo for their good suggestions for my Ph study and the pleasant time together for dinner, playing poker and so on.

Beate Schmitt, Jasmin Kirch, Christina Lo Porto and Victoria Weinhold, Eva Dilly, to whom I owe a great debt of gratitude, helped me in sequencing, mice breeding and so on.

For Dr. Gilles Gasparoni, I am really grateful to him for his nice R course, from which I learned and benefit a lot for the future work.

For Dr. Monika Frings, I wish to thank her for her useful Tips to inject the mice.

I also consider it an honor to have Michael Glander as my colleague, who helped me several times in resolving the computer problems, for which I am really grateful.

In addition, I am indebted to many of my colleagues and alumni, Dr. Nina Gasparoni, Diana Santacruz, Anna Tartakowski, Tatiana Guerrero Marçola, Tabea Trampert, Wachiraporn Wanichnopparat, Stefanie Geisen, Dr. Karl Nordström, Abdulrahman Salhab, Sam Ringle, Dirk Schumacher, for the support and pleasant time in the lab or in Mensa.

At the end, a special thanks to my parents, words cannot express how much gratitude I want to extend to my mother and father for all of the sacrifices that they have made during all these years. All the support and encouragement from my parents pushed me forward on the way to pursue my PhD degree. Meanwhile, I would like to express appreciation to my engaged wife, Ping Zhong, who is always giving me the full support and understanding in getting me through my PhD study, which made this dissertation possible. Her role in both my work and daily life was, is and will be so important that gratitude is always both inadequate and superfluous.

Contents

1 Introduction	1
1.1 Epigenetic reprogramming in mammalian development	1
1.2 Dynamics of histone variants in mouse zygotes	1
1.2.1 Histone H1 and its variants	2
1.2.2 Histone H2A and its variants	2
1.2.3 Histone H2B and its variants	3
1.2.4 Histone H3 and its variants	4
1.2.5 Histone H4 and its variants	5
1.3 Dynamics of histone modifications and related modifying enzymes in mouse zygotes ..	6
1.3.1 Modifications on histone H1	6
1.3.2 Modifications on histone H2A	6
1.3.3 Modifications on histone H2B	7
1.3.4 Modifications on histone H3	7
1.3.5 Modificaitons on histone H4	10
1.4 Dynamics of DNA modifications in mouse zygotes	12
1.5 Cross talks between histone variants, histone modifications and DNA methylation in mouse zygotes	13
1.6 Aims and objectives	14
2 Materials and Methods	15
2.1 Materials	15
2.1.1 Mouse strains	15
2.1.2 Chemicals	15
2.1.3 Antibodies	16
2.1.4 Enzymes	17
2.1.5 Prokaryotic cells	17
2.1.6 Mediums	17
2.1.7 Solutions and buffers	18
2.1.8 Primers	18
2.1.9 Reaction kits	20
2.1.10 Instruments	20
2.2 Methods	21
2.2.1 Mouse superovulation and execution	21
2.2.2 RNA isolation	21
2.2.3 cDNA reverse transcription	21
2.2.4 Polymerase chain reaction (PCR)	21
2.2.5 Plasmids preparation	21
2.2.6 Site-specific mutagenesis	22
2.2.7 Acetylation-mimetic mutant of H3.1	22
2.2.8 <i>In vitro</i> transcription of mRNAs	22
2.2.9 Protein Purification	23
2.2.10 Verification of H3K9me2 by Western blotting	23

2.2.11 <i>In vitro</i> fertilization	23
2.2.12 Embryo culture	23
2.2.13 Chaetocin treatment.....	23
2.2.14 Cycloheximide treatment and Edu labelling	24
2.2.15 Preparation of microinjection needles	24
2.2.16 Microinjection of mRNAs or proteins into zygotes	24
2.2.17 Triton treatment of zygotes	24
2.2.18 Chromatin incorporation of histone H3 variants monitored by live imaging	24
2.2.19 Immunofluorescence staining	24
2.2.20 IF Microscopy, quantification and statistical analysis	25
2.2.21 Hairpin bisulfite sequencing.....	25
3 Results	26
3.1 Effects of K9R mutation of H3.1/2/3 on modifications of both histone and DNA in mouse zygotes	26
3.1.1 Dynamic pattern of H3K9me2 through DNA replication	26
3.1.2 Dynamic pattern of H3K9me3 through DNA replication	26
3.1.3 Dynamic pattern of H3K9ac through DNA replication	27
3.1.4 Nuclear localization and chromatin incorporation of H3.1/2/3-GFPWTs and K9R mutants	27
3.1.5 Effects of H3.1/2/3-GFPK9R on H3K9me2	29
3.1.6 Effects of H3.1/2/3-GFPK9R on H3K9me3	30
3.1.7 Effects of H3.1/2/3-GFPK9R on H3K9ac.....	31
3.1.8 Effects of H3.1/2/3-GFPK9R on 5mC and 5hmC.....	32
3.2 Effects of S10A and T11A mutations of H3.1/2/3-GFP on modifications of both histone and DNA in mouse zygotes.....	33
3.2.1 Dynamic patterns of H3S10phos and H3T11phos throughout the mouse zygotic stage.....	34
3.2.2 Effects of H3.1/2/3-GFPS10A on H3K9me2, 5mC and 5hmC	34
3.2.3 Effects of H3.1/2/3-GFPT11A on H3T11phos, H3K9me2, 5mC and 5hmC	36
3.3 Introduction of H3K9me2 into the paternal chromatin of mouse zygotes by G9aFL-GFP and G9aCat-NLS-GFP	41
3.3.1 Effects on H3K9me2	41
3.3.2 Effects on 5mC and 5hmC	43
3.4 Dissecting relations between H3K9me2 and histone H3.1/2/3 by co-injection of G9aCat-NLS-GFP and H3.1/2/3-GFPT11A	45
3.4.1 Effects on H3K9me2	45
3.5 Microinjection of H3.3-GFPK9me2 proteins.....	46
3.5.1 Localization of purified proteins of H3.3-GFPK9me2	46
3.6 Relation between H3K9ac and DNA methylation	48
3.6.1 Effect on DNA methylation by loss of H3K9ac	48
3.6.2 Effect on H3K9me2 by co-injection of G9aCat-NLS-GFP and HDAC1-GFP	50
4 Discussion	51

4.1 Inefficient disruption in H3K9me2/me3/ac by H3.1/2/3-GFPK9R in both parental genomes of mouse zygotes.....	51
4.2 Phosphorylation on H3.1/2S10 and H3.1/2T11 serving as a double switch for H3K9me2 in the maternal genome of mouse zygotes	53
4.3 Artificial introduction of H3K9me2 on H3.1 and H3.2 fails to block global active DNA demethylation in the paternal genome of mouse zygotes.....	55
4.4 Relation between H3.3 and active DNA demethylation in both parental genomes of mouse zygotes	57
4.5 Conclusions	58
4.6 Perspectives	59
Zusammenfassung	60
Summary	61
References	62
Appendices	75
Abbreviations	78
Curriculum Vitae	80

1 Introduction

1.1 Epigenetic reprogramming in mammalian development

After experiencing a stage of being buried for more than one century when the “Lamarckian inheritance” was proposed and another period of being silenced for half a century when the term “epigenetics” was first coined by Conrad Waddington in the early 1940s (Waddington, 1942), as a new subject, “epigenetics” has been extensively and substantially studied from the late 1990s on. Notably, the current concept of epigenetics has been narrowed to some extent from its original definition with the rapid development of genetics over the past decades, with its general acceptance as changes in phenotype without changes in genotype. More accurately speaking, on the molecular level, epigenetics involves the modifications occurring on DNA, RNA or histones which are inherited mitotically and/or meiotically from the parent cells to the daughter cells and could decisively determine the gene functions or expressions without the changes to the underlying DNA sequence itself (Wu and Morris, 2001). In 1997, as a hallmark event in the cloning history, the birth of “Dolly” greatly boosted the interests in epigenetic reprogramming in mammalian embryos (Wilmut et al., 1997), which suggested the great powerful ability of a mammalian oocyte to reprogram a differentiated somatic cell into a totipotent status. Naturally, the formation of a mammalian zygotes is created by the fusion of an oocyte with a spermatozoon, which immediately triggers the epigenetic reprogramming of both highly differentiated gametes involving replacement of protamines with histone variants, dynamic changes of histone modifications, iterative oxidation of 5mC possibly followed by DNA repair-related pathways, RNA-mediated regulation as well as interactions among them and so forth, comprising and displaying rather complicated and multiple regulation layers essential for normal embryo development. For mice, it is rather significant in the zygotic stage, for it is preparing for the zygotic genome activation occurring at the 2-cell stage and its epigenetic dysregulation could cause embryo development failure. Therefore, the dissection of the roles of histone modifications and DNA methylation in mouse zygotic stage is really helpful for a better understanding of epigenetic reprogramming in embryo development, which will shed a light on reprogramming in stem cells, induced pluripotent cells as well as somatic cell nuclear cloning.

1.2 Dynamics of histone variants in mouse zygotes

Two copies each of the core histones H2A, H2B, H3, and H4, together with approximately 146 base pairs of DNA, form a nucleosome, the basic repeating unit for eukaryotic chromatin (Luger et al., 1997). Between the two adjacent nucleosomes, histone H1 is located, which could facilitate the packaging of DNA into the octamer of core histones. Upon fertilization, the replacement of the protamines in sperm with maternally-derived histones and their variants in oocytes causes a decondensation structure in the paternal genome during the formation of pronuclei. Soon after entering into the replication phase, there is another wave of histone incorporation in both pronuclei in zygotes, which is dependent on DNA synthesis. Notably, histone chaperones also participate in both processes so as to ensure that all the histone variants are deposited into the proper regions. In general, histones could fall into two groups, canonical and non-canonical histones, which differ in their primary structure, as well

as in the organization of their genes (intron-less) and mRNAs (Marzluff et al., 2002; Marzluff et al., 2008).

1.2.1 Histone H1 and its variants

Histone H1 is defined as a linker histone, which consists of three different regions, that is, a short C-terminal tail of around 35 amino acids, a central globular domain with roughly 80 amino acids long and a rather long N-terminal tail of approximately 100 amino acids (Hartman et al., 1977). It is located between the adjacent nucleosomes, binds to the nucleosome where the DNA enters or exits and protects the linker DNA via its evolutionarily conserved globular domain, and facilitates to stabilize the formation of higher-order chromatin structures by its two highly variable flanking terminal tails (Allan et al., 1980; Harshman et al., 2013; Zhou et al., 2013). In mice, there are at least 9 members of histone H1 family have been identified in mice so far, including five somatic subtypes H1a, H1b, H1c, H1d and H1e, one testis-specific linker histone H1t, one differentiation-specific linker histone H1⁰ as well as another two isoforms of oocyte-specific linker histone H1FOO (formerly H1OO), namely H1FOO α and β . The variety of H1 isoforms is summarized in Fig. 1.1 (Lennox and Cohen, 1983; Lennox and Cohen, 1984; Seyedin and Kistler, 1979; Tanaka et al., 2005). Apart from H1⁰ and H1FOO, the others follow a replication dependent way (Marzluff et al., 2002). Notably, oocyte-specific linker histone H1FOO appears in both pronuclei during 1-cell stage, decreases in the nuclei at 2-cell stage and becomes undetectable after 4-cell stage (Gao et al., 2004), with H1FOO α isoform being much more abundant than the β one in the zygotes (Tanaka et al., 2005). The somatic variants are absent throughout oogenesis up to 1-cell stage and become detectable from 2-cell-stage on (Gao et al., 2004). However, an opposite observation has been reported that the depositions of somatic variants into the chromatin occur as soon as the formation of the pronuclei after fertilization (Adenot et al., 2000). The discrepancy could be resulted from the specificities of the antibodies. As for the differentiation-specific linker histone H1⁰, it has been proved that H1⁰ knockout mice have a normal development, suggesting that it is indispensable for mouse embryogenesis (Sirotkin et al., 1995).

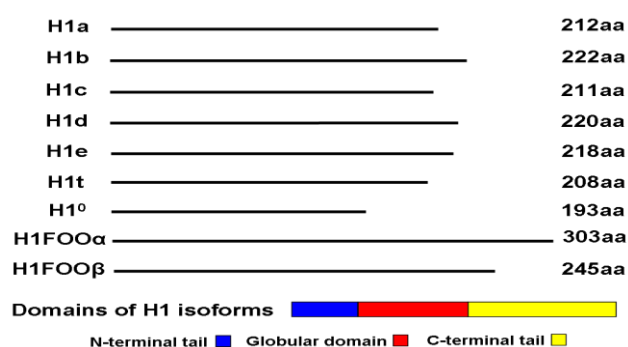


Fig. 1.1 The schematic overview of mouse histone H1 variants

1.2.2 Histone H2A and its variants

Among the core histones, the canonical H2A harbors a rather extended family, including H2A isoforms, H2A.X, H2A.Z isoforms, H2A.B subtypes as well as macroH2A subtypes, with N-terminal tails and fold domains being relatively conserved and C-terminal tails being rather

divergent (Costanzi and Pehrson, 2001; Govin et al., 2007; Marzluff et al., 2002; Matsuda et al., 2010; Rasmussen et al., 1999; West and Bonner, 1980), which are summarized in Fig. 1.2. Although many isoforms of H2A in mouse have been identified, no reports concerning the site variation related functions have emerged. In mouse zygotes, one of the isoforms of H2A has been described to be rather lowly abundant after fertilization till 4-cell stage (Nashun et al., 2010), which is in line with the expression data (Kafer et al., 2008). In contrast, H2A.X is highly expressed throughout the preimplantation stage (Nashun et al., 2010). Particularly in zygotic period, H2A.X reaches the signal peak and shows equal distribution in both pronuclei. However, H2A.X is nonessential for mouse embryo development, for the H2A.X^{-/-} mice are viable, although pleiotropic effects are rather obvious in chromosomal instability, repair defects and so forth (Celeste et al., 2002). Another variant, H2A.Z, although it is highly incorporated in the chromatin of GV and MII oocytes, is gradually evicted from the maternal genome from the beginning of fertilization to 6 hours post fertilization (hpf) and reappeared into the nuclei in the morula stage (Nashun et al., 2010). Inconsistent with the observation, Ana Bošković et al reported the presence of H2A.Z as early as the late 2-cell stage by using the freshly flushed embryos (Boskovic et al., 2012), which may explain the discrepancy between these two experiments. Indeed, the H2A.Z^{-/-} knockout embryos have shown the normal formation of blastocyst, although the severe defects emerge shortly after implantation (Faast et al., 2001). As for H2A.B and its subtypes, they express in a tissue-specific manner, strongly in testis and less abundantly in brain (Chadwick and Willard, 2001; Ishibashi et al., 2010; Soboleva et al., 2012). Furthermore, Wu et al. have reported that its subtypes, H2ALap2 and Lap3, which are strongly detected in sperms, become undetectable by being excluded from the paternal pericentric heterochromatin regions after sperm-egg fusion (Wu et al., 2008). As the largest member in this family, macroH2A, which is structurally rather diverse in its C-terminal tail containing a nonhistone domain (NHD) (Pehrson and Fried, 1992), is abundantly present in the form of mH2A1.2 in chromatin of MII oocytes while absent in the sperm during fertilization, begins to be progressively stripped from the maternal genome upon fertilization and becomes undetectable from PN3 stage on until reaching the morula stage (Chang et al., 2005; Nashun et al., 2010). However, the biological meanings of the transient asymmetry and the lost of macroH2A are still unknown.

1.2.3 Histone H2B and its variants

Together with H2A, H2B forms a heterotypic dimer and is relatively less diverse than its partner. Thus far, 14 variants of H2B have been reported, namely 11 canonical isoforms and 3 testis-specific subtypes (Fig. 1.3). The canonical ones are constantly appearing in the nuclei during the preimplantation development, while the noncanonical ones play yet unknown roles in spermatogenesis (Govin et al., 2007; Kamakaka and Biggins, 2005; Marzluff et al., 2002; Nashun et al., 2010). Notably, H2BL1 may be involved during the protamine-histone exchange soon after fertilization, for it has been detected in mature sperms at a certain amount (Govin et al., 2007).

Introduction

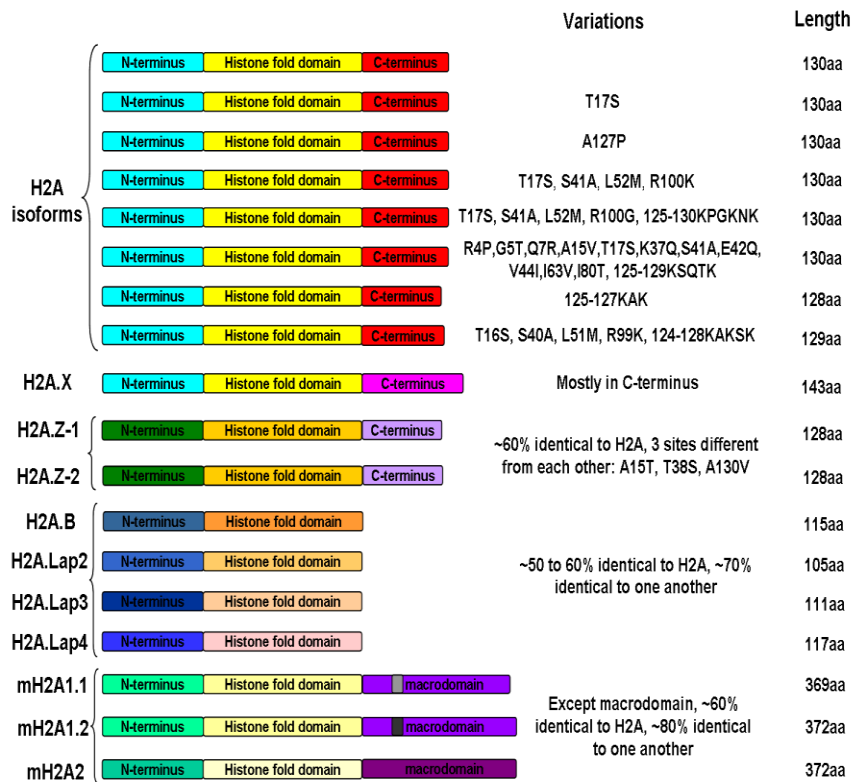


Fig. 1.2 The schematic overview of mouse histone H2A variants

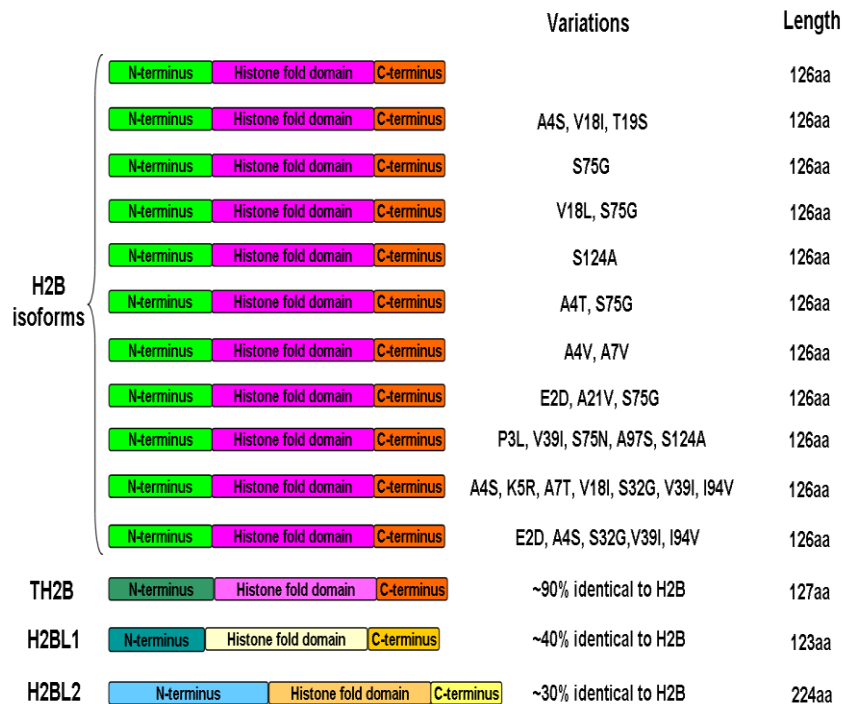


Fig. 1.3 The schematic overview of mouse histone H2B variants

1.2.4 Histone H3 and its variants

In mice, structurally, histone H3 variants could fall into two subgroups. One subgroup consists of H3.1, H3.2 and H3.3, which have the same size but differ from one another by only five amino acids (Loyola and Almouzni, 2007). And another subgroup encompasses

Introduction

CENP-A isoforms produced by different splicing, which differentiate either in the N-terminus or in the C-terminal histone fold domain (Craig et al., 1999; Marzluff et al., 2002; Van Hooser et al., 1999). The currently identified histone H3 variants are exhibited in Fig. 1.4. Although a testis-specific histone H3 variant (H3t) in human has been isolated and purified (Tachiwana et al., 2008), the counterpart in mice has still not been found so far. During the zygotic stage, the immunostaining using the H3.1/2-specific antibody has shown that both canonical histones are only confined to the maternal chromatin in G1 phase, begin to incorporate into both pronuclei at the commencement of S phase and remain like this through G2 phase (van der Heijden et al., 2005). Likewise, with eGFP being tagged in the C-terminus, H3.1 is observed to deposit into both male and female chromatins in a replication-dependent manner (Santenard et al., 2010). Similar to H3.1-eGFP, Flag-H3.2 also shows an equal distribution between both pronuclei during replication phase (Akiyama et al., 2011). Nevertheless, the ability of H3.1 to localize into the pronuclei is abolished when the Flag or eGFP is fused to its N-terminus (Akiyama et al., 2011), implying the importance of proper fusion strategy for histones possibly in a variant-specific manner. As a noncanonical histone variant, H3.3 is preferentially located in the male pronucleus after fertilization up to replication phase. It starts to appear in the female chromatin concomitant with replication. Later, it is equivalent in both pronuclei when G2 phase is reached. The dynamic pattern of H3.3 is consistent with that of its specific chaperon, Hira (Inoue and Zhang, 2014; van der Heijden et al., 2005). It has been demonstrated that H3.3 is indispensable for the formation of the paternal pronucleus (Inoue and Zhang, 2014), while the absence of H3.1 and H3.2 has a severe effect on blastocyst formation (Akiyama et al., 2011). CENP-A is another variant in the histone H3 family and plays a rather critical role in the post-implantation stages, because no CENP-A null mice could be obtained beyond 6.5 days postconception (Howman et al., 2000). The distribution patterns of histone H3 variants in mouse zygotes are schematically illustrated in Fig. 1.5.

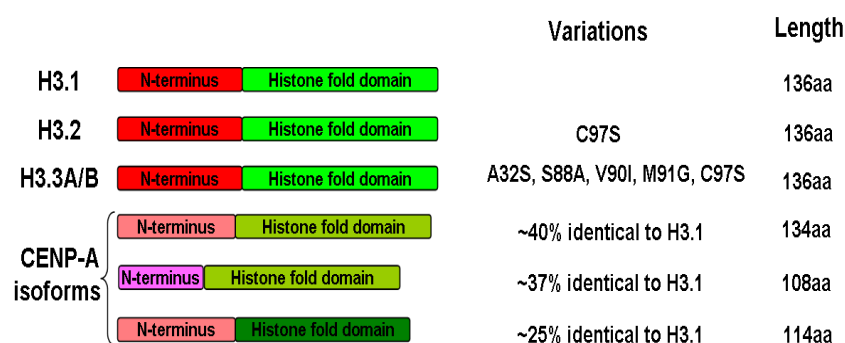


Fig. 1.4 The schematic overview of mouse histone H3 variants

1.2.5 Histone H4 and its variants

Evolutionarily, H4 is rather conserved, although it is encoded by multiple genes, for no non-allelic variants have been discovered so far and even the isoforms which could be derived from the alternative splicing are not found (Kamakaka and Biggins, 2005). In mice, H4 shares the same dynamic pattern with H3.3 in zygotic stage (Akiyama et al., 2011; Inoue and Zhang, 2014), since they could bind with each other to form a heterotypic dimer and later a tetramer. In Fig. 1.5, the distribution patterns of the main histone variants are summarized.

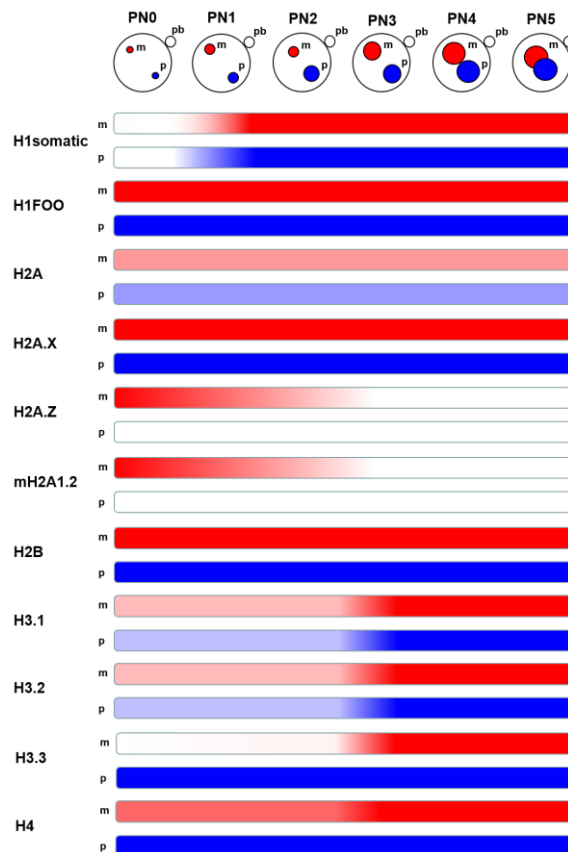


Fig. 1.5 The schematic of distribution patterns of histones in mouse zygotes

1.3 Dynamics of histone modifications and related modifying enzymes in mouse zygotes

Histone posttranscriptional modifications function in a wide variety of biological processes, for instance, DNA repair, gene regulation and chromosome condensation (Cosgrove et al., 2004; Zhou et al., 2011). Typically, these marks are performed via addition or removal of chemical attachments, such as acetyl, methyl, phosphate, polypeptide ubiquitin and so forth to multiple targeting sites including lysine, arginine, serine, threonine and so on. This occurs mostly within the histone N-terminal tails protruding from the nucleosome body as well as on the histone fold domains by the histone modifying enzymes either before or after histone incorporation into the chromatin. In mouse zygotes, the patterns of histone modifications in both pronuclei are rather dynamic and many of them still have to be characterized.

1.3.1 Modifications on histone H1

Currently, multiple modifications on several sites of Histone H1 have been identified in different species. These modifications include phosphorylation, methylation, acetylation and so forth (Harshman et al., 2013; Villar-Garea and Imhof, 2008). Note that the related writers for these modifications have redundant activities, for example Aurora B kinase (Daujat et al., 2005; Hergeth et al., 2011), G9a/KMT1C (Weiss et al., 2010) and GCN5 (Kamieniarz et al., 2012) modify histone H1 but are also responsible for H3S10phos, H3K9me2, H3K9ac/H3K14ac, respectively. However, their dynamics in mouse zygotes are yet to be described.

1.3.2 Modifications on histone H2A

The well-studied modification on the H2A variant, H2A.X, is the phosphorylation on serine139 in its C-terminal, also called γ H2A.X. It responds to DNA double strand breaks (DSBs) and serves as a sensor for the assembly of DNA repair proteins at the damaged sites. In mouse zygotes, it shows the preferential localization in the paternal pronucleus (Wossidlo et al., 2010; Ziegler-Birling et al., 2009). Even if the zygotes are exposed to DNA damaging agents, still much more γ H2A.X foci are observed in the male genome than in the female one, from which the authors have concluded that female chromatin has a much more proficient capacity in DNA repair (Derijck et al., 2006). Another described modification in mouse zygotes is the acetylation at K4+K7+ K11 of H2A.Z, which is at detectable level but rather weak from PN0 to PN3 in both pronuclei, and then becomes undetectable up to 2-cell stage (Boskovic et al., 2012). Apart from the marks above, the N-terminal part of human canonical H2A could also be phosphorylated, acetylated and methylated at the sites of S1, K3 as well as K5 and K9, respectively (Ancelin et al., 2006; Wyrick and Parra, 2009; Zhang et al., 2004). So far, on H2A, only the pattern of K5ac has been shown in mouse zygotes, namely equal distribution in both pronuclei (Stein et al., 1997) and those of the other marks in mouse embryos are still lacking. The other modifications like ubiquitination on H2A or H2A.Z are also worth considering in mouse zygotes, for they could establish the cross talk with H3K4me_{2/3} or H3S10phos, and influence the histone replacement (Joo et al., 2007; Nakagawa et al., 2008; Sarcinella et al., 2007; Weake and Workman, 2008).

1.3.3 Modifications on histone H2B

Based on the literature, profiles of few modifications on histone H2B in mouse zygotes are available till now. Only general acetylation on H2B using an unspecific antibody has been described to be located throughout both pronuclei uniformly in mouse zygotes (Stein et al., 1997). However, acetylation on K5, K12, K15 and K20, phosphorylation on S14 and S36, methylation on K30 and K34 have been reported in human, bovine, chicken and so on (Kurdistani et al., 2004; Zhang and Tang, 2003; Zhang et al., 2003). Due to the rather conserved sequences across the species, how these modifications change and whether they play any roles or not in mouse embryo development should be addressed in the future.

1.3.4 Modifications on histone H3

In mouse embryos, the modifications of lysine and serine residues on the N-terminal tail of histone H3 have been very intensively investigated, including monomethylation (me₁), dimethylation (me₂), trimethylation (me₃), acetylation (ac) as well as phosphorylation (phos). Methylation on lysine 4 is typically regarded as an active mark for gene transcription (Barski et al., 2007; Bernstein et al., 2007; Guenther et al., 2007), although there are recent evidences which indicate that it could indicate the repressive state in some cases (Cheng et al., 2014; Margaritis et al., 2012). For H3K4me₁, it appears only in the maternal genome upon fertilization, becomes detectable in both parental genomes after the formation of pronuclei with showing more abundantly in the maternal one and displays equal signal intensities in PN4/5 stage, while H3K4me₂ and me₃ are undetectable from the male side up to late PN3, begin to emerge into male pronucleus at around PN4 and reach comparable distribution in both pronuclei at PN5 (Lepikhov and Walter, 2004; Santenard et al., 2010; van der Heijden et al., 2005). The meaning behind the delayed setting of H3K4me_{2/3} is still mysterious.

Introduction

However, rather intriguingly, two groups reported that asymmetric di-methylation of histone H3 arginine 2 (H3R2me2a) is mutually antagonistic to H3K4me2/3 in human cells and budding yeast, respectively (Guccione et al., 2007; Kirmizis et al., 2007). Furthermore, based on Chip-sequencing data, two groups have claimed that it is H3R2 symmetric dimethylation (H3R2me2s) that is highly correlated with H3K4me3 on the genome wide scale in mice (Migliori et al., 2012; Yuan et al., 2012). Besides this, H3T6phos may also be involved in regulation of deposition of methyl group on lysine4 due to the observation that ablation of H3T6phos strongly enhances the demethylation on lysine 4 (Metzger et al., 2010). Together, they strongly imply a possible coordination mechanism in mouse zygotes which should be tested in the near future. Another neighboring site, threonine 3, once being phosphorylated, is essential for the activation of Aurora B, despite in *Xenopus* eggs (Zierhut et al., 2014), pointing out that H3T3phos could serve as a upstream switch for H3S10phos, the well-known target for Aurora B. Using the specific antibodies to trace H3K9 methylation patterns, it shows that H3K9me1 is positive in both genomes throughout the zygotic stage, which is the same for H3K9ac, whereas both H3K9me2 and H3K9me3 are regarded negative in male pronucleus, in which, notably, H3K9me2 is gradually placed during replication at a rather low but detectable level (Arney et al., 2002; Lepikhov and Walter, 2004; Santenard et al., 2010; Santos et al., 2005; Stein et al., 1997; van der Heijden et al., 2005). Its neighboring modification, H3S10phos, displays the following dynamic pattern: it disappears from G1 stage on, becomes almost invisible during replication, and appears *de novo* in G2 stage. However, the different commercial antibodies against H3S10phos perform differently in immunostaining, that is, completely absent or still detectable to some degree during replication in different experiments from two independent research groups, respectively (Ribeiro-Mason et al., 2012; Teperek-Tkacz et al., 2010). As a typical case for crosstalk on histone 3, phosphorylation at serine 10, together with methylation on K9, could serve as a critical “switch” on the transcription according to the barcode hypothesis (Strahl and Allis, 2000), which is supported by some evidence (Lo et al., 2001; Ng et al., 2007). For phosphorylation at threonine 11, no reports about its dynamics are available. Because phosphorylation on either serine 10 or threonine 11 could influence H3K9ac in somatic cells (Dinant et al., 2008; Metzger et al., 2008), whether this effect exists in mouse zygotes or not should be investigated. Also, similar effect might be applied to H3K14ac, because it follows the same pattern as H3K9ac and could also be introduced by the histone acetyltransferase, GCN5 (Cheung et al., 2000; Kim et al., 2003; Lo et al., 2000). The *in vitro* data on interactions among the modifications on these four sites, K9, S10, T11 and K14, have provided some hints that pre-acetylation of K9 regulates phosphorylation of S10 in a positive manner while pre-acetylation of K14 causes a negative effect on phosphorylation of S10, but not vice versa for these two cases (Cheung et al., 2000; Lo et al., 2000). In addition, a decrease of H3S10phos is observed when H3T11 phos pre-exists (Demidov et al., 2009), consistent with the observation from another group that they are mutually exclusive (Liokatis et al., 2012). The same observation is obtained for the crosstalk (mutually exclusive) between H3S10phos and H3T6phos (Liokatis et al., 2012). The other modifications on neighboring sites, like H3R17me2, H3K18ac and H3K23ac, show uniform distribution in both pronuclei in mouse zygotes (Sarmiento et al., 2004; Stein et al., 1997; van der Heijden et al., 2005). Different methylation grades of H3K27 show rather similar patterns to H3K4 methylation.

Introduction

Briefly, H3K27me1 is observed in both pronuclei with stronger staining in female one throughout the PN stages. For H3K27me2 and me3, they are beyond detection in the paternal pronucleus during the early PN stages and become increasingly accumulated until comparable to those in the maternal one in the late PN stages (Santenard et al., 2010; Santos et al., 2005). Furthermore, Santenard et al. have provided the evidence that H3.3K27 is critical for heterochromatin formation in mouse zygotes (Santenard et al., 2010). Another form of K27 modification is acetylation, which appears to be opposite to H3K27me3, namely no H3K27ac in the maternal genome in the PN1-2 stages and getting appeared in both genomes in late stages (Hayashi-Takanaka et al., 2011; Santenard et al., 2010). The adjacent amino acid, serine 28, exists in the form of phosphorylation from the metaphase to telophase upon fertilization, and then undergoes dephosphorylation (van der Heijden et al., 2005). Its dynamics in the later stages remains elusive. The questions that to what extent H3S28phos could crosstalk with H3K27me (1/2/3) and whether H3S28phos could be responsible for the absence of H3K27me2/3 in the PN1-2 stages should be interrogated in mouse zygotes. For serine 31, which is specific to H3.3, could experience phosphorylation in the metaphase of mitosis, which could lead to target gene transcription (Hake et al., 2005), suggesting that H3.3S31phos might play a role in the metaphase of the first cell cycle of mouse embryo and prepare for the major zygotic genome activation (ZGA). For lysine 36, its trimethylated form has been reported to be located only in the maternal genome in mouse zygotes (Boskovic et al., 2012), although it serves as an active mark distributing in gene bodies (Butler and Dent, 2012; Wagner and Carpenter, 2012), which may potentially establish a crosstalk with H3K27me2/3, as reported by Yuan et al (Yuan et al., 2011). Based on the data above, we could speculate that H3K36me2 may follow the same pattern as H3K36me3. Intriguingly, H3K36me2 has been confirmed to be associated with H3.3 but not H3.1 in mouse embryos (Lin et al., 2013). These observations raise the question: why H3K36 methylation is absent from the paternal genome even if H3.3 is preferentially deposited into the male pronucleus. Like other lysine sites, K36 could also be modified by an acetyl group via the histone acetyltransferases, such as GCN5. And H3K36ac has been found to be predominantly mapped to the promoters of RNA polymerase II-transcribed genes in yeast (Morris et al., 2007). However, the pattern of H3K36ac has not been defined yet in mouse embryos. For K56 on H3, it is located at the entry–exit point of the DNA on the nucleosome. Its acetylation could respond to DNA repair (Vempati et al., 2010; Yuan et al., 2009), which may contribute to active DNA demethylation in the paternal genome of mouse zygotes, because BER or NER have been suggested to be involved in active DNA demethylation (Santos et al., 2013; Wossidlo et al., 2010). As a novel identified histone mark, H3K56me3 is found to be enriched in the pericentromeres and plays a role in heterochromatin formation, together with H3K9me3 (Jack et al., 2013), probably showing the similar pattern to H3K9me3 in mouse zygotes. Recently, H3K64me3 has been described to have the preferential localization in the maternal genome in mouse zygotes (Daujat et al., 2009), which is dependent on H3K9me3 (Lange et al., 2013). However, its counterpart, H3K64ac, serves as an active mark for gene transcription (Di Cerbo et al., 2014), about which the data are still unknown in mouse embryos to our knowledge. Apart from modifications on the tail of histone H3, the other marks residing in the folding domain could also be of interest, such as H3K79 methylation, which is rather abundantly enriched in the chromosomes in MII oocytes. Nevertheless, demethylation takes

place immediately after fertilization on lysine 79, causing an unmethylated status throughout the zygotic stage (Ooga et al., 2008), which may be occupied by an acetyl group after that. In general, the crosstalks between different modifications are rather more complicated than expected due to the existence of distinct histone variants.

1.3.5 Modifications on histone H4

In mouse zygotes, hyperacetylation of histone H4 is strongly associated with male and weakly with female chromatin upon the entry of sperm into the MII oocytes. From the paternal side, acetylations at lysine 8 and 12 are inherited from the sperm, while the maternal chromatin is largely de-acetylated in mature MII oocyte (van der Heijden et al., 2006). Later, equivalent acetylation levels are observed in both pronuclei in advanced PN stages (Sarmiento et al., 2004). Similar results have been obtained by using the antibody specific for acetylation at lysine 5 on histone H4, showing asymmetric pattern throughout the G1 phase and symmetric one during S and G2 phases (Adenot et al., 1997). In parallel, Sarmiento et al. evaluate histone H4 arginine 3 methylation (H2A/4R3me2) in the zygotic stage, which shows no or rather weak signals (Sarmiento et al., 2004). Another studied site on histone H4 is lysine 20, on which mono, di and tri methyl groups could be added. In mouse zygotes, H4K20me1 is already detectable in both chromatins immediately after sperm-oocyte fusion, while H4K20me2 is at undetectable level in both pronuclei throughout the zygotic stage and H4K20me3 is only present in the perinucleolar ring in the female pronucleus (Kourmouli et al., 2004; Probst et al., 2007; van der Heijden et al., 2005; Wongtawan et al., 2011). The pattern of H4K20me3 resembles that of H3K9me3, which supports the observation that both these two marks are highly associated with heterochromatin formation (Burton and Torres-Padilla, 2010). The dynamic profiles of different histone modifications in mouse zygotes are summarized in the Fig. 1.6.

Introduction

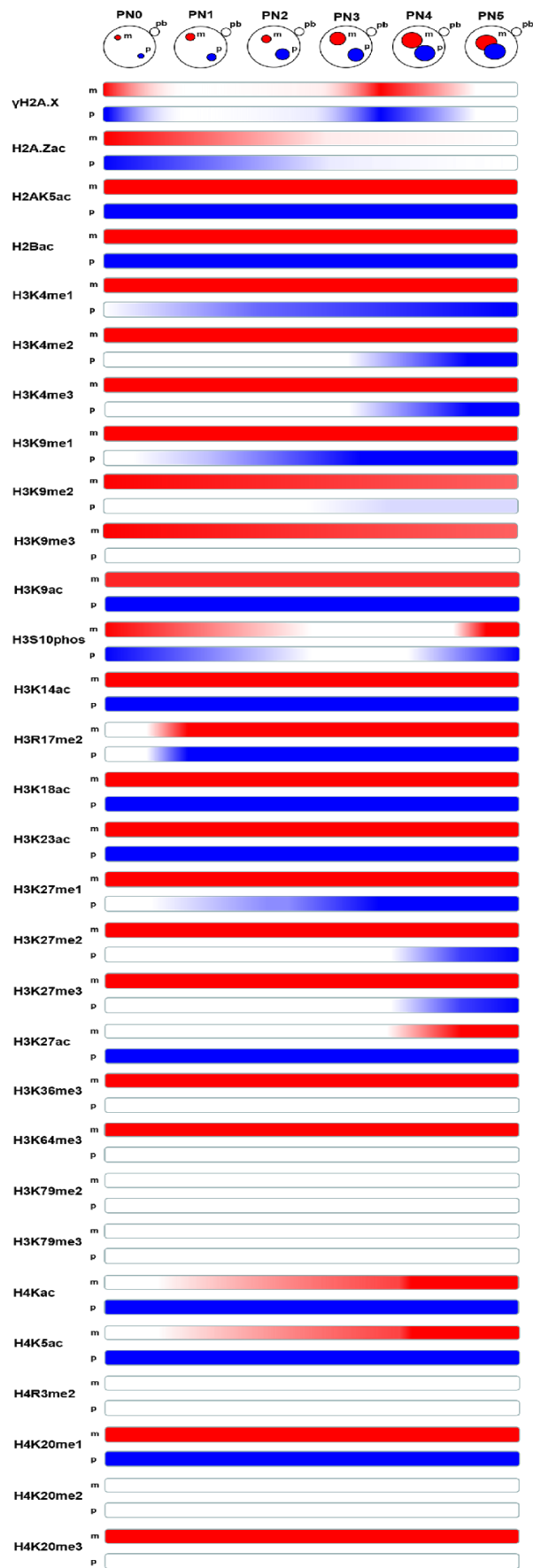


Fig. 1.6 The schematic illustration of histone modifications dynamics in mouse zygotes

1.4 Dynamics of DNA modifications in mouse zygotes

DNA methylation is a modification where a methyl group (CH₃) is covalently added to the 5-carbon of the cytosine ring, which is referred to as 5-methylcytosine (5mC). Recently, with the discovery of ten-eleven translocation (TET) family enzymes, the oxidized forms of 5mC are sequentially identified, namely 5-Hydroxymethylcytosine (5hmC), 5-formylcytosine (5fC) and 5-carboxylcytosine (5caC), which are regarded as the new 6th, 7th and 8th bases of the mammalian genome, respectively (He et al., 2011; Ito et al., 2011; Tahiliani et al., 2009). Around one decade ago, the phenomenon that active DNA demethylation takes place preferentially in the paternal genome prior to DNA replication in mouse zygotes was described (Mayer et al., 2000; Oswald et al., 2000). In 2011, several groups demonstrated that 5hmC is accumulated preferentially in the paternal genome, which is catalyzed by Tet3 enzyme from 5mC in mouse zygotes (Gu et al., 2011; Iqbal et al., 2011; Wossidlo et al., 2011), pointing out that oxidation of 5mC is at least one of the major upstream pathway for DNA demethylation. Later, Santos et al. proved that Tet3-based oxidation is confined to the time window of DNA replication (Santos et al., 2013). By generation of antibodies specific for 5fC and 5caC, Inoue et al. have provided the dynamic patterns of 5fC and 5caC in mouse zygotes, similar to 5hmC (Inoue et al., 2011). Based on the immunostaining, all the oxidized forms are diluted in a replication-dependent manner during the later cleavage stages (Inoue et al., 2011). The TDG-mediated pathway which is potentially very efficient for removal of 5fC and 5caC is somehow limited in mouse zygotes, for no influences on these two bases have been observed in TDG-knockout mice (Guo et al., 2014a), probably due to the regulatory mechanism that TDG could be inactivated by acetylation at 4 lysine sites in the N-terminal part shown recently by the *in vitro* data (Madabushi et al., 2013). Obviously, the other possible pathways, like deamination of 5mC to thymine, followed by Tets-mediated oxidation of thymine to 5-hydroxymethyluracil, or processed by DNA base excision repair in the final step, seem to be responsible for active DNA demethylation (Pfaffeneder et al., 2014; Santos et al., 2013; Wossidlo et al., 2010). Except the active pathway, DNA demethylation could also be managed in a replication-dependent manner, which is assumed to be resulted from the absence of DNMT1. However, whether it is due to the missing of DNMT1 or other essential factors should be further investigated. Very recently, a very interesting result has been reported by three different groups that both active and passive DNA demethylation occur to distinct extents in parental genomes in mouse zygotes (Arand et al., 2015; Guo et al., 2014b; Shen et al., 2014), suggesting that the discrepancy in DNA demethylation between male and female pronuclei may be caused by the chromatin modifications and configuration. The dynamic patterns of 5mC and its oxidized forms in mouse zygotes are shown in Fig. 1.7.

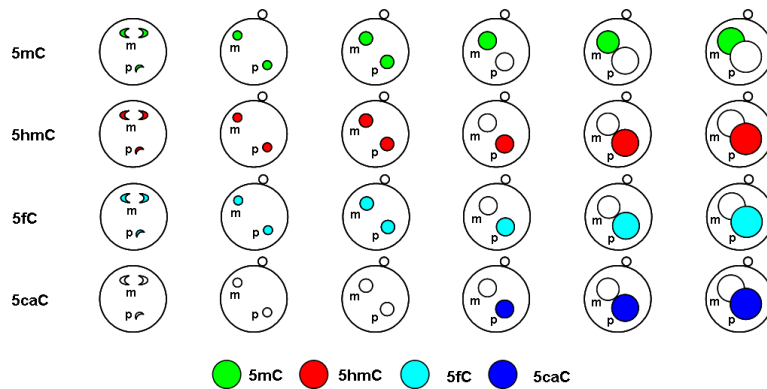


Fig. 1.7 The schematic of dynamics of DNA modifications in mouse zygotes

1.5 Cross talks between histone variants, histone modifications and DNA methylation in mouse zygotes

In mouse zygotes, reprogramming involves chromatin reorganization and DNA demethylation (Mayer et al., 2000; Oswald et al., 2000; Santos et al., 2005). The crosstalk between these two cases has been being investigated for years. Globally, H3K9 methylation (me2 or me3) has been shown to be associated with DNA methylation across the species, such as *Neurospora crassa* (Tamaru and Selker, 2001), *Arabidopsis thaliana* (Bernatavichute et al., 2008; Jackson et al., 2004; Jackson et al., 2002) and mice (Lehnertz et al., 2003), although Soppe et al. have shown the opposite results in *Arabidopsis thaliana* (Soppe et al., 2002). Indeed, it has been reported recently that in mouse zygotes, H3K9me2 attracts PGC7 and together they protect against DNA demethylation in the maternal genome as well as some loci in the paternal one (Nakamura et al., 2007; Nakamura et al., 2012). As the potential carriers for H3K9me2 as well as other modifications, histone H3 variants H3.1, H3.2, and H3.3, play a role in separating the chromatin into different functional compartments and are targets for distinct posttranslational "signatures" (Hake and Allis, 2006). Although we know that H3.1 and H3.2 are reported to be equally deposited into both pronuclei during replication and that H3.3 is preferentially incorporated into the replicating paternal pronucleus before and during replication (Akiyama et al., 2011; Torres-Padilla et al., 2006; van der Heijden et al., 2005), so far no data available about the relation between the dynamics of histone H3 variants, the deposition of H3K9me2 and DNA methylation in mouse zygotes. Hence, the dissection of the relations among these three players would definitely give us a deeper insight in chromatin reorganization and DNA demethylation. Additionally, whether histone modifications at other lysine residues contribute to DNA methylation or demethylations - this issue has to be addressed in the nearest future. For example, unmethylated histone 3 at lysine 4 could be well recognized by DNMT3A–DNMT3L complex both *in vivo* and *in vitro*, respectively, which further leads to *de novo* methylation (Hashimoto et al., 2010; Hu et al., 2009; Ooi et al., 2007; Otani et al., 2009; Zhang et al., 2010). Moreover, genome-wide mapping of DNA methylation and H3K27 trimethylation in mouse embryonic stem cells shows that a certain portion of repressed genes encompass these two marks in parallel (Fouse et al., 2008), indicating that H3K27me3 may be the protector for 5mC in some local regions in mouse zygotes. Additionally, H3K36me3 is observed to appear asymmetrically only in the maternal pronucleus (Boskovic et al., 2012). Combined with the recently published data indicating that Dnmt3a, which has been shown the localization in both pronuclei (Gu et al., 2011; Hirasawa

et al., 2008), recognizes H3K36me3 and triggers *de novo* DNA methylation *in vitro* (Dhayalan et al., 2010), it is tempting to speculate the potential mechanistic link between H3K36me3 and *de novo* methylation in mouse zygotes. As for histone variants, they add another layer of complexity for regulation of modifications on either histones or DNA, among which H3.3 is the most studied one in mouse zygotes. By knocking down of either H3.3 or its chaperone Hira, the formation of the paternal pronucleus is completely abolished due to the inability to form functional nucleosomes (Inoue and Zhang, 2014). Furthermore, site mutation experiment of H3.3 at lysine 27 to arginine has shown that heterochromatin formation of pericentromeric domains could be greatly disrupted in 2-cell mouse embryos. Unfortunately, no data about DNA methylation have been displayed in this publication (Santenard et al., 2010). Another interesting player is H2A.Z. In other species, like *Arabidopsis thaliana* and human cells, it has been shown that H2A.Z is mutually exclusive with DNA methylation and facilitates DNA repair pathway by creating a relatively open chromatin (Xu et al., 2012; Zilberman et al., 2008). Notably, the deposition of H2A.Z has been demonstrated to be regulated by H3K56 acetylation (Watanabe et al., 2013). It still remains to be investigated that to what extent the role of H2A.Z in mouse zygotes is evolutionarily conserved. Taken together, histone variants are important players in chromatin reorganization and DNA demethylation in mammalian zygotes.

1.6 Aims and objectives

In mouse zygotes, the conversion of 5-methylcytosine (5mC) to 5-hydroxymethylcytosine (5hmC) and further oxidized forms by the Tet dioxygenase 3 (Tet3) in paternal and maternal genomes has been associated to the modification status of histone H3 at lysine 9 (H3K9me2/3). Notably, as potential carriers for this histone mark, histone H3 variants, namely H3.1, H3.2, H3.3, are dynamically deposited into the chromatin in DNA replication dependent and independent manners, which may be responsible for the asymmetry. Additionally, based on the histone code hypothesis that phosphorylation, together with methylation, could serve as a critical “switch” on the transcription level, we speculate that the neighbouring sites to lysine 9 on histone H3 may potentially and coordinately function in maintenance of the asymmetry, further influencing DNA methylation in mouse zygotic stage.

In this thesis, the following questions would be addressed.

(I) How does the differential deposition of histone H3 variants into maternal and paternal pronuclei contributes to histone H3 and DNA modifications asymmetry?

(II) Does any other modification act as an upstream switch for regulation of H3K9me2 in the maternal pronucleus?

(III) Does the preferential accumulation of H3.3 variant in paternal pronucleus plays role in paternal DNA demethylation?

(IV) How would the induced artificial abundance of H3K9me2 in the paternal genome influence DNA methylation reprogramming in mouse zygote?

2 Materials and Methods

2.1 Materials

2.1.1 Mouse strains

We used adult F1 (♂BDA x ♀C57Bl6) mice (at least two-month-old), which were bred in our laboratory.

2.1.2 Chemicals

Chemicals	Suppliers
Acidic Tyrode's	Sigma-Aldrich, Taufkirchen, Germany
Acrylamide/Bis-acrylamide(30%)	Carl Roth, Karlsruhe, Germany
Agar	Carl Roth, Karlsruhe, Germany
APS (10%)	Carl Roth, Karlsruhe, Germany
Blotting Grade Blocker	Bio-Rad, California, USA
Bromophenol blue	Serva, Heidelberg, Germany
BSA	Sigma-Aldrich, Taufkirchen, Germany
Calcium chloride	Sigma-Aldrich, Taufkirchen, Germany
Chaetocin	Sigma-Aldrich, Taufkirchen, Germany
Chromo-sulphuric acid	Sigma-Aldrich, Taufkirchen, Germany
Chloroform	Sigma-Aldrich, Taufkirchen, Germany
Cycloheximide	Sigma-Aldrich, Taufkirchen, Germany
DAPI	Sigma-Aldrich, Taufkirchen, Germany
DAB	Carl Roth, Karlsruhe, Germany
dNTPs	MBI Fermentas, St.Leon-Rot, Germany
Dextran Tetramethylrhodamine	Invitrogen, Karlsruhe, Germany
DMSO	Sigma-Aldrich, Taufkirchen, Germany
5%DMDCS in toluene	Supelco, Bellefonte, USA
Disodium hydrogen phosphate	Carl Roth, Karlsruhe, Germany
DNA Ladder 1kb	Thermoscientific, Schwerte, Germany
DTT	Sigma-Aldrich, Taufkirchen, Germany
EDTA	Sigma-Aldrich, Taufkirchen, Germany
Ethanol	Carl Roth, Karlsruhe, Germany
Ethidium bromide	Carl Roth, Karlsruhe, Germany
Glucose	Carl Roth, Karlsruhe, Germany
Glycerol	Carl Roth, Karlsruhe, Germany
hCG	Interved, Unterschleissheim, Germany
HEPES	Serva, Heidelberg, Germany
Hoechst 33342	Invitrogen, Karlsruhe, Germany
Hydrogen peroxide	Sigma-Aldrich, Taufkirchen, Germany
Imidazole	Carl Roth, Karlsruhe, Germany
IPTG	Carl Roth, Karlsruhe, Germany
Isopropyl alcohol	Carl Roth, Karlsruhe, Germany
Kanamycin sulfate	Sigma-Aldrich, Taufkirchen, Germany
Manganese(II) chloride	Sigma-Aldrich, Taufkirchen, Germany
Magnesium sulfate	Sigma-Aldrich, Taufkirchen, Germany
Methanol	Carl Roth, Karlsruhe, Germany
Mercury	Sigma-Aldrich, Taufkirchen, Germany
Mineral oil	Sigma-Aldrich, Taufkirchen, Germany

Materials and Methods

Milli-Q Water	Millipore Milli Q plus
Mounting Medium	Vector Labs, Loerrach, Germany
NEB buffer 3	New England Biolabs, USA
NEB buffer 4	New England Biolabs, USA
NEB BSA (100x)	New England Biolabs, USA
Nickel(II) chloride	Sigma-Aldrich, Taufkirchen, Germany
Nuclease-Free Water	Ambion, Darmstadt, Germany
Paraformaldehyde	Sigma-Aldrich, Taufkirchen, Germany
PCR Buffer 10x	Qiagen, Hilden, Germany
Pefabloc® SC-Protease Inhibitor	Carl Roth, Karlsruhe, Germany
Penicillin/Streptomycin	PAA, Coelbe, Germany
Phenol:Chloroform:Isoamyl Alcohol Mixture	Sigma-Aldrich, Taufkirchen, Germany
Phusion® HF Buffer	New England Biolabs, USA
PMSG	Interved, Unterschleissheim, Germany
Polyvinylpyrrolidone	Sigma-Aldrich, Taufkirchen, Germany
Potassium chloride	Carl Roth, Karlsruhe, Germany
Potassium dihydrogen phosphate	Carl Roth, Karlsruhe, Germany
Potassium hydroxide	Sigma-Aldrich, Taufkirchen, Germany
Q5® Reaction Buffer	New England Biolabs, USA
Salmon Sperm DNA	Thermoscientific, Schwerte, Germany
Sodium azide	Sigma-Aldrich, Taufkirchen, Germany
Sodium chloride	Carl Roth, Karlsruhe, Germany
Sodium dodecyl sulfate (SDS)	Sigma-Aldrich, Taufkirchen, Germany
Sodium hydroxide	Sigma-Aldrich, Taufkirchen, Germany
TEMED	Carl Roth, Karlsruhe, Germany
Tetracycline	Sigma-Aldrich, Taufkirchen, Germany
Tris-HCl	Carl Roth, Karlsruhe, Germany
Triton X-100	Sigma-Aldrich, Taufkirchen, Germany
Tween 20	Sigma-Aldrich, Taufkirchen, Germany
Tryptone	Carl Roth, Karlsruhe, Germany
X-Gal	Carl Roth, Karlsruhe, Germany
Yeast extract	Carl Roth, Karlsruhe, Germany

2.1.3 Antibodies

Name (Manufacture, Catalog#)	Dilution	Application
Anti-H3K9me2 (gift from Thomas Jenuwein, rabbit polyclonal)	1:1000	IF/WB
Anti-H3K9me2 (Abcam, #ab1220, mouse monoclonal)	1:1000	WB
Anti-H3K9me3 (Millipore, #07-442, rabbit polyclonal)	1:200/1:500	IF/WB
Anti-H3K9ac (Cell Signaling, #9671, rabbit polyclonal)	1:200	IF
Anti-H3S10phos (Cell Signaling, #3377, rabbit monoclonal)	1:100	IF
Anti-H3T11phos (Cell Signaling, #9767, rabbit monoclonal)	1:100	IF
Anti-gH2AX (US Biological, #H5110-03K2, rabbit polyclonal)	1:250	IF
Anti-G9a (abcam, #ab31874, rabbit polyclonal)	1:100	IF

Materials and Methods

Anti-5mC (Calbiochem, #NA81, mouse monoclonal)	1:1000	IF
Anti-5hmC (Active motif, #39791, rabbit ployclonal)	1:1000	IF
Anti-5caC (Active motif, #61225, rabbit ployclonal)	1:2000	IF
Anti-ssDNA (Immuno-Biological Laboratories, #18731, rabbit ployclonal)	1:400	IF
Anti-GFP (Roche #11814460001, mouse monoclonal)	1:1000	WB
Anti-GFP (Antibodies-online GmbH, #AA1-246, goat polyclonal)	1:2000	IF/WB
Anti-mouse IgG Alexa Fluor® 647 (Life Technologies, #A-21237)	1:200	IF
Anti-rabbit IgG Rhodamine Red-X (Jackson ImmunoResearch Laboratories Inc., #83473)	1:500	IF
Donkey Anti-Goat IgG Antibody (abcam, #ab6566)	1:1000	IF
Goat Anti-Mouse IgG Antibody, HRP conjugate (Millipore, #AP308P)	1:5000	WB
Goat Anti-Rabbit IgG Antibody, HRP-conjugate (Millipore, #12-348)	1:2500	WB
Donkey Anti-Goat IgG H&L (HRP) (abcam, #ab6885)	1:5000	WB

2.1.4 Enzymes

Enzymes	Suppliers
GeneRuler 1 kb DNA Ladder	Thermoscientific, Schwerte, Germany
HotFire DNA Polymerase	Solis BioDyne, Tartu, Estonia
Hyaluronidase	Sigma-Aldrich, Taufkirchen, Germany
Klenow Fragment	Thermoscientific, Schwerte, Germany
Pfu DNA Polymerase	New England Biolabs, USA
Phusion® DNA Polymerase	New England Biolabs, USA
Proteinase K	Zymo Research Europe, Germany
Protein Ladder (SM0671)	Thermoscientific, Schwerte, Germany
Q5® DNA Polymerase	New England Biolabs, USA
Taq DNA Polymerase	New England Biolabs, USA
T4 DNA ligase	New England Biolabs, USA
BsaWI	New England Biolabs, USA
Eco47I	Thermoscientific, Schwerte, Germany
NcoI	New England Biolabs, USA
NdeI	New England Biolabs, USA
SaII	New England Biolabs, USA
XhoI	New England Biolabs, USA

2.1.5 Prokaryotic cells

E.coli Top10 cells were used for sub-cloning the coding sequences, to generate plasmid templates for in vitro transcription, or to generate vectors for proteins expression in Rosetta (DE3) E.coli cells (Novagen).

2.1.6 Mediums

Mediums	Suppliers
Gibco Fetal Bovine Serum	Life Technologies, Darmstadt, Germany
KSOM	Millipore, Schwalbach-Ts, Germany

Materials and Methods

M2-Medium	Millipore, Schwalbach-Ts, Germany
M2-Medium without BSA	Millipore, Schwalbach-Ts, Germany
KSOM with 30 mg/ml BSA	Self-made
LB-Medium	Self-made
SOC-Medium	Self-made

2.1.7 Solutions and buffers

- (1) Blocking solution: 1% BSA, 0.01% triton X-100, 0.05% NaN₃, dissolved in 1x PBS solution.
- (2) DNA loading buffer (6x): 4g sucrose, 25mg bromophenol blue, 25mg xylene cyanol, add distilled water to 10mL.
- (3) Elution buffer (1L): 50mM NaH₂PO₄, 500mM NaCl, 300mM imidazole, adjust pH to 8.0 using NaOH.
- (4) Lysis buffer (1L): 50mM NaH₂PO₄, 500mM NaCl, adjust pH to 8.0 using NaOH.
- (5) PBS (1L, 10x) without Mg²⁺ and Ca²⁺: 80g NaCl, 2g KCl, 2.7g KH₂PO₄, 14.4g Na₂HPO₄, adjust pH to 7.4.
- (6) Permeabilization solution: 0.2% triton X-100, 0.05% NaN₃, dissolved in 1x PBS solution.
- (7) Sample loading buffer (10mL, 4x): 2.5ml of 1M Tris-HCl (pH 6.8), 1.0g SDS, 0.8mL of 0.1% bromophenol blue, 4mL of 100% glycerol, 2mL of 14.3M β-mercaptoethanol (100% stock).
- (8) TAE buffer (1L, 50x): 242g Tris base, 57.1mL glacial acetic acid, 100mL 0.5M EDTA, bring final volume to 1L and store at room temperature.
- (9) Washing buffer (1L): 50mM NaH₂PO₄, 500mM NaCl, 5mM imidazole, adjust pH to 8.0 using NaOH.

2.1.8 Primers

Name	Sequence (5' to 3')	Application
H3.1-GFPWild type FWD	CATGCCATGGCTCGTACTAAGCAGACCGC	Cloning
H3.1-GFPWild type REV	CCGCTCGAGGCCGCCAGCCCTCTCCCCGCGGATGCGGC	Cloning
H3.2-GFPWild type FWD	CATGCCATGGCCCCGTACGAAGCAGACTGC	Cloning
H3.2-GFPWild type REV	CCGCTCGAGGCCGCCAGCGCGCTCCCCACGGATGCGG	Cloning
H3.3-GFPWild type FWD	CATGCCATGGCTCGTACAAAGCAGACTGC	Cloning
H3.3-GFPWild type REV	CCGCTCGAGGCCGCCAGCACGTTCTCCGCGTATGCGGC	Cloning
MutGeneralPCR1 FWD	CCTGCCACCATACCCACGCCGAAAC	Mutagenesis
H3.1-GFPK9RPCR1 REV	GCCTTGCCGCCGGTAGAGCGGCGAGCGGTCTGCTTAGT	Mutagenesis
H3.1-GFPK9RPCR2 FWD	ACTAAGCAGACCGCTCGCCGCTCTACCGGCGGCAAGGC	Mutagenesis
MutGeneralPCR2 REV	CGTAGGTCAGGGTGGTCACGAGGGT	Mutagenesis
H3.2-GFPK9RPCR1 REV	GCCTTGCCGCCAGTGGAGCGGCGAGCGGTCTGCTTCG	Mutagenesis
H3.2-GFPK9RPCR2 FWD	CGAAGCAGACCGCTCGCCGCTCCACTGGCGGCAAGGC	Mutagenesis
H3.3-GFPK9RPCR1 REV	GTGCTTTACCACCGGTGGAGCGGCGGGCAGTCTGCTTTGT	Mutagenesis
H3.3-GFPK9RPCR2 FWD	ACAAAGCAGACTGCCCGCGCTCCACCGGTGGTAAAGCAC	Mutagenesis
H3.1-GFPS10APCR1 REV	CGGGGCCTTGCCGCCGGTGGCCTTGCAGCGGTCTGCT	Mutagenesis

Materials and Methods

H3.1-GFPS10APCR2 FWD	AGCAGACCGCTCGCAAGGCCACCGGCGGCAAGGCCCCG	Mutagenesis
H3.2-GFPS10APCR1 REV	CGGGGCCTTGCCGCCAGTGGCCTTGCGAGCGGTCTGCT	Mutagenesis
H3.2-GFPS10APCR2 FWD	AGCAGACCGCTCGCAAGGCCACTGGCGGCAAGGCCCCG	Mutagenesis
H3.3-GFPS10APCR1 REV	CTGGGTGCTTTACCACCGGTGGCTTTGCGGGCAGTCTGC	Mutagenesis
H3.3-GFPS10APCR2 FWD	GCAGACTGCCCCGAAAGCCACCGGTGGTAAAGCACCCAG	Mutagenesis
H3.1-GFPT11APCR1 REV	CGCGGGGCCTTGCCGCCGGCAGACTTGCGAGCGGTCTGC	Mutagenesis
H3.1-GFPT11APCR2 FWD	GCAGACCGCTCGCAAGTCTGCCGGCGGCAAGGCCCCGCG	Mutagenesis
H3.2-GFPT11APCR1 REV	CGCGGGGCCTTGCCGCCGGGACTTGCGAGCGGTCTGC	Mutagenesis
H3.2-GFPT11APCR2 FWD	GCAGACCGCTCGCAAGTCCGCCGGCGGCAAGGCCCCGCG	Mutagenesis
H3.3-GFPT11APCR1 REV	CTGGGTGCTTTACCACCGGCGGATTTGCGGGCAGTCTGC	Mutagenesis
H3.3-GFPT11APCR2 FWD	GCAGACTGCCCCGAAATCCGCCGGTGGTAAAGCACCCAG	Mutagenesis
H3.1-GFPK9QPCR1 REV	GCCTTGCCGCCGGTAGACTGGCGAGCGGTCTGCTTAGT	Mutagenesis
H3.1-GFPK9QPCR2 FWD	ACTAAGCAGACCGCTCGCCAGTCTACCGGCGGCAAGGC	Mutagenesis
HDAC1-GFP FWD	GCGCAGACTCAGGGCACCAAGAGGAAAG	Cloning
HDAC1-GFP REV	AGAATTTCGTCGACCTCGAGGCCGGCCAACTTGACCTCTTCTTTGAC	Cloning
HDAC2-GFP FWD	GCGTACAGTCAAGGAGGGCGCAAGAAGAAAGTGT	Cloning
HDAC2-GFP REV	GAATTCCTCGAGGCCAGGGTTGCTGAGTTGTTCTGACTTGCT	Cloning
G9aFL-GFP FWD	CGGGGTCTGCCGAGAGGGAGGGGGCTGATGCGGGCCCG	Cloning
G9aFL-GFP REV	CCGCTCGAGGGTGTGATGGGGGGCAGGGAGCTGAG	Cloning
G9aCat FWD	GTCTTCTGTCCCCACTGTGGAG	Cloning
G9aCat REV	CCGCTCGAGTTAGGTGTTGATGGGGGGCAGGGAGCTGAG	Cloning
G9aCat-GFP FWD	GTCTTCTGTCCCCACTGTGGAG	Cloning
G9aCat-GFP REV	CCGCTCGAGGGTGTGATGGGGGGCAGGGAGCTGAG	Cloning
G9aCat-NLS-GFP FWD	GTCTTCTGTCCCCACTGTGGAG	Cloning
G9aCat-NLS-GFP REV	TGGCCGACGTCGACGGTGTGATGGGGGGCAGGGAGCTGAG	Cloning
LINE1 FWD	TGGTAGTTTTTAGGTGGTATAGAT	Sequencing
LINE1 REV	TCAAACACTATATTACTTTAACAATTCCCA	Sequencing
IAP FWD	TTTTTTTTTTAGGAGAGTTATATTT	Sequencing
IAP REV	ATCACTCCCTAATTAACTACAAC	Sequencing
mSAT FWD	GGAAAATTTAGAAATGTTTAATGTAG	Sequencing
mSAT REV	AACAAAAAACTAAAAATCATAAAAA	Sequencing
T7 promoter	TAATACGACTCACTATAGGG	Sequencing
T7 upstream	TGCGTCCGGCGTAGAGGATCG	mRNA prep
T7 terminator	GCTAGTTATTGCTCAGCGG	mRNA prep
eGFP1 REV	GACACGCTGAACTTGTGGC	Sequencing
LINE1-Hairpin linker	Tggtagtttttagtggtatagattctcactaagcagactaaattcctaagttccttgaggtcccgggacca agatg gcgaccgctgctgctgtggcttagcgccccccagccggcgggcacctgtctccggtCCGGaG nGRC CATnnnnnnnnATGGGRCCtcngaccggaggacaggtcccggcggctggggagggc ggccT aagccAcagcagcagcggtgccaatctgtgcccggactccaaggaacttaggaatttagtctgctta agtctgtaccacctgggaattgtaagtaataatagtttga	Sequencing
IAP-Hairpin linker	Tcccttttttaggagagttatatttcgcttagacgtgtcactccctgattggctgcagcccacgcccaggt tgactg caAgtgacgtcacgggaaggcagagcacatggagtagagaaccacctcgcatatgcccagatta ttgttta ccacTTAaggRTTatNNNNNNNnatgggRTTtaagtgtaacaaataatctgcgcatat Gccgag ggtggttctactccatgtgctctccttccgtgacgtcaactcggccgatgggctgcagccaatcaggg agtgc	Sequencing

Materials and Methods

mSAT-Hairpin linker	GgaaaatttagaaatgttaatgtaggaCGtggaatatggcaagaaaactgaaatcatgggaaatgag aaac atccactgtCGactgaaaaatgaCGaaatcactaaaaaaCGtgaaaaatgagaaatgcacactga aggN TgggRTTatNNNNNNNNatgggRTTgNccttcagtgtgcatttcattttcaCGttttta gtgattt CGcattttcaagtCGacaagtggatgtttctcatttttatgatttttagtttttgtt	Sequencing
---------------------	---	------------

2.1.9 Reaction kits

The DNA replication in mouse zygotes was confirmed by using Click-iT® EdU kit (Life Technologies, Darmstadt, Germany). The mRNA extraction from oocytes was performed by using Dynabeads® mRNA Purification Kit (Life Technologies, Darmstadt, Germany). The subsequent cDNA reverse transcription was completed with EndoFree Reverse Transcription Kit (Life Technologies, Darmstadt, Germany). The *In vitro* mRNA transcription and purification were done by using AmpliCap-Max™ T7 High Yield Message Maker Kit (CELLSCRIPT) and RNA Clean & Concentrator™-25 Kit (Zymo research), respectively. The bisulfite treatment was performed using EZ DNA Methylation-Gold™ Kit (Zymo research). The PCR fragments were purified with Gel/PCR DNA Fragments Extraction Kit (GeneAid). Plasmids were extracted by using GenElute™ Plasmid Miniprep Kit (Sigma-Aldrich).

2.1.10 Instruments

Instruments	Manufactures
Axiovert 200M Inverted Microscope	Zeiss, Germany
Balance	Sartorius, Bradford, USA
BioStation IM Live Cell Recorder	Nikon, Germany
Borosilicate glass (GC100 TF-10)	Harvard Apparatus, UK
Borosilicate glass (GC100 TF-15)	Harvard Apparatus, USA
Cell Tram Air	Eppendorf, Germany
Cell Tram Vario	Eppendorf, Germany
Centrifuge	Eppendorf, Germany
CO ₂ Incubator	Sanyo, Wood Dale, USA
Concavity Slides	Menzel, Germany
Femtojet	Eppendorf, Germany
French Press Cell Disrupter	Thermo scientific, Germany
Gel Documentation System	PEQLAB, Germany
Glass capillary (Ringcaps® 50 µl)	Hirschmann GmbH, Germany
Heraeus® CO ₂ -Inkubator	Thermo scientific, Germany
Micro-forge De Fonbrune	Technical Products international
Micromanipulator	Eppendorf, Germany
NanoDrop2000 Spectrophotometers	Thermo scientific, Germany
Needle Puller, Model P-87	Sutter, Novato, USA
Nunc™ IVF Petri Dishes	Thermo scientific, Germany
PCR Cyclers (Applied Biosystems)	Life Technologies, Germany
Piezo Drill, PMAS-CT 150	Prime Tech, Japan
Preparation instruments	Fine Science Tools, Germany
Semi-Dry Blotting Systems	Bio-Rad, Germany
SMZ 800 Stereomicroscope	Nikon, Germany

Glass Bottom Culture Dish (35mm)	MatTek, Ashland, USA
----------------------------------	----------------------

2.2 Methods

2.2.1 Mouse superovulation and execution

All animal experiments were performed according to the German Animal Welfare law in agreement with the authorizing committee. For superovulation, females were treated by injection of 6 IU pregnant mare serum gonadotropin (PMSG) and 6 IU human chorionic gonadotropin (hCG) in an intraperitoneal manner, with a time interval of around 48 hours. Mice were executed via cervical dislocation.

2.2.2 RNA isolation

The mRNA from oocytes was prepared by using the Reverse Transcription System according to the manufacture's instructions. Briefly, oocytes were incubated with Lysis/Binding Buffer for 10min. Then 10µl Dynabeads oligo (dT)₂₅ was added to the sample for another 10min incubation at room temperature (RT). After incubation, the sample tubes were placed in the Magnetic Separation Rack which could immobilize the magnetic beads with mRNAs on. Subsequently, Washing Buffer A and B in a volume of 100µl were applied to remove contaminating RNA species in this order, respectively. Lastly, the mRNAs were eluted in as little as 10µl of elution butter, which was used for downstream experiment immediately.

2.2.3 cDNA reverse transcription

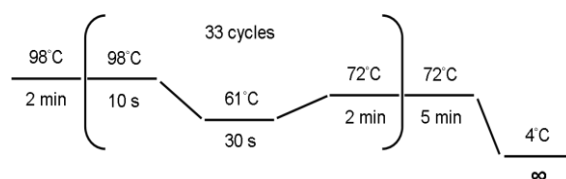
The reverse transcription was performed in the following steps. Firstly, the mixture of RNA (7µl) and RT (1µl) primer was prepared. Meanwhile, a reaction mix was also done, including 2µl 10x RT buffer, 8µl dNTPs, 1µl RNase inhibitor as well as 1µl Nuclease-free water. Secondly, incubation of the RNA: RT primer mixture at 72°C for 3min was done in a thermal cycler. After that, it was quickly moved to 50°C for 3min. The reaction mix was done in the same way in parallel. Then the reaction mix was added to the RNA: RT primer mixture. Note that the temperature should be avoided below 48°C. Lastly, incubation was continued at 50°C for 2 hours after being added with 1µl of Reverse Transcriptase. The produced cDNA was immediately used for PCR amplification.

2.2.4 Polymerase chain reaction (PCR)

The cloning of G9a catalytic domain was performed using the cDNA mentioned above as template in the following PCR reaction.

PCR components: (1) 10µl 10x Reaction buffer; (2) 2.5µl forward primer (10µM); (3) 2.5µl reverse primer (10µM); (4) 4µl dNTPs (2.5mM each); (5) 1µl cDNA template; (6) 0.5µl Phusion polymerase; (7) 29.5µl Nuclease-free water.

PCR conditions:



2.2.5 Plasmids preparation

Materials and Methods

The cDNAs of H3.1, H3.2 (gifts from Prof. Dr. Fugaku Aoki, Japan), H3.3 (purchased from ImaGenes GmbH) were cloned to pEGUP1 (a modified pET28b containing eGFP after multiple cloning sites) by using NcoI and XhoI. The cDNA of G9a full length (gift from Prof. Dr. Y. Shinkai, M. Tachibana, M. Brand and M. R. Stallcup) was subcloned to our vector pEGUP1 by ligation with one end being blunt and the other end being sticky cut by XhoI. The same strategy was applied to G9aCat-GFP, HDAC1 (purchased from Addgene) as well as HDAC2 (gift from Prof. Dr. Richard M. Schultz, USA). For G9aCat-NLS-GFP, the fragment was ligated to pEGUP1-NLS (a modified pET28b containing NLS after multiple cloning sites) with one blunt end and one sticky end cut by SaII. For G9aCat, it was cloned into pET15Am (a modified pET28b containing ampicillin resistance marker, p15 origin and no His-tag sequences). All the positive constructs were verified by Sanger sequencing.

Ligation components: (1) 1µl 10x Ligation buffer; (2) 1µl digested vector; (3) 4µl digested PCR fragments; (4) 1µl T4 DNA Ligase; (5) 3µl Milli-Q water.

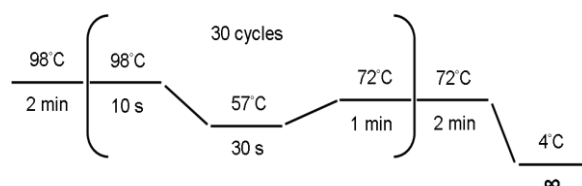
2.2.6 Site-specific mutagenesis

The generation of all mutants (K9R, S10A, T11A) of histone H3.1/2/3 was done by overlapping PCR-based mutagenesis. Briefly, two PCRs, namely PCR1 and PCR2, were applied with two sets of primers in which reverse primer for PCR1 and forward primer for PCR2 are complementary and contain the mutation sites. After gel purification, the cleaned up fragments from PCR1 and PCR2 were mixed as templates in the Overlap PCR reactions. The expected PCR products were then double-digested by NcoI and XhoI, followed by ligation with pEGUP1. The positive clones containing the corresponding mutations were selected and confirmed by Sanger sequencing.

PCR1 or PCR2 components: (1) 10µl 10x Reaction buffer; (2) 2.5µl forward primer (10µM); (3) 2.5µl reverse primer (10µM); (4) 4µl dNTPs (2.5mM each); (5) 0.5µl plasmid template; (6) 0.5µl Phusion polymerase; (7) 30µl Nuclease-free water.

Overlap PCR components: (1) 20µl 10x Reaction buffer; (2) 5µl forward primer (10µM); (3) 5µl reverse primer (10µM); (4) 8µl dNTPs (2.5mM each); (5) 5µl PCR1 product; (6) 5µl PCR2 product; (7) 0.5µl Phusion polymerase; (8) 51.5µl Nuclease-free water.

PCR conditions:



2.2.7 Acetylation-mimetic mutant of H3.1

The mutation of lysine 9 to glutamine of H3.1 was performed using the same strategy aforementioned to mimic the acetylation status.

2.2.8 *In vitro* transcription of mRNAs

For preparation of cRNAs of all the constructs mentioned above, highly purified DNAs were extracted with Phenol:Chloroform, and high-quality capped mRNAs were generated by *in vitro* transcription using AmpliCap-Max T7 High Yield Message Maker Kit (CellScript, Inc.),

followed by purification using RNA Clean & Concentrator™-25 Kit (Zymo research) according to the manufacturers' instructions. Finally, transcribed mRNAs were eluted with nuclease-free water (Life technologies), and stored at -80°C for later use within one month.

2.2.9 Protein Purification

For co-expression of G9aCat with histone H3.1-GFPWT, or H3.1-GFPT11A or H3.3-GFPWT, both constructs were transformed into Rosetta™ 2 Competent Cells. Cells containing both constructs were grown in SOC medium with ampicillin (100mg/mL) and kanamycin (25mg/mL) until OD value reached 0.5-0.6 at 37°C , followed by 0.5mM isopropyl-b-D-thiogalactopyranoside (IPTG) induction for 24h at 16°C . Modified proteins of H3.1-GFPWT, H3.1-GFPT11A, H3.3-GFPWT were purified through Nickel nitrilotriacetic (Ni-NTA) resin by taking advantage of the 6xHis tag. The same procedure was respectively applied to H3.1-GFPWT and H3.3-GFPWT without co-expression. H3.3-GFPWT and H3.3-GFPK9me2 proteins were further gradually dialysed with PBS buffer overnight at 4°C . The protein expression was confirmed by Coomassie Blue staining of SDS-PAGE gel.

2.2.10 Verification of H3K9me2 by Western blotting

Western blotting was performed to check whether dimethyl group was successfully transferred to K9 on histone H3.1-GFP, H3.1-GFPT11A or H3.3-GFP. After purification, the proteins were added with loading buffer, heated at 100°C for 3-5min and loaded onto the SDS-PAGE gel. After running, the proteins were electrotransferred to the PVDF membrane at 15V for 45min, followed by blocking for around 2h. Then the membrane was incubated with primary antibodies, followed by HRP conjugated secondary antibody incubation with three times washing between two steps. In the end, DAB was applied for detection following the manufacturer's instructions.

2.2.11 *In vitro* fertilization

Spermatozoa isolation, oocytes collection and IVF procedures were carried out as previously published protocol with small modifications (Wossidlo et al., 2010). Briefly, sperm were isolated from the cauda epididymis of male mice and capacitated in pre-gassed modified KSOM medium supplemented with 30 mg/ml BSA for 2h. Mature oocytes were collected 15h post-human chorionic gonadotropin (hCG) injection of female mice according to the standard protocol (Nagy et al., 2003). Cumulus–oocyte complexes (COCs) were placed into a 400 μl drop of KSOM medium, mixed with capacitated sperm and incubated at 37°C in a humidified atmosphere of 5% CO_2 and 95% air.

2.2.12 Embryo culture

At around 2 to 3hpf, the zygotes were collected and washed several times in M2 medium. Subsequently, they were transferred to 100 μl drops of pre-gassed KSOM medium covered with mineral oil in a Petri dish. They were cultured to the desired stage for fixation.

2.2.13 Chaetocin treatment

At 3h post fertilization, Chaetocin with a concentration of 1 μM was added into the 400 μl drop of KSOM medium. Meanwhile, ethonal was applied as the control treatment. Then the

zygotes were cultured to post-replication stage (PN4/5), followed by fixation for immunostaining.

2.2.14 Cycloheximide treatment and Edu labelling

At the beginning of fertilization, cycloheximide with a concentration of 50 μ g/ml was added into the 400 μ l drop of KSOM medium, as used in the literature (Liu et al., 2004). For the Edu labelling, it was performed according to manufacture's instructions. Briefly, after 3hpf, the zygotes were transferred into 100 μ l KSOM containing 2 μ l of cycloheximide and 1 μ l of Edu diluted from the stock solution in the kit. Then the zygotes were cultured to replication stage (late PN3 or PN4), followed by fixation for 30min, permeabilization for 30min, and blocking for 3h at RT. Then the reaction cocktail was applied for incubation for 1h at RT. After washing in the blocking solution, the anti-gamma H2A.X antibodies were incubated, followed by the protocol mentioned below for immunostaining.

2.2.15 Preparation of microinjection needles

Fine tipped glass needles were prepared by a puller under the following conditions. (1) Temperature: Ramp-Test+5; (2) Traction force: 80; (3) Speed: 80; (4) Time: 200; (5) Druck: 200;

2.2.16 Microinjection of mRNAs or proteins into zygotes

At around 1hpf, just before microinjection, zygotes were collected, washed in M2 medium for several times and transferred into 100 μ l drops of pre-gassed KSOM medium. Microinjection was performed under a Zeiss Axiovert 200M inverted microscope (Zeiss) equipped with a microinjector and Piezo-driven micromanipulators (Eppendorf). After a quick setup according to the procedures described in the laboratory manual entitled "Manipulating the mouse embryo" (Nagy et al., 2003), zygotes were placed into a M2 medium drop of 20 μ l and cytoplasm injection was done with mRNAs or proteins, respectively.

2.2.17 Triton treatment of zygotes

Zygotes injected with histone H3WTs and K9R mutants were treated exactly as previously reported (Nakamura et al., 2012). After the last washing with PBS, the zygotes were fixed for immunostaining as mentioned below.

2.2.18 Chromatin incorporation of histone H3 variants monitored by live imaging

After being microinjected with mRNAs of histone H3 WT or K9R mutants at around 1hpf, respectively, the zygotes were transferred into a KSOM drop of 10 μ l on a glass bottom culture dish (35mm) and placed into the chamber of Live Cell Screening Systems. The chamber was under the condition of 37°C in a humidified atmosphere of 5% CO₂ and 95% air. The pictures were captured every 15min for 97 cycles with the exposure time being 1/250s.

2.2.19 Immunofluorescence staining

The embryos were fixed at desired stages in 3.7% PFA. The detailed protocol was well described in the published papers (Wossidlo et al., 2010; Wossidlo et al., 2011). All the antibodies used were shown in Materials Part (2.1.3 Antibodies).

2.2.20 IF Microscopy, quantification and statistical analysis

The mounted embryos were analysed on Zeiss Axiovert 200M inverted microscope equipped with the fluorescence module and B/W digital camera for imaging. The IF images were captured, pseudocoloured and merged using AxioVision software (Zeiss). GIMP and Image J softwares were applied together to complete quantification of the signals of z-stack computed images. For each group, at least 10 zygotes were analysed from at least two repeated experiments. Student's t-test was employed for statistical analysis.

2.2.21 Hairpin bisulfite sequencing

The tube containing the zygotes in M2 medium was added with 1µl lysis buffer, 1µl salmon sperm DNA (100ng/µl) as well as 1µl proteinase K (1ng/µl) and incubated at 55°C over night. The reaction was stopped by putting 0.7µl Pefabloc (8.14µM) to the sample. The DNA was then cut in an 8µl reaction mixture containing 0.8µl buffer, 5-10U of restriction enzyme and 1µl 5mM MgCl₂. As for restriction enzymes, BsaWI (NEB) was used for LINE1, DdeI (NEB) for IAPs and Eco47I (Thermo Scientific) for mSat. The reaction was incubated for 3h. Temperatures were adjusted according to the enzymes. After digestion, the ligation of the hairpin linker was done by adding 200U T4 DNA ligase, 1µl ATP and 1µl HP-Linker and incubating for 16h at 16°C. The bisulfite treatment was performed using the GOLD kit from Zymo Research. Amplicons were generated in a PCR using the HotFire polymerase (SolisBioDyne) and the primers shown in Materials Part (2.1.8 Primers). In the case of L1 and IAP the reactions were supplied with HotStartIT binding protein. The fragments were purified by gel electrophoresis and cleaned with Gel/PCR DNA Fragments Extraction Kit. The Sequencing was performed on an Illumina MiSeq platform. The analysis was done using BiQAnalyzerHT and python scripts.

3 Results

3.1 Effects of K9R mutation of H3.1/2/3 on modifications of both histone and DNA in mouse zygotes

DNA demethylation preferentially occurs in the paternal genome of mouse zygotes based on the Immunofluorescence, which is further confirmed by deep sequencing on the molecular level (Arand et al., 2015; Smallwood et al., 2011; Smith et al., 2012). Recently, Nakamura et al. demonstrated that H3K9me2, together with PGC7, serves as a protector for DNA methylation in the maternal genome, as well as some imprinted loci in the paternal one (Nakamura et al., 2007; Nakamura et al., 2012). Notably, H3K9me2 could theoretically take place on different histone H3 variants, namely H3.1, H3.2 and H3.3. For this reason, the site mutation of K9R was introduced on H3.1, H3.2 and H3.3 to address the question that which histone H3 variant is enriched with K9me2.

3.1.1 Dynamic pattern of H3K9me2 through DNA replication

To dissect the relations between histone H3 variants and H3K9me2 in mouse zygotes, we first evaluated the dynamic pattern of H3K9me2 during replication. It showed a reduction via DNA replication in the maternal pronucleus. In contrast, a slight but significant increase in *de novo* H3K9me2 was obtained in the paternal pronucleus (Fig. 3.1a, b), as reported previously (Liu et al., 2004; Santos et al., 2005).

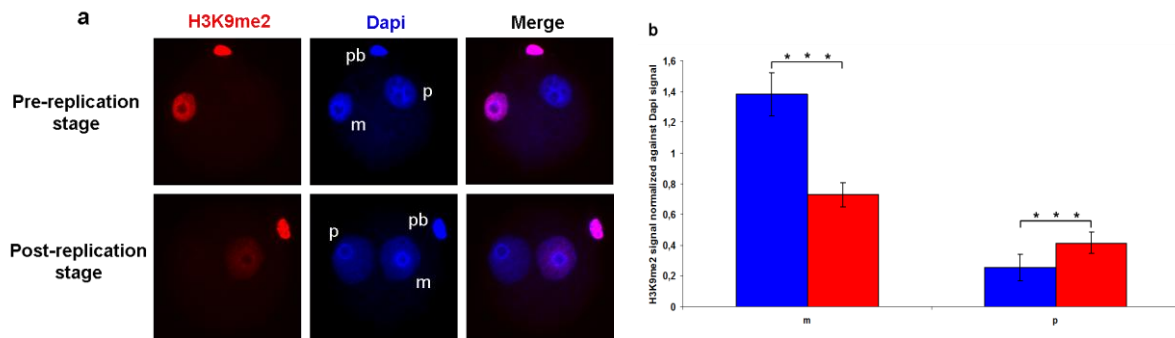


Fig. 3.1 Dynamic changes of H3K9me2 through DNA replication in mouse zygotes. **a**, Representative images of pre- and post replication stage zygotes stained with antibodies against H3K9me2. H3K9me2, red; Dapi, blue; **b**, Quantification of H3K9me2 signal normalized against Dapi signal in both parental genomes in pre- and post replication stages. Blue and red stand for pre-replication and post-replication stage, respectively. m, the maternal pronucleus; p, the paternal pronucleus; pb, polar body. Asterisks showed significant changes using Student's t-tests (***) ($P < 0.001$). Error bars indicated s.d. For each group, at least 10 zygotes were analysed from at least two repeated experiments.

3.1.2 Dynamic pattern of H3K9me3 through DNA replication

Through quantification of H3K9me3 signal in pre- and post-replicative stages, it showed that H3K9me3 followed a similar to H3K9me2 dilution model in the maternal pronucleus, while it was completely absent from the paternal one.

Results

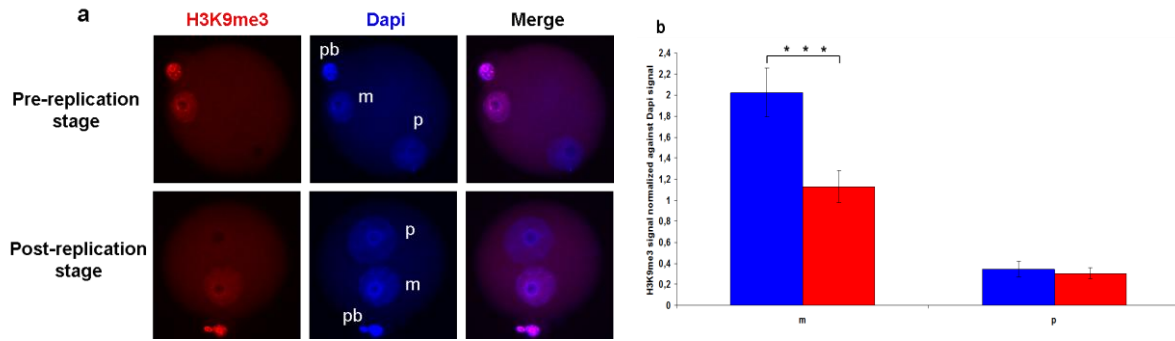


Fig. 3.2 Dynamic changes of H3K9me3 through DNA replication in mouse zygotes. **a**, Representative images of pre- and post replication stage zygotes stained with antibodies against H3K9me3. **b**, Quantification of H3K9me3 signal normalized against Dapi signal in both parental genomes in pre- and post replication stages. Blue and red stand for pre-replication and post-replication stage, respectively. H3K9me3, red; Dapi, blue; m, the maternal pronucleus; p, the paternal pronucleus; pb, polar body. Asterisks showed significant changes using Student's t-tests ($***=P<0.001$). Error bars indicated s.d.. For each group, at least 10 zygotes were analysed from at least two repeated experiments.

3.1.3 Dynamic pattern of H3K9ac through DNA replication

Upon fertilization, H3K9ac is readily detectable in both pronuclei. It is slightly more abundant in the paternal genome. At the commencement of replication, H3K9ac is increasingly accumulated in both genomes.

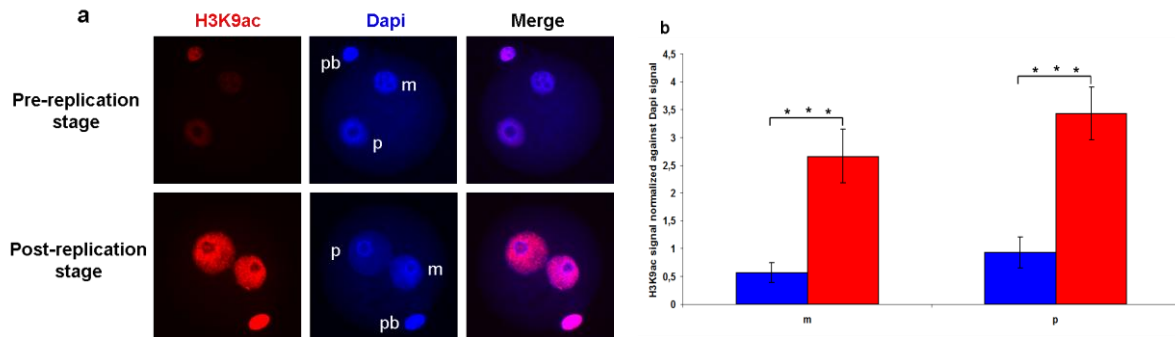


Fig. 3.3 Dynamic changes of H3K9ac through DNA replication in mouse zygotes. **a**, Representative images of pre- and post replication stage zygotes stained with antibodies against H3K9ac. **b**, Quantification of H3K9ac signal normalized against Dapi signal in both parental genomes in pre- and post replication stages. Blue and red stand for pre-replication and post-replication stage, respectively. H3K9ac, red; Dapi, blue; m, the maternal pronucleus; p, the paternal pronucleus; pb, polar body. Asterisks showed significant changes using Student's t-tests ($***=P<0.001$). Error bars indicated s.d.. For each group, at least 10 zygotes were analysed from at least two repeated experiments.

3.1.4 Nuclear localization and chromatin incorporation of H3.1/2/3-GFPWTs and K9R mutants

By tracing the GFP signal, we could clearly see the nuclear distribution of both H3.1/2/3-GFPWTs and K9R mutants in mouse zygotes (Fig. 3.4). Only PN3 stage was shown for H3.1 and H3.2, because they are replication-dependent.

Results

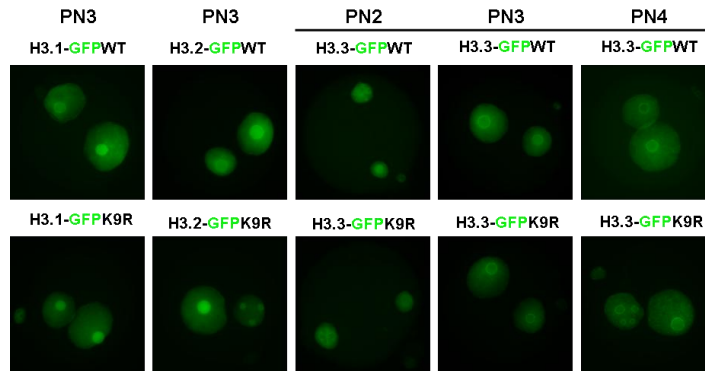


Fig. 3.4 Nuclear localization of H3.1/2/3-GFPWT and K9R mutants. H3.1 or H3.2-GFPWTs or K9R injected groups were fixed at replication stage (PN3), whereas H3.3-GFPWT or K9R injected groups were captured at pre (PN2), middle (PN3) and post (PN4) replication stages, respectively. GFP signal, green. For each group, at least 10 zygotes were analysed from at least two repeated experiments.

However, notably, the nuclear localization does not mean histone incorporation into the chromatin. Due to this fact, we first introduced triton treatment before fixation, which in principle could drive the free histones out of the nuclear, leaving the chromatin-bound histones inside the nuclear. As expected, we found that H3.3-GFPWT displayed a preferential localization in the paternal pronucleus before and during replication. Later, a balanced distribution of H3.3-GFPWT was seen between paternal and maternal pronuclei after replication, which is consistent with the published data (Santenard et al., 2010; Torres-Padilla et al., 2006; van der Heijden et al., 2005), while H3.1/2-GFPWTs exhibited the same pattern regardless of introduction of triton treatment. Intriguingly, when lysine 9 on H3.3 was replaced by arginine, it showed generally weaker signals than its WT counterpart in PN2 stage. Also, during replication stage, it showed equal deposition into the chromatin in both pronuclei, while its wild type remained to be asymmetrically distributed during this time window. Taken together, it gave a hint that lysine 9 on H3.3 might be involved in its deposition into chromatin (Fig. 3.5).

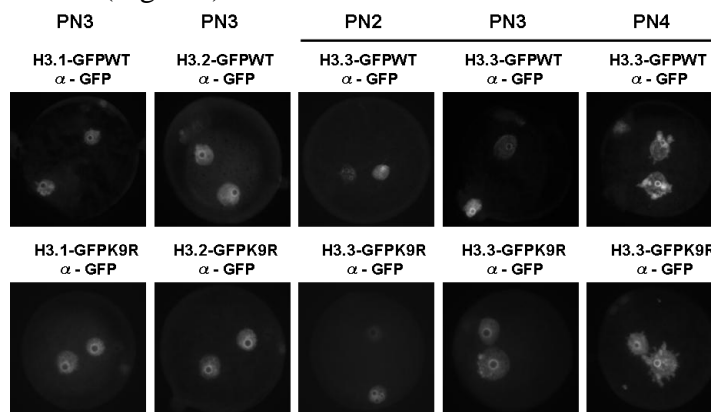


Fig. 3.5 Chromatin incorporation of H3.1/2/3-GFPWT and K9R mutants after introducing triton treatment before fixation. H3.1/H3.2-GFPWTs or K9R expressing zygotes were fixed at PN3, and H3.3-GFPWT or K9R expressing zygotes were arrested at PN2, PN3 and PN4 stages. Representative images of zygotes stained with antibodies against GFP were shown. For each group, at least 10 zygotes were analysed from at least two repeated experiments.

Results

Later, H3.1/2/3-GFPWTs and K9R mutants expressing zygotes were monitored by live imaging, which clearly showed the chromosomal localization of ectopically expressed histones during metaphase stage, strongly indicative of their successful incorporation into the chromatin after microinjection (Fig. 3.6). Otherwise, the green signal would show a homogenous localization in the cytoplasm.

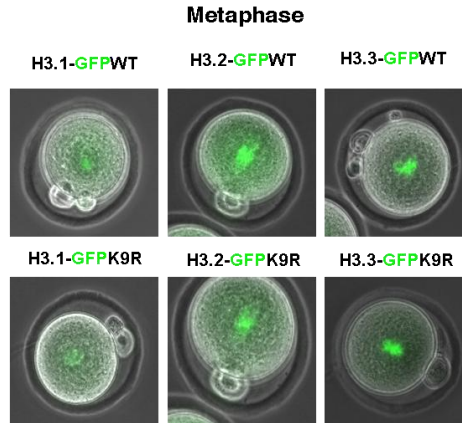


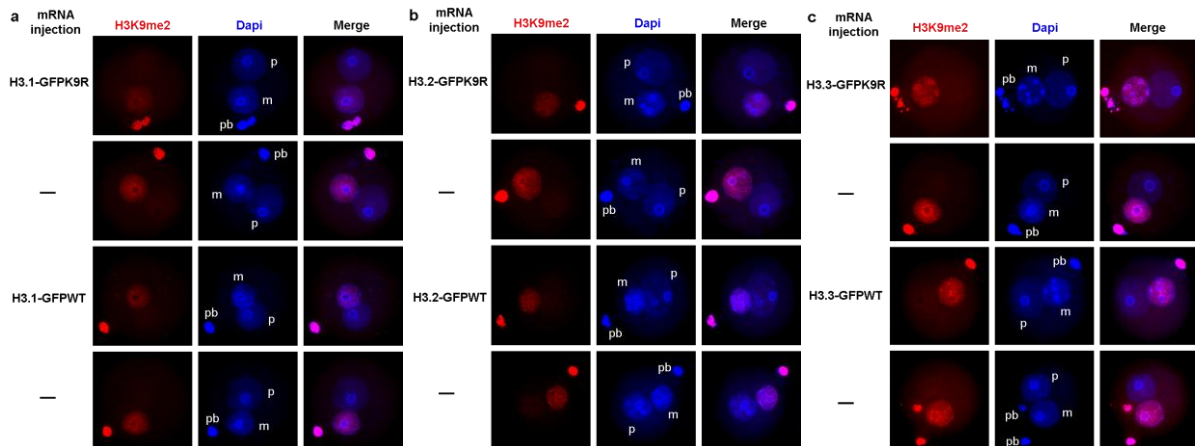
Fig. 3.6 Chromatin incorporation of H3.1/2/3-GFPWT and K9R mutants monitored by live cell imaging. The representative images of H3.1/2/3-GFPWTs or K9R mutants expressing mouse zygotes were shown at metaphase stage. GFP signal, green. For each group, at least 10 zygotes were analysed from at least two repeated experiments.

3.1.5 Effects of H3.1/2/3-GFPK9R on H3K9me2

Next, we tried to address the following questions:

- (I) Does the reduction of H3K9me2 during replication follow a simple dilution model or whether it involves the *de novo* methylation activity?
- (II) Can newly synthesized exogenous histone H3.1/2/3-GFPK9R replace the old histones carrying H3K9me2 during the replication coupled dilution process?
- (III) Which histone variant would be the main carrier of H3K9me2?

In fact, the immunostaining results showed rather comparable signal intensities of H3K9me2 between K9R mutants, WT injected and non-injected groups (Fig. 3.7a, b, c).



Results

Fig. 3.7 Influences on H3K9me2 in zygotes expressing H3.1/2/3-GFPWT and K9R. a, b, c, Representative images of PN4/5 stage zygotes stained with antibodies against H3K9me2. H3K9me2, red; Dapi, blue. m, the maternal pronucleus; p, the paternal pronucleus; pb, polar body. For each group, at least 10 zygotes were analysed from at least two repeated experiments.

Having a closer view by signal quantification, we found that WT's indeed failed to disrupt H3K9me2. However, all the K9R mutants caused a minor reduction in H3K9me2 in the maternal pronucleus, of which H3.1/2K9R and H3.3K9R showed a relatively major and minor but significant effect, respectively, compared to the non-injected controls (Fig. 3.8), suggesting that H3.1 and H3.2 are more enriched with H3K9me2 than H3.3. Moreover, K9R mutants but not WT's slightly impaired H3K9me2, indicating that *de novo* H3K9me2 indeed took place during replication and strongly pointing out that the loss of H3K9me2 in a replication-dependent manner does not follow a simple dilution pathway but involves re-methylation process.

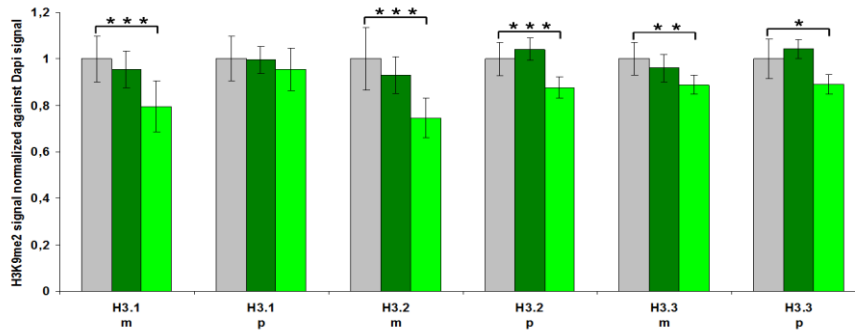


Fig. 3.8 Quantification of H3K9me2 signal normalized against Dapi signal in both parental genomes of zygotes expressing H3.1/2/3-GFPWT or K9R. Non-injected groups, grey; H3.1/2/3-GFPWT injected groups, dark green; H3.1/2/3-GFPK9R injected groups, light green; Asterisks showed significant changes using Student's t-tests (***=P<0.001, **=P<0.01, *=P<0.05). The quantified values in control group were set to 1. Error bars indicated s.d.. For each group, at least 10 zygotes were analysed from at least two repeated experiments.

3.1.6 Effects of H3.1/2/3-GFPK9R on H3K9me3

Since the minor effects on H3K9me2 by H3.1/2/3K9R-GFP were observed, we also checked the alteration of H3K9me3. As a result, similar observations were obtained for H3K9me3 based on the immunostaining, shown in Fig. 3.9 a, b, c.

Results

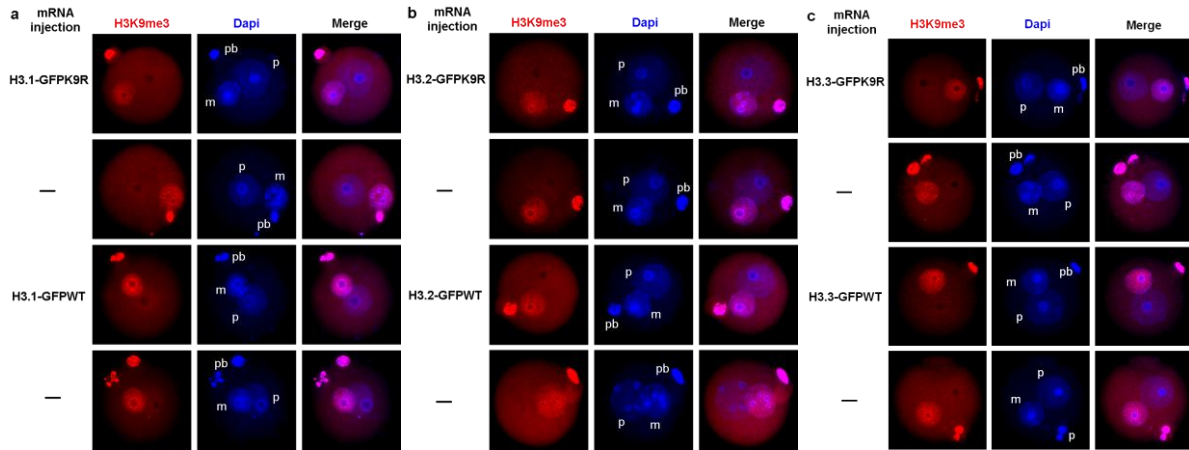


Fig. 3.9 Influences on H3K9me3 in zygotes expressing H3.1/2/3-GFPWT and K9R a, b, c, Representative images of PN4/5 stage zygotes stained with antibodies against H3K9me3. H3K9me3, red; Dapi, blue. m, the maternal pronucleus; p, the paternal pronucleus; pb, polar body. For each group, at least 10 zygotes were analysed from at least two repeated experiments.

Then we quantified the signals of H3K9me3 only from the maternal pronucleus in different groups, owing to its absence in the paternal one. As indicated on Fig. 3.10, significant reduction in H3K9me3 was caused by K9R mutation on H3.1/2-GFP, but not H3.3-GFP, indicating that the repressive mark H3K9me3 is distributed on H3.1 and H3.2, but not on H3.3.

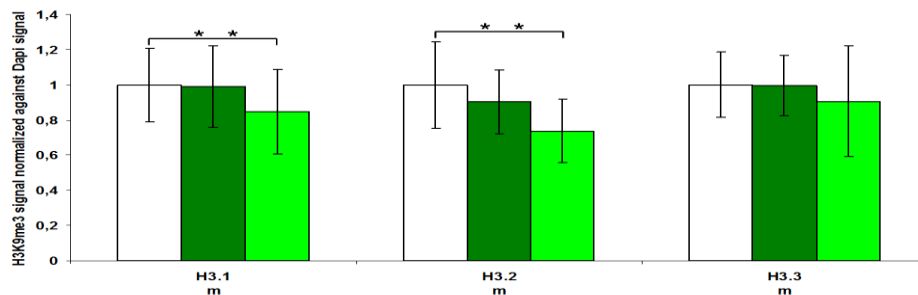


Fig. 3.10 Quantification of H3K9me3 signal normalized against Dapi signal in the maternal genome of zygotes expressing H3.1/2/3-GFPWT or K9R. Non-injected groups, grey; H3.1/2/3-GFPWT injected groups, dark green; H3.1/2/3-GFPK9R injected groups, light green; Asterisks showed significant changes using Student's t-tests (**=P<0.01). The quantified values in control group were set to 1. Error bars indicated s.d.. For each group, at least 10 zygotes were analysed from at least two repeated experiments.

3.1.7 Effects of H3.1/2/3-GFPK9R on H3K9ac

Due to the fact that the rather dramatic increase of H3K9ac was obtained through replication in both pronuclei, we anticipated that, theoretically, K9R mutation at least on one of H3.1/2/3-GFP variants may affect H3K9ac level. Nevertheless, unexpectedly, it displayed no differential signal intensities of H3K9ac between groups based on the immunofluorescence (Fig. 3.11).

Results

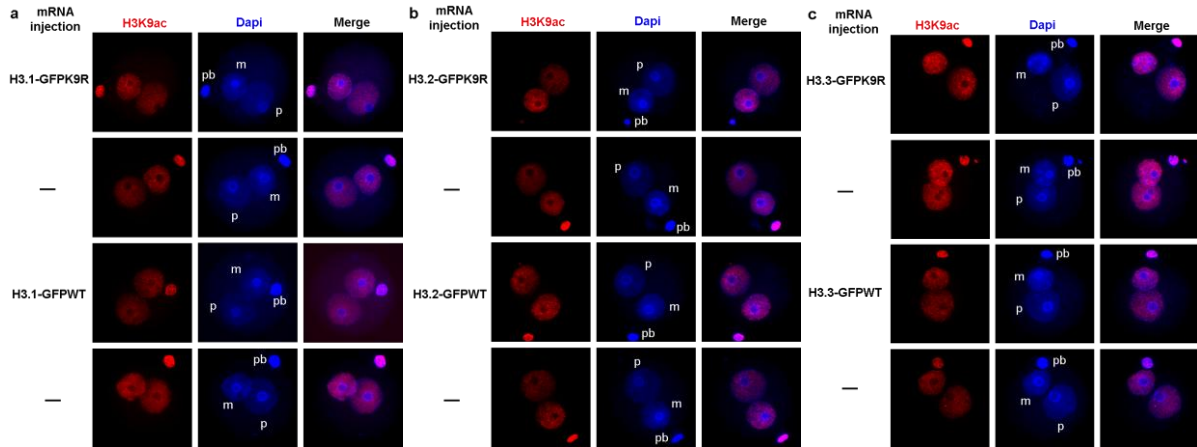


Fig. 3.11 Influences on H3K9ac in zygotes expressing H3.1/2/3-GFPWT and K9R. a, b, c, Representative images of PN4/5 stage zygotes stained with antibodies against H3K9ac. H3K9ac, red; Dapi, blue. m, the maternal pronucleus; p, the paternal pronucleus; pb, polar body. For each group, at least 10 zygotes were analysed from at least two repeated experiments.

To verify the staining results, we compared H3K9ac signal intensities by quantification between groups, indeed showing no alterations in H3K9ac by K9R mutation (Fig. 3.12), although lysine 9 on histone H3 is highly aggressively acetylated through replication and H3.1/2/3-GFPK9R mutants were proved to be clearly incorporated into the chromatin after microinjection. The results implied that mutation of K9R might cause the inability of histone H3 variants to get access to the acetylation-required areas but not to the non-acetylation related ones across the whole genome.

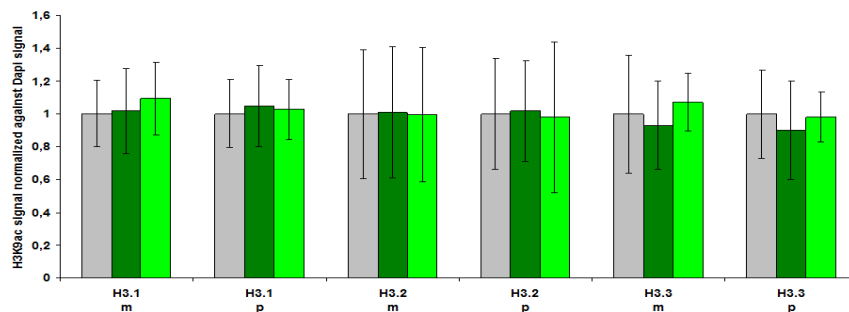


Fig. 3.12 Quantification of H3K9ac signal normalized against Dapi signal in both parental genomes of zygotes expressing H3.1/2/3-GFPWT or K9R. Non-injected groups, grey; H3.1/2/3WT-GFP injected groups, dark green; H3.1/2/3K9R-GFP injected groups, light green; The quantified values in control group were set to 1. Error bars indicated s.d.. For each group, at least 10 zygotes were analysed from at least two repeated experiments.

3.1.8 Effects of H3.1/2/3-GFPK9R on 5mC and 5hmC

Though only slight impacts on H3K9me2 were observed in all the injected groups, we still evaluated the influence of K9R mutation on the conversion of 5mC to 5hmC. However, no significant loss in 5mC was observed by immunostaining, which was further confirmed by quantification (Fig. 3.13 a, b, c, d). Correspondingly, 5hmC showed similar patterns between

Results

groups (Fig. 3.13 e, f, g). We have to admit, that due to the technical problem related to mouse-derived anti-ssDNA antibody, we failed to quantify the signal intensity of 5hmC.

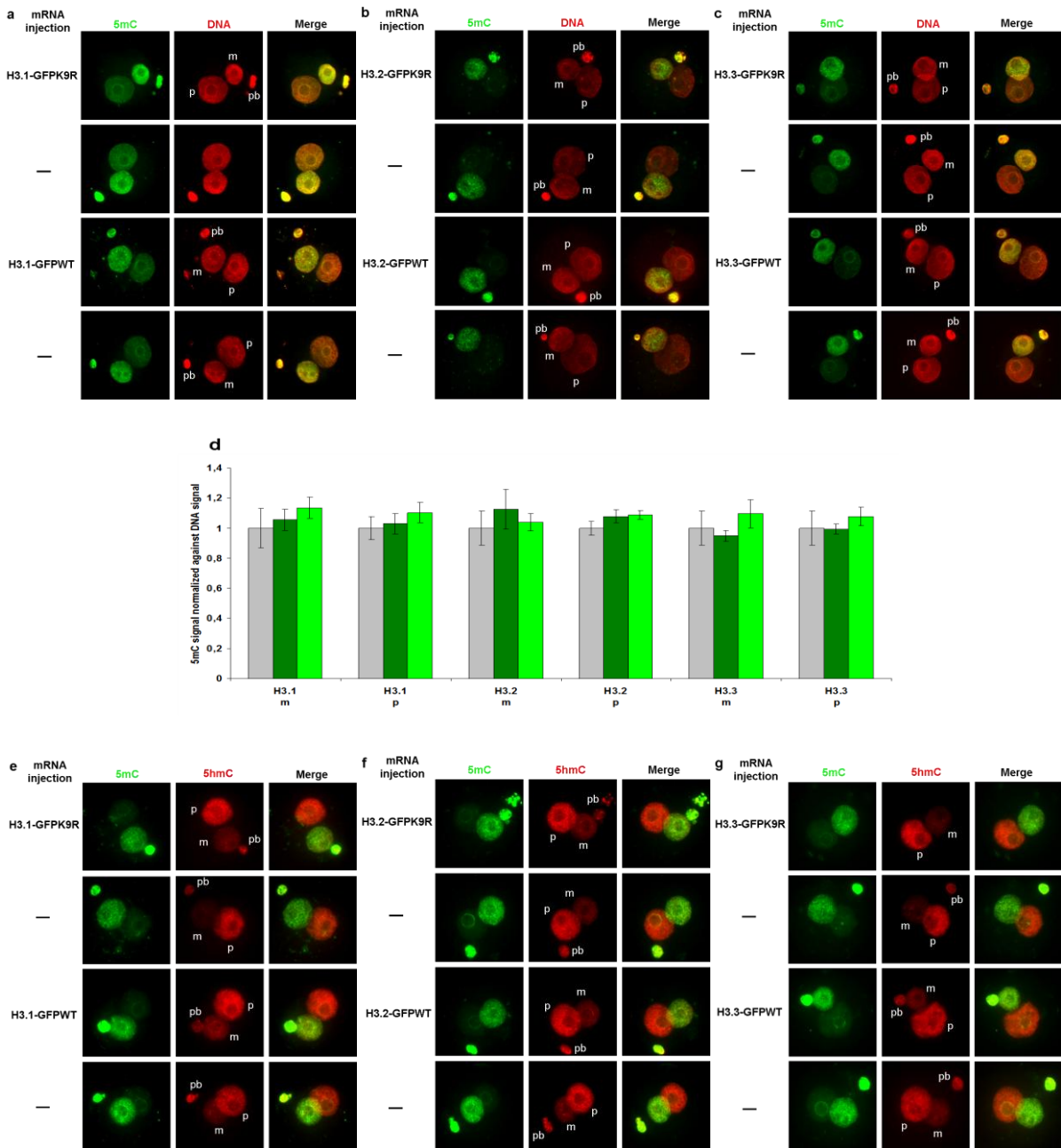


Fig. 3.13 Influences on 5mC and 5hmC in zygotes expressing H3.1/2/3-GFPWT and K9R. **a, b, c**, Representative images of PN4/5 stage zygotes stained with antibodies against 5mC and DNA. 5mC, green; DNA, red. **d**, Quantification of 5mC signal normalized against DNA signal in both parental genomes of zygotes at PN4/5. Non-injected groups, grey; H3.1/2/3WT-GFP injected groups, dark green; H3.1/2/3K9R-GFP injected groups, light green; The quantified values in control group were set to 1. Error bars indicated s.d.. **e, f, g**, Representative images of PN4/5 stage zygotes stained with antibodies against 5mC and 5hmC. 5mC, green; 5hmC, red. m, the maternal pronucleus; p, the paternal pronucleus; pb, polar body. For each group, at least 10 zygotes were analysed from at least two repeated experiments.

3.2 Effects of S10A and T11A mutations of H3.1/2/3-GFP on modifications of both histone and DNA in mouse zygotes

Results

As the neighboring sites to lysine 9, serine 10 (S10) and threonine 11 (T11) could potentially be phosphorylated by different kinases (Hirota et al., 2005; Metzger et al., 2008). The growing evidence shows the crosstalks between K9 methylation (K9me), S10 phosphorylation (S10phos) and T11 phosphorylation (T11phos) (Baek, 2011; Fischle, 2008; Metzger et al., 2008; Ng et al., 2007; Sabbattini et al., 2014), which prompted us to investigate the potential links among them.

3.2.1 Dynamic patterns of H3S10phos and H3T11phos throughout the mouse zygotic stage

First, we examined the dynamic patterns of phosphorylation at S10 and T11 on histone H3. As shown in Fig. 3.14a, H3S10phos was clearly detectable in G1 stage, was almost invisible during replication, and again appeared in G2 stage, which is in line with the published data (Ribeiro-Mason et al., 2012; Teperek-Tkacz et al., 2010). Notably, H3S10phos signal intensities were variable depending on the antibodies used. As for H3T11phos, it was absent in G1 stage, appeared from S phase on, and further accumulated in G2 phase (Fig. 3.14b). To our knowledge, it is the first description of H3T11phos pattern in mouse zygotes. Hence the two phosphorylation marks follow different dynamics during the first cell cycle.

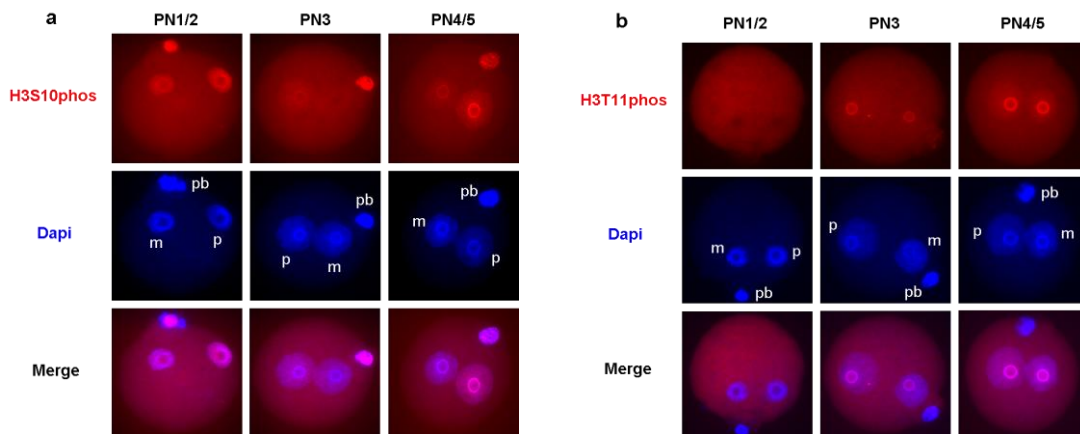


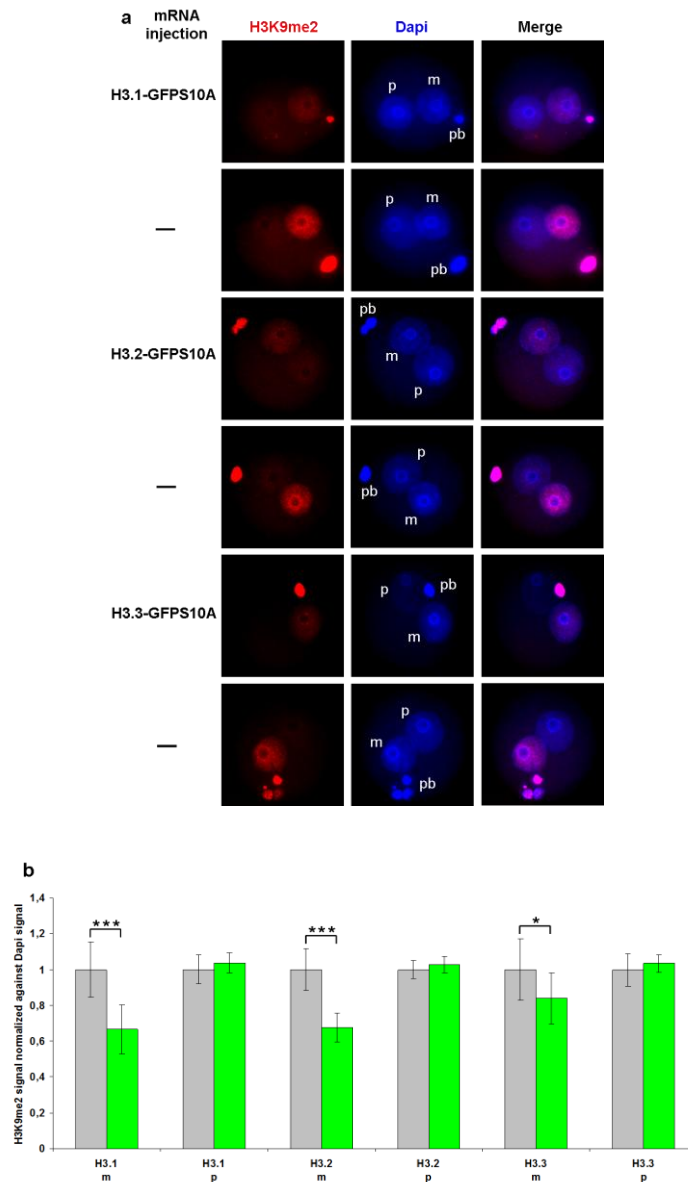
Fig. 3.14 Dynamic patterns of H3S10phos and H3T11phos in mouse zygotes. **a**, Representative images of zygotes at different PN stages stained with antibodies against H3S10phos. H3S10phos, red; Dapi, blue; **b**, Representative images of zygotes at different PN stages stained with antibodies against H3T11phos. H3T11phos, red; Dapi, blue; m, the maternal pronucleus; p, the paternal pronucleus; pb, polar body. For each group, at least 10 zygotes were analysed from at least two repeated experiments.

3.2.2 Effects of H3.1/2/3-GFPS10A on H3K9me2, 5mC and 5hmC

To dissect the relations between H3S10phos, H3K9me2 and 5mC, we microinjected mRNAs encoding histone H3 variants, either WT or bearing S10A mutations, into early mouse zygotes (very critical: around 1 hour post fertilization). As shown in Fig. 3.15a and b, H3K9me2 was significantly reduced by around 30% in both H3.1-GFPS10A and H3.2-GFPS10A expressing zygotes, by around 15% in H3.3-GFPS10A expressing zygotes, when compared to the controls. Furthermore, the quantification results showed that 5mC was only impaired by 15% to 20% in the maternal genomes of H3.1-GFPS10A and H3.2-GFPS10A injected groups, while it remained comparable between H3.3-GFPS10A injected and non-injected control (Fig. 3.15c and d), indicative of the weak but significant H3S10phos-switch role in maintaining

Results

H3.1/2K9me2 and further protecting 5mC from being oxidized. Notably, the impact on 5mC is less than that on H3K9me2. Such discrepancies reflected that H3K9me2 and 5mC were hardly overlapped with each other in some certain regions. As expected, gain of 5hmC in the maternal pronucleus was observed in both H3.1-GFPS10A and H3.2-GFPS10A expressing groups (Fig. 3.15e). Intriguingly, despite of no alteration in 5mC, there seemed to be an observable increase of 5hmC in both parental genomes in H3.3-GFPS10A injected group (Fig. 3.15e), which is consistent with that in H3.3-GFPT11A injected group mentioned later. Collectively, H3.1/2/3S10phos served a weak protection for H3K9me2 in the maternal genome of mouse zygotes, of which H3.1 and H3.2 were related to the maintenance of 5mC to a low extent. Such low correlation could be explained by dephosphorylation of H3S10 during replication, at the time when massive 5mC to 5hmC conversion was shown to take place (Wossidlo et al., 2011). Due to this reason, it was also hard to evaluate the effect of S10A mutation on H3S10phos in mouse zygotes.



Results

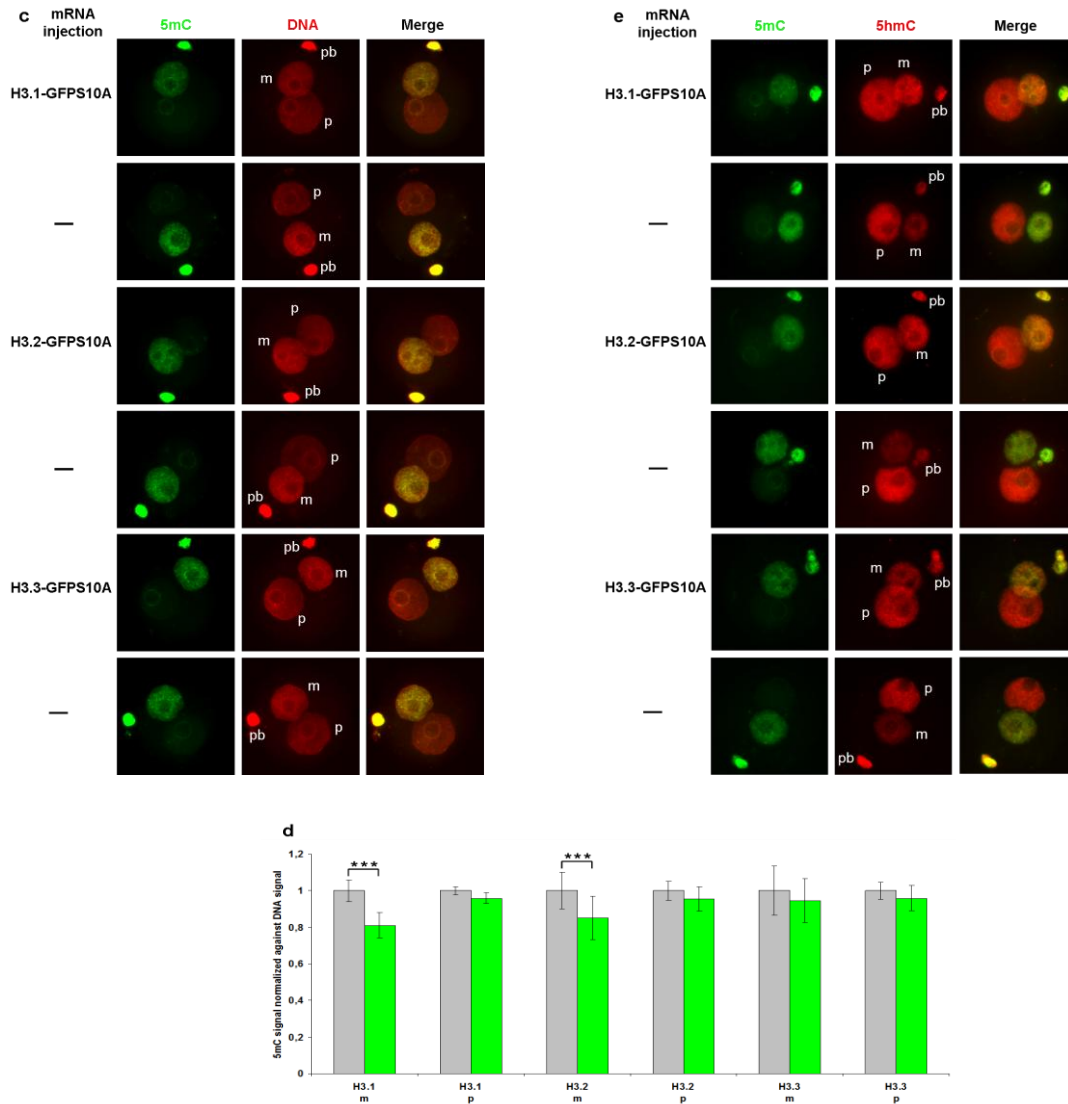


Fig. 3.15 Influences on H3K9me2, 5mC and 5hmC in zygotes expressing H3.1/2/3-GFPS10A. **a, c, e,** Representative images of PN4/5 stage zygotes zygotes stained with antibodies against H3K9me2, 5mC and 5hmC, respectively. H3K9me2, red; Dapi, blue; 5mC, green; DNA, red; 5hmC, red; m, the maternal pronucleus; p, the paternal pronucleus; pb, polar body. **b, d,** Quantification of H3K9me2 and 5mC signals normalized against Dapi and DNA signals in both parental genomes of zygotes at PN4/5, respectively. Non-injected groups, grey; H3.1/2/3-GFPS10A injected groups, green; The quantified values in control group were set to 1. Asterisks showed significant changes using Student's t-tests ($*=P<0.05$, $***=P<0.001$). Error bars indicated s.d. For each group, at least 10 zygotes were analysed from at least two repeated experiments.

3.2.3 Effects of H3.1/2/3-GFP11A on H3T11phos, H3K9me2, 5mC and 5hmC

Next, we asked whether the appearance of H3T11phos during replication regulates the persistence of H3K9me2 on maternal chromosomes. First, to dissect the enrichment of threonine11 phosphorylation on all three histone variants, we therefore microinjected mRNAs encoding histone H3 variants (WT) or T11A mutations, respectively into early mouse zygotes. T11A mutation on H3.1 and H3.2 rather than on H3.3 resulted in dramatic loss in H3T11phos (Fig. 3.16a, b), suggesting that H3.1 and H3.2 but not H3.3 are the prime substrates for H3T11phos. Surprisingly, zygotes injected with H3.1-GFPWT and H3.2-

Results

GFPWT isoforms exhibited a variable but reproducible reduction in H3T11phos (Fig. 3.17a, b). This variable effect might be due to an altered abundance of free nuclear or cytoplasmic H3.1-GFPWT and H3.2-GFPWT that act as free substrates for H3T11 kinases, further impairing the H3T11phos antibody binding to the epitopes on the nucleosomes incorporated histones. To test this possibility, Triton treatment was introduced before fixation in immunostaining, which, theoretically, could wash away the same amount of free histones between groups from the zygotes. However, H3.1-GFPWT and H3.2-GFPWT injected groups still displayed higher background than other groups (Fig. 3.17c, d), which could be regarded as an artifact because of the existence of the zona pellucida (ZP). For this reason, it is hard to confirm because the Triton treatment can not be applied to zygotes without ZP. In zygotes injected with H3.3-GFPWT, in contrast, H3T11phos signals remained unchanged compared to non-injected controls (Fig. 3.17e), suggesting that H3T11phos is not linked to H3.3 competition or incorporation into the chromatin.

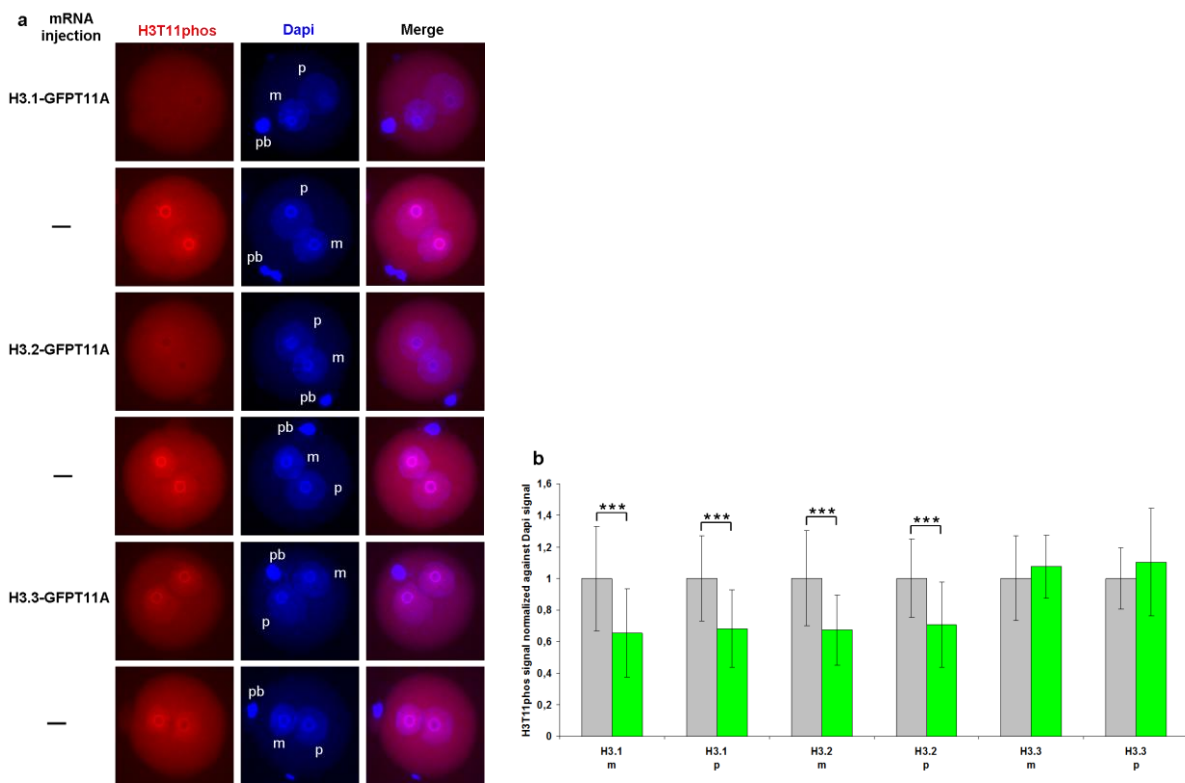


Fig. 3.16. Influences on H3T11phos in zygotes expressing H3.1/2/3-GFP11A. **a**, Representative images of PN4/5 stage zygotes stained with antibodies against H3T11phos. H3T11phos, red; Dapi, blue. m, the maternal pronucleus; p, the paternal pronucleus; pb, polar body. **b**, Quantification of H3T11phos signal normalized against Dapi signal in both parental genomes of zygotes at PN4/5. Non-injected groups, grey; injected groups, green. The quantified values in control group were set to 1. Asterisks showed significant changes using Student's t-tests (***)= $P < 0.001$). Error bars indicated s.d.. For each group, at least 10 zygotes were analysed from at least two repeated experiments.

Results

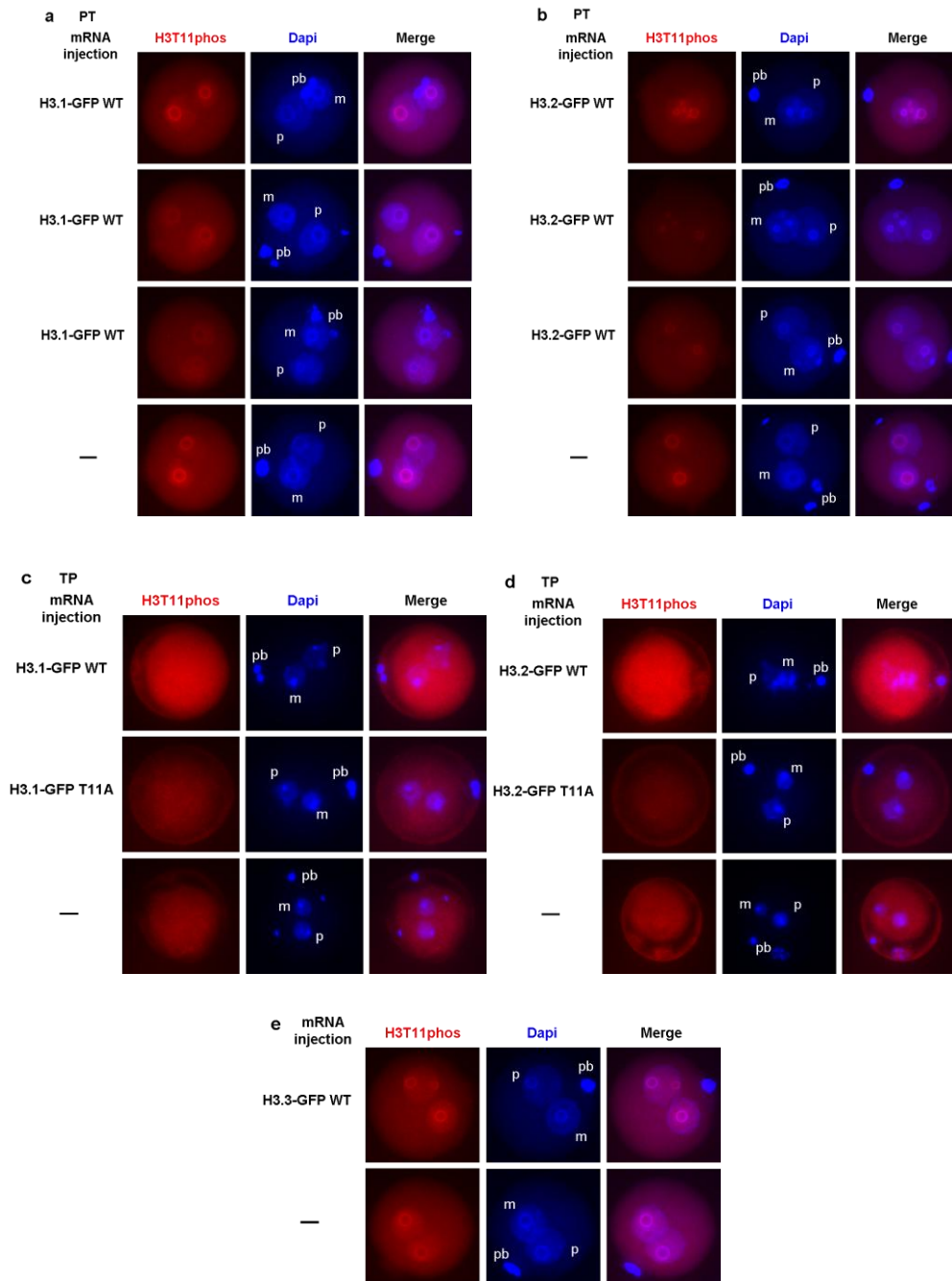


Fig. 3.17 Influences on H3T11phos in zygotes expressing H3.1/2/3-GFPWT. **a, b, e,** Representative images of PN4/5 stage zygotes stained with antibodies against H3T11phos under PT condition. **c, d,** Representative images of PN4/5 stage zygotes stained with antibodies against H3T11phos under TP condition. H3T11phos, red; Dapi, blue. m, the maternal pronucleus; p, the paternal pronucleus; pb, polar body. For each group, at least 10 zygotes were analysed from at least two repeated experiments.

Next we analysed the effect of H3.1/2/3-GFPT11A overexpression on H3K9me2. We indeed observed a very strong and highly significant reduction of H3K9me2 in H3.1-GFPT11A and H3.2-GFPT11A injected zygotes, but in not H3.3-GFPT11A, in comparison to the non-injected controls (Fig. 3.18a, b).

Results

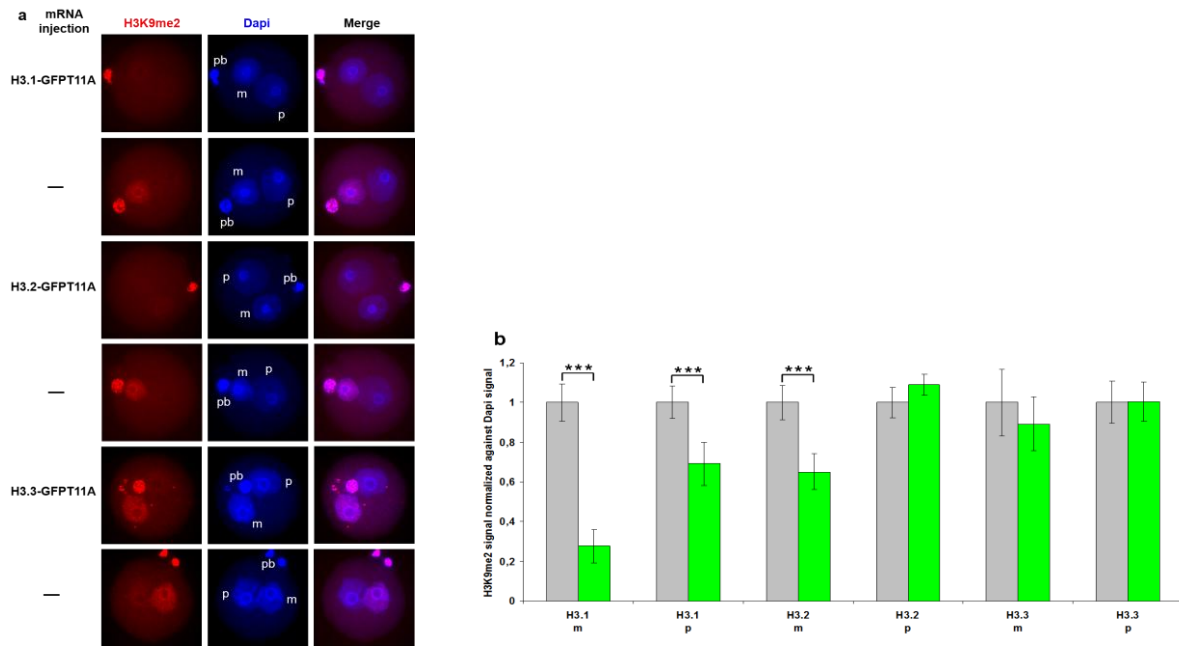


Fig. 3.18 Influences on H3K9me2 in zygotes expressing H3.1/2/3-GFPT11A. **a**, Representative images of PN4/5 stage zygotes stained with antibodies against H3K9me2. H3K9me2, red; Dapi, blue. m, the maternal pronucleus; p, the paternal pronucleus; pb, polar body. **b**, Quantification of H3Kme2 signal normalized against Dapi signal in both parental genomes of zygotes at PN4/5. Non-injected groups, grey; injected groups, green; The quantified values in control group were set to 1. Asterisks showed significant changes using Student's t-tests (***)= $P < 0.001$). Error bars indicated s.d.. For each group, at least 10 zygotes were analysed from at least two repeated experiments.

A possible explanation for this effect is that the T11A mutation influences the methylation and/or binding of anti-H3K9me2 antibody to its epitopes. To exclude the latter possibility, we therefore co-expressed H3.1-GFPT11A or H3.1-GFP together with the catalytical domain of G9a histone methyltransferase (G9aCat) in E.coli cells. The partially purified wild-type or mutated histones were probed by Western blot using the same anti-H3K9me2 antibody in IF immunostaining. As demonstrated on Supplementary Fig 4, the antibody clearly detects H3K9me2 on T11A mutated form (Fig. 3.19a, b).

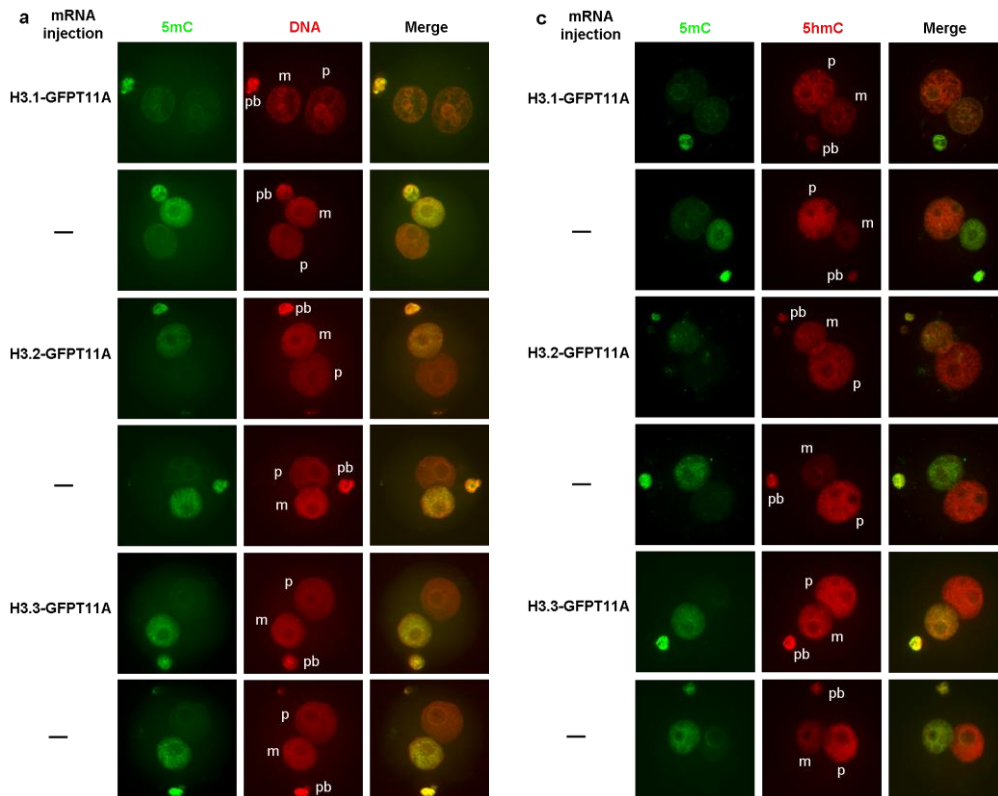


Fig. 3.19 The effect of H3T11A mutation on H3K9me2 recognition by the specific antibody, used in this study, verified by Western blotting. **a**, Verification of expression of the recombinant histones by using antibody against histone H3. **b**, Verification of H3K9me2 presence on H3.1-GFPWT and T11A proteins. Lane 1, expression of H3.1-GFPWT alone as a negative control; Lane 2, coexpression of H3.1-GFPWT and G9aCat as a positive control; Lane3, coexpression of H3.1-GFPT11A and G9aCat; Lane 4, marker.

Then we further detected the changes in 5mC and 5hmC, because H3K9me2 could serve as a protector against oxidation of 5mC to 5hmC in mouse zygotes according to the published data (Nakamura et al., 2012). Concomitant with the changes in H3K9me2 also DNA methylation (5mC) was strongly altered in the maternal pronuclei of H3.1/H3.2-GFPT11A expressing

Results

zygotes (Fig. 3.20a and b). Correspondingly 5hmC signals were strongly enhanced in both H3.1-GFPT11A and H3.2-GFPT11A expressing groups compared to the controls (Fig. 3.20c). To our surprise, 5hmC signal was slightly decreased in the paternal pronuclei of either H3.1-GFPT11A or H3.2-GFPT11A expressing zygotes, although 5mC and 5caC signals were comparable to those in the control group (Fig. 3.20a, b, c and d). Again despite of no significant change of 5mC in H3.3-GFPT11A injected zygotes, we observed an obvious increase of 5hmC in both parental genomes in H3.3-GFPT11A (and in the H3.3GFP1S10A) injected group not coupled to a significant reduction of 5mC (Fig. 3.20c). The mechanism responsible for the observed 5hmC fluctuation remains to be investigated in the future. Next we examined potential changes in DNA methylation by hairpin-bisulfite high-throughput sequencing of LINE1 repetitive elements. We only found a very minor reduction of fully methylated sites (CpG sites, methylated on both complementary DNA strands) in H3.1-GFPT11A injected group compared to H3.1-GFPWT injected and non-injected groups (Fig. 3.21). This indirectly supports the conclusion that most 5mC is converted to 5hmC – and both modifications are indistinguishable in bisulfite sequencing (Huang et al., 2010). However, we observed a significant increase in hemimethylated sites in the H3.1-GFPT11A expressing group (Fig. 3.21), suggesting that the increased level of 5hmC apparently affects the DNA methylation maintenance during replication. In summary, the introduction of mutated histone variants H3.1 and 3.2 at threonine 11 and, to minor extent at serine 10, has a strong influence on the presence of H3K9me2 in the maternal pronucleus and enhances the oxidation of 5mC to 5hmC. In contrast, the overrepresentation of H3.1T11A or H3.2-GFPT11A causes a partial loss of 5hmC in the paternal genome.



Results

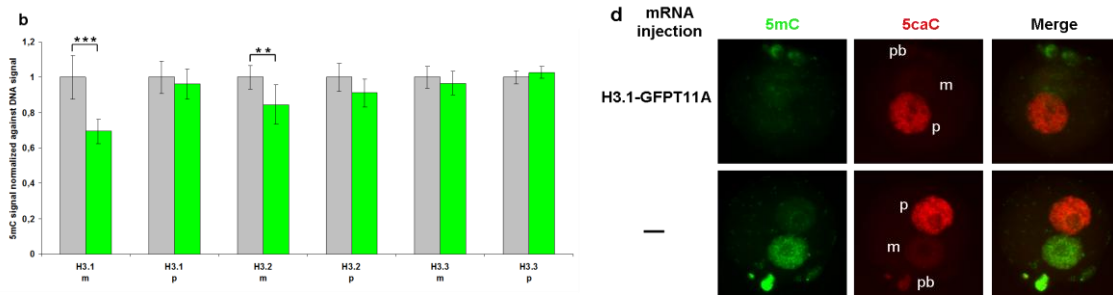


Fig. 3.20 Influences on 5mC, 5hmC and 5caC in zygotes expressing H3.1/2/3-GFP11A. **a**, Representative images of PN4/5 stage zygotes stained with antibodies against 5mC and DNA. 5mC, green; DNA, red. **b**, Quantification of 5mC signal normalized against DNA signal in both parental genomes of zygotes at PN4/5. Non-injected groups, grey; injected groups, green; The quantified values in control group were set to 1. Asterisks showed significant changes using Student's t-tests (**= $P < 0.01$, ***= $P < 0.001$). Error bars indicated s.d.. **c**, Representative images of PN4/5 stage zygotes stained with antibodies against 5hmC and 5mC. 5hmC, red; 5mC, green; **d**, Representative images of PN4/5 stage zygotes stained with antibodies against 5caC and 5mC. 5caC, red; 5mC, green. m, the maternal pronucleus; p, the paternal pronucleus; pb, polar body. For each group, at least 10 zygotes were analysed from at least two repeated experiments.

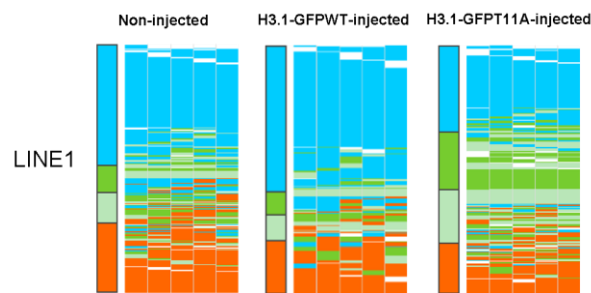


Fig. 3.21 Methylation patterns of LINE1 repetitive element in non-injected, H3.1-GFPWT injected and H3.1-GFP11A injected groups. The bars represented the DNA methylation status of all CpG dyads. The maps beside the bars showed the distribution of methylated sites. Columns and lines stand for CpG sites and sequence reads, respectively. Red, fully methylated CpG dyads; light green and dark green, hemi-mCpG dyads on the upper and lower strand; blue, unmethylated CpG dyads; white, mutated or not analysable.

3.3 Introduction of H3K9me2 into the paternal chromatin of mouse zygotes by G9aFL-GFP and G9aCat-NLS-GFP

It was demonstrated that H3K9me2 contributes to maintenance of 5mC in the maternal genome as well as at some loci in the paternal one (Nakamura et al., 2012) and that H3K9me2 has an asymmetrical distribution pattern in parental genomes, being much more abundant in the maternal pronucleus and nearly undetectable in the paternal one (Lepikhov and Walter, 2004; Liu et al., 2004; Santos et al., 2005). Currently, the absence of H3K9me2 in the paternal chromatin is viewed as a main reason for the dominant occurrence of DNA demethylation of the paternal genome in mouse zygotes. Here, we investigated that whether the discrepancy in DNA methylation is really caused by the asymmetry of H3K9me2 between the parental genomes or not. Furthermore, we evaluated the contribution of H3 variants to the DNA methylation reprogramming.

3.3.1 Effects on H3K9me2

Results

To challenge this assumption and to boost H3K9me2 in mouse zygotes artificially, G9a (also known as EHMT2), an H3K9me2-specific histone methyltransferase, was considered as a promising candidate to be employed. First, we examined the distribution of endogenous G9a by immunostaining, which showed that G9a was totally absent from the pronuclei in the zygotic stage, seemed to be rather sparsely distributed in the nuclei in the 2-cell stage and began to accumulate in the nucleus from 4-cell stage on (Fig. 3.22), in agreement with the published data (Li et al., 2013).

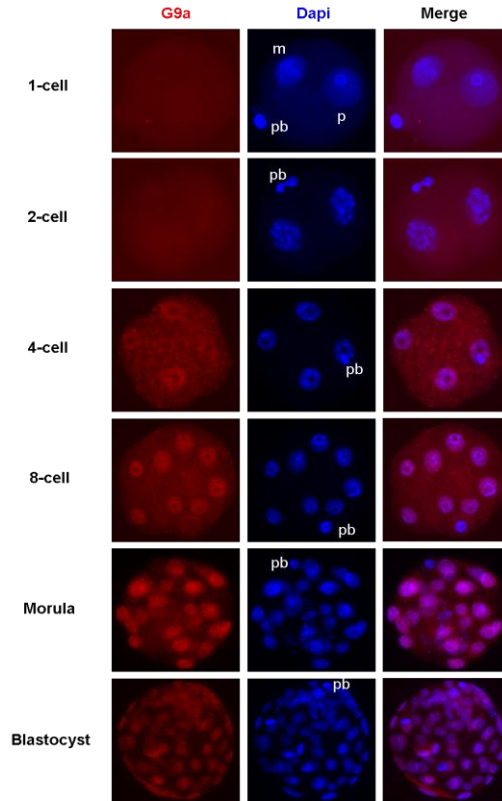


Fig. 3.22 Dynamic patterns of G9a during mouse preimplantation development. Representative images of different staged embryos stained with antibodies against G9a. G9a, red; Dapi, blue; m, the maternal pronucleus; p, the paternal pronucleus; pb, polar body. For each group, at least 10 zygotes were analysed from at least two repeated experiments.

Then we ectopically expressed G9a in early mouse zygotes (around 1 hpf). When expressing a full length GFP tagged G9a version (G9aFL-GFP) we only found a minor effect on H3K9me2 (Fig. 3.23). The N-terminus of G9A apparently interferes with its function in the zygote - a finding that is in agreement with the observation that the oocyte triggers a mechanism suppressing G9a function (Liu et al., 2004). The injection of a shorter G9aCat-NLS-GFP version (G9a catalytical domain fused with NLS of SV40 and GFP) overcame these restrictions and efficiently enhanced the H3K9me2 (Fig. 3.23). Meanwhile, H3K9me3 was also evaluated in order to confirm the specificity of G9a (Fig. 3.24). It is noteworthy that the observed effects were also strictly associated with time point of microinjection (the injection should take place within 1.5hpf).

Results

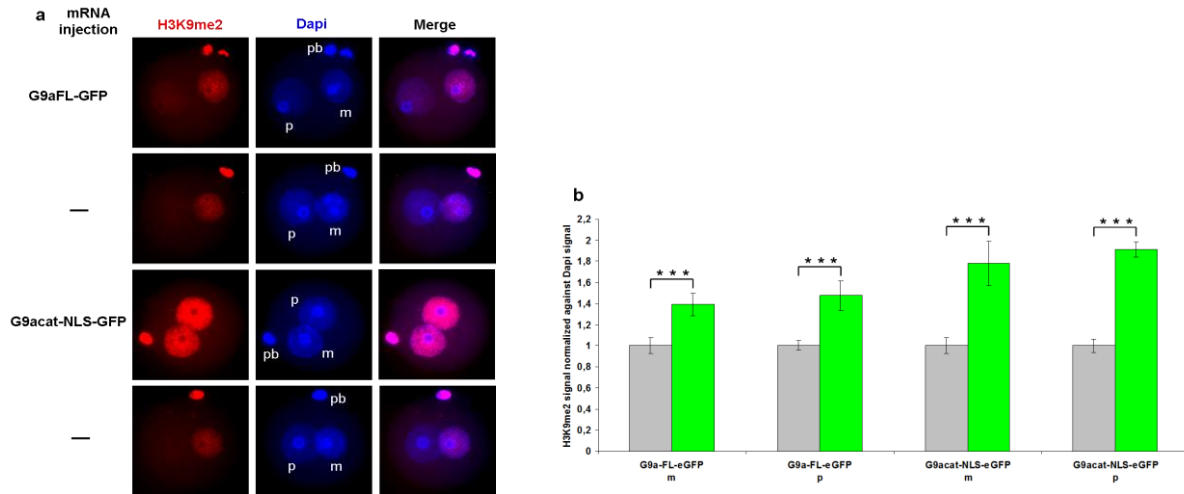


Fig. 3.23 Introduction of H3K9me2 into both genomes of mouse zygotes by ectopically expressed G9aFL-GFP and G9aCat-NLS-GFP. **a**, Representative images of PN4/5 stage zygotes stained with antibodies against H3K9me2. H3K9me2, red; Dapi, blue. m, the maternal pronucleus; p, the paternal pronucleus; pb, polar body. **b**, Quantification of H3Kme2 signal normalized against Dapi signal in both parental genomes of zygotes at PN4/5. Non-injected groups, grey; injected groups, green; The quantified values in control group were set to 1. Asterisks showed significant changes using Student's t-tests (***=P<0.001). Error bars indicated s.d.. For each group, at least 10 zygotes were analysed from at least two repeated experiments.

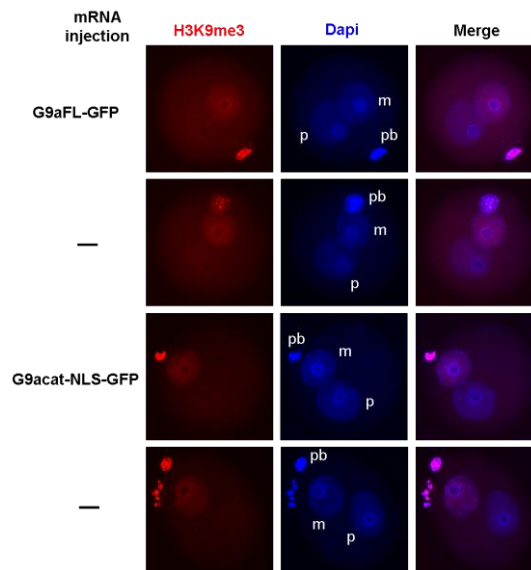


Fig. 3.24 No influences on H3K9me3 in mouse zygotes expressing G9aFL-GFP and G9aCat-NLS-GFP. Representative images of PN4/5 stage zygotes stained with antibodies against H3K9me3. H3K9me3, red; Dapi, blue. m, the maternal pronucleus; p, the paternal pronucleus; pb, polar body. For each group, at least 10 zygotes were analysed from at least two repeated experiments.

3.3.2 Effects on 5mC and 5hmC

Since a dramatic increase of H3K9me2 appeared in both pronuclei of mouse zygotes expressing G9aCat-NLS-GFP, we further checked the changes in 5mC and 5hmC by immunostaining. Very surprisingly, the signal intensities of 5mC and 5hmC were comparable in both parental genomes between injected and noninjected groups (Fig. 3.25a, c), suggesting

Results

that artificial introduction of H3K9me2 failed to block active DNA demethylation (5mC to 5hmC conversion) in the paternal genome on a global scale. However, through quantification, a minor but significant increase of 5mC was found in both parental genomes of mouse zygotes expressing G9aCat-NLS-GFP (Fig. 3.25b), indicating that a small amount of 5mC was indeed protected from being oxidated by the acquisition of H3K9me2. In contrast, in G9aFL-GFP injected zygotes, only rather small amount of 5mC was rescued after introduction of H3K9me2 in the paternal genome (Fig. 3.25b). Notably, this small fraction of 5mC rescued by the reacquisition of H3K9me2 in both parental genomes on one hand confirmed the protection role of H3K9me2 in 5mC and, on the other hand, may reflect the passive dilution mechanism in which the replication-dependent loss of H3K9me2 could lead to the exposure of 5mC to Tet3 dioxygenase.

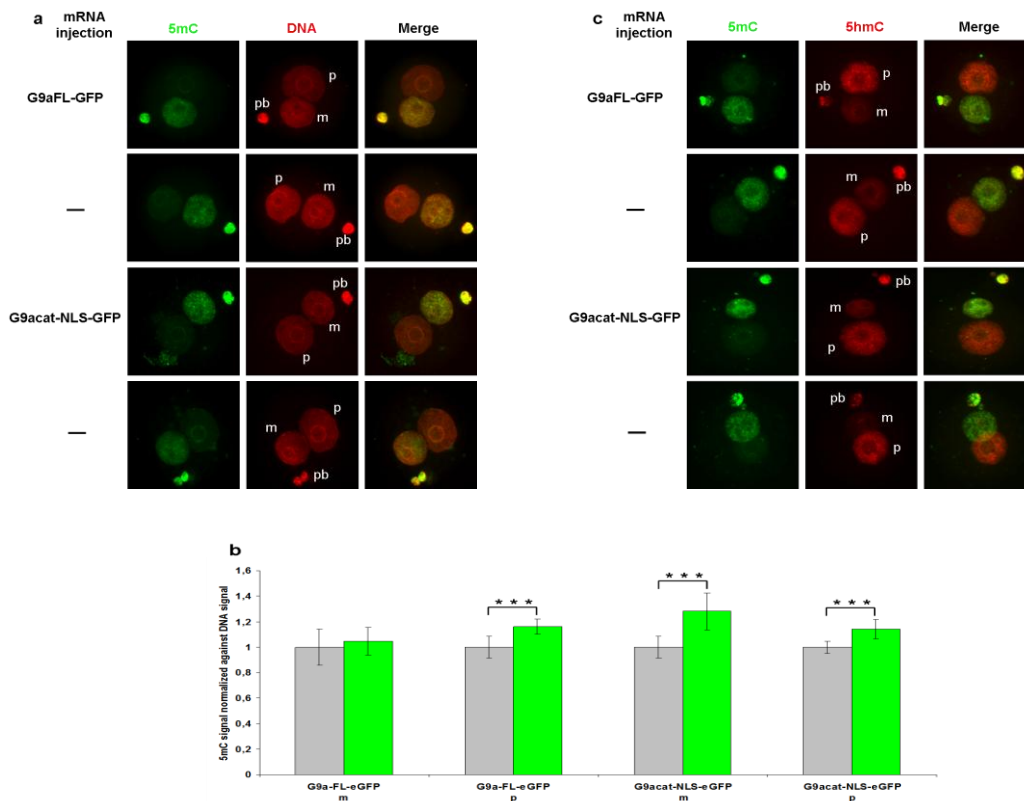


Fig. 3.25 Influences of G9aFL-GFP and G9aCat-NLS-GFP expression in zygotes on 5mC and 5hmC. a, Representative images of PN4/5 stage zygotes stained with antibodies against 5mC and DNA. 5mC, green; DNA, red. **b,** Quantification of 5mC signal normalized against DNA signal in both parental genomes of zygotes at PN4/5. Non-injected groups, grey; injected groups, green; The quantified values in control group were set to 1. Asterisks showed significant changes using Student's t-tests (***=P<0.001). Error bars indicated s.d.. **c,** Representative images of PN4/5 stage zygotes stained with antibodies against 5mC and 5hmC. 5mC, green; 5hmC, red. m, the paternal pronuclei; p, the paternal pronuclei; pb, polar body. For each group, at least 10 zygotes were analysed from at least two repeated experiments.

Subsequently, the methylation levels on three repetitive elements, including long interspersed elements (LINE1), intracisternal A-particle element (IAP) and major satellites (mSat) were evaluated in G9aCat-NLS-GFP injected zygotes by the hairpin bisulfite sequencing. As a result, the methylation heatmaps displayed the similar patterns between groups (Fig. 3.26),

Results

further confirming the immunostaining results that active DNA demethylation was not globally affected given the fact that these three repetitive elements have a rather broad distribution across the whole genome.

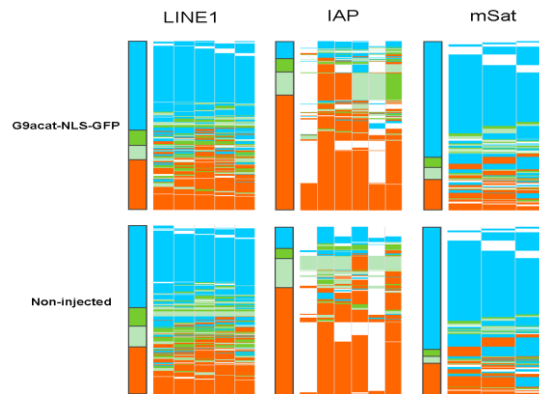


Fig. 3.26 Methylation patterns of repetitive elements in G9aCat-NLS-GFP injected and non-injected groups. The bars represented the DNA methylation status of all CpG dyads. The maps beside the bars showed the distribution of methylated sites. Column and line stood for CpG sites and sequence read, respectively. Red, fully methylated CpG dyads; light green and dark green, hemi-mCpG dyads on the upper and lower strand; blue, unmethylated CpG dyads; white, mutated or not analysable.

3.4 Dissecting relations between H3K9me2 and histone H3.1/2/3 by co-injection of G9aCat-NLS-GFP and H3.1/2/3-GFPT11A

The failure to arrest oxidation of 5mC to 5hmC in the paternal genome on a global level by introduction of H3K9me2 strongly indicates the differences in chromatin structure and DNA methylation distribution between male and female pronuclei. One explanation could be that the regions artificially covered with H3K9me2 by G9aCat-NLS-GFP are rather sparsely enriched with 5mC. Hence, it is necessary to address the question that which histone H3 variants could be linked to the 5mC-poor regions in the paternal genome of mouse zygotes, which will help us to locate the main player (H3.3?) related to the active DNA demethylation by excluding the unrelated ones (H3.1 and/or H3.2?). So far, we have already demonstrated that T11A mutation on H3.1 and H3.2, but not on H3.3, abolished H3K9me2 in the maternal genome of mouse zygotes. In addition, it must be mentioned that G9a could target and methylate the histone H3 as a substrate even including T11A mutant form, which has been demonstrated by *in vitro* assay (Chin et al., 2005) and our Western blotting results (Fig. 3.19). Therefore, by taking advantage of this protection mechanism that T11A mutation could negatively interfere with H3K9me2-specific methylation activity, we performed coinjection of G9aCat-NLS-GFP and H3.1-GFPT11A or H3.2-GFPT11A or H3.3-GFPT11A, which makes it possible to uncover the potential links between histone variants, H3K9me2 and 5mC.

3.4.1 Effects on H3K9me2

As a result, H3K9me2 dramatically decreased in both pronuclei by co-injection of G9aCat-NLS-GFP either with H3.1-GFPT11A or with H3.2-GFPT11A. At the same time, the dramatic enhancement of H3K9me2 in both pronuclei, caused by G9aCat-NLS-GFP (Fig. 3.27a, b), was not affected by H3.3-GFPT11A co-expression (Fig. 3.27a, b). The signal intensity was similar to that in zygotes expressing G9aCat-NLS-GFP alone (Fig. 3.23a, b).

Results

This result clearly indicates that H3.1 and H3.2, but not H3.3, served as the substrates for G9aCat-NLS-GFP. Therefore, H3.1 and H3.2, which lose K9me2 during replication, are involved in passive DNA demethylation in both parental genomes. Also indirectly, it implies that H3.3 could be a promising player linked to global active DNA demethylation in mouse zygotes.

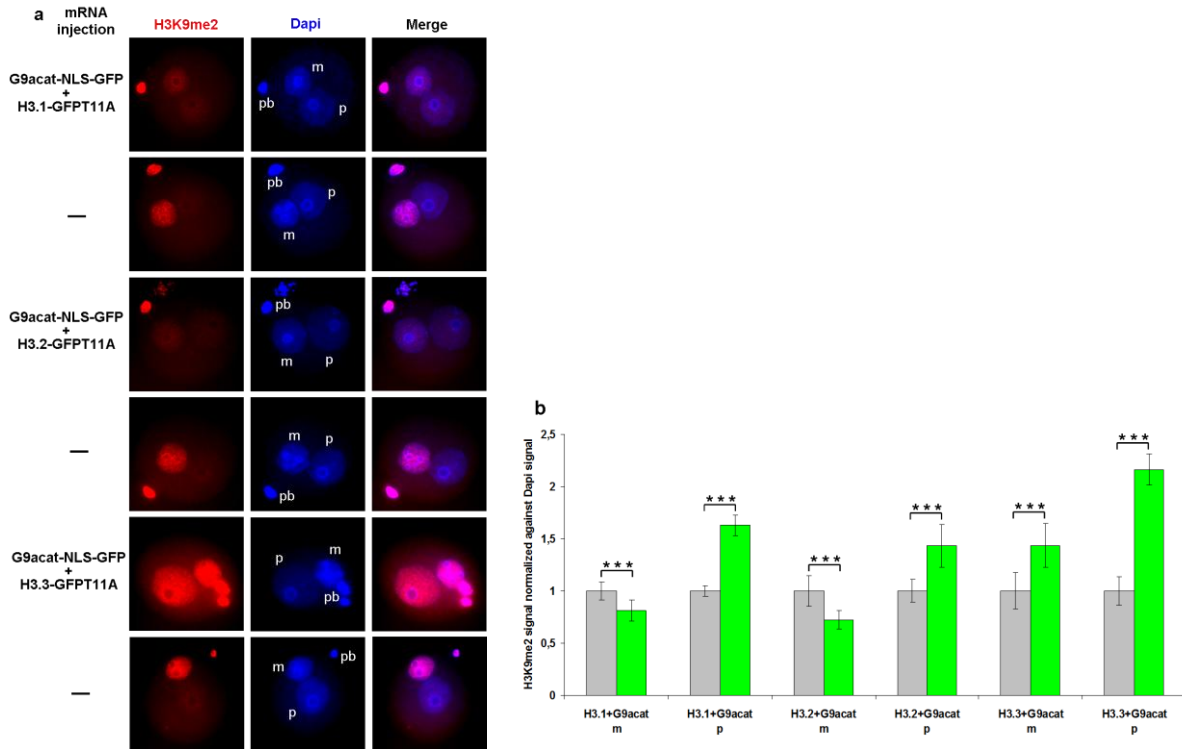


Fig. 3.27 Ablation of H3K9me2 by co-injection of G9aCat-NLS-GFP with H3.1-GFP11A or H3.2-GFP11A, respectively. **a**, Representative images of PN4/5 stage zygotes stained with antibodies against H3K9me2. H3K9me2, red; Dapi, blue. m, the maternal pronucleus; p, the paternal pronucleus; pb, polar body. **b**, Quantification of H3K9me2 signal normalized against Dapi signal in both parental genomes of zygotes at PN4/5. Non-injected groups, grey; injected groups, green; The quantified values in control group were set to 1. Asterisks showed significant changes using Student's t-tests (***=P<0.001). Error bars indicated s.d.. For each group, at least 10 zygotes were analysed from at least two repeated experiments.

3.5 Microinjection of H3.3-GFPK9me2 proteins

As shown above, H3.1 and H3.2 were not responsible for the major loss of DNA methylation in the paternal genome of mouse zygotes, this prompted us to verify the hypothesis that H3.3 would be a potential major player involving in global active DNA demethylation, as suggested by many groups based on the fact that H3.3 is preferentially located in male pronucleus before and during DNA replication (Torres-Padilla et al., 2006; van der Heijden et al., 2005; Wu and Zhang, 2010).

3.5.1 Localization of purified proteins of H3.3-GFPK9me2

To test this hypothesis, we decided to microinject the premodified H3.3-GFPK9me2 proteins into early mouse zygotes, which may have the chance to block the active DNA demethylation pathway to some degree. First, we coexpressed G9aCat and H3.3-GFP or expressed H3.3-

Results

GFP just alone in Rosetta™ 2 E.coli cells. Western blot analysis of thus produced recombinant histone H3.3-GFP protein has shown, that dimethylation but not trimethylation was successfully introduced onto K9 residue (Fig. 3.28a, b, c).

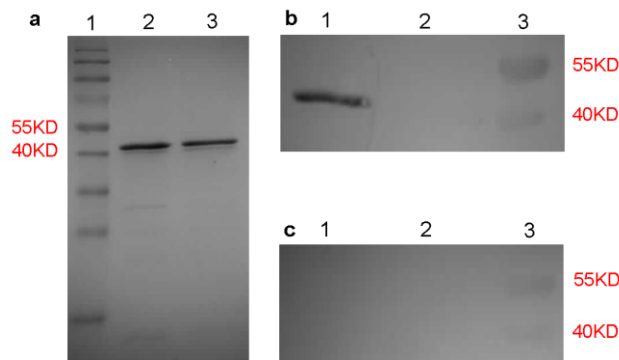


Fig. 3.28 Western blotting detection of H3.3-GFPK9me2 (modified) and H3.3-GFP (unmodified) proteins after purification. **a**, Verification of purification of H3.3-GFPK9me2 and H3.3-GFP by using antibody against GFP. Lane1, marker; lane 2, H3.3-GFPK9me2 protein; lane 3, H3.3-GFP protein. **b**, **c**, Verification of dimethylation and trimethylation at lysine 9 of H3.3-GFP and H3.3-GFP by using antibodies against H3K9me2 and H3K9me3, respectively. Lane1, H3.3-GFPK9me2 protein; marker; lane 2, H3.3-GFP protein; lane 3, marker.

Then, protein purification was performed, which was followed by dialysis. In the end, modified H3.3-GFPK9me2 and unmodified proteins were microinjected into very early zygotes (around 1-1.5hpf), respectively. Surprisingly, H3.3-GFPK9me2 protein failed to enter into both pronuclei compared to H3.3-GFPWT (Fig. 3.29), indicating that the site K9 may be very crucial for nuclear trafficking of histone H3.3 or that at least dimethylation on K9 should be avoided before deposition into the chromatin, which was to some extent in line with the published data that K9 of histone H3 is essential for histone incorporation across some species (Kuo et al., 1996; Sobel et al., 1995; Turner and O'Neill, 1995). It is noteworthy that this view was also supported by our H3.1/2/3-GFPK9R mutation data that none of the histone H3 variants could affect H3K9ac level in both pronuclei (Fig. 3.11 and 3.12), although H3K9ac exhibited a dramatic increase through replication in mouse zygotic stage (Fig. 3.3). Additionally, due to its inability to deposit into the chromatin, H3.3-GFPK9me2 protein seemed to be cleared away via degradation, because the GFP signal vanished in a few hours after microinjection. Therefore, practically, it is not feasible to impede global active DNA demethylation by microinjection of premodified H3.3-GFPK9me2 protein.

Results

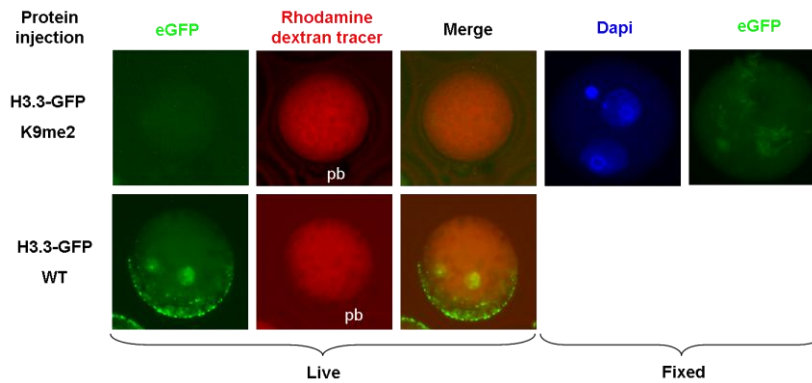


Fig. 3.29 Localization of H3.3-GFPK9me2 and WT proteins. H3.3-GFPWT showed a clear nuclear localization by GFP signals. As for the H3.3-GFPK9me2 protein, it failed to enter both pronuclei and showed gradual degradation in the cytoplasm. And fertilization was verified by Dapi staining in the H3.3-GFPK9me2 injected group. GFP, green; Rhodamine dextran tracer, red. Dapi, blue. For each group, at least 10 zygotes were analysed from at least two repeated experiments.

3.6 Relation between H3K9ac and DNA methylation

As an active transcription marker, H3.3 is claimed to be highly correlated with H3K9ac across the species (Ahmad and Henikoff, 2002; Loyola and Almouzni, 2007). Meanwhile, given the potential critical role of preacetylation at K9 in histone H3.3 for the deposition into the chromatin, we speculate that, the failure of G9aCat-NLS-GFP to modify H3.3 was due to the pre-occupancy of K9 residue with acetyl group. Indeed, our result showed that H3K9ac was not altered by the ectopic expression of G9aCat-NLS-GFP (Supplementary Fig. 6). In that case, removal of acetyl group from K9 on H3.3 seems to be a necessary step for creating an ideal substrate for G9aCat-NLS-GFP in mouse zygotes.

3.6.1 Effect on DNA methylation by loss of H3K9ac

Before introducing a dimethyl group to K9 site on H3.3, we first performed the evaluation on the DNA methylation changes by abolishing H3K9ac. By microinjection of mRNAs, encoding histone deacetylases HDAC1-GFP and/or HDAC2-GFP into early zygotes, we successfully released acetyl groups from K9 sites of histone H3. As shown in Fig. 3.30, a great loss of H3K9ac was observed in injected groups compared to non-injected ones. The efficiencies between HDAC1-GFP, HDAC2-GFP and combination of these two were rather similar (Fig. 3.30). Moreover, the decrease of H3K9ac by HDAC1-GFP did not cause any increase of K9me2 (Fig. 3.31d). This finding supports the notion that indeed H3.3 is the main target of H3K9ac. Furthermore, we examined the changes in 5mC as well as 5hmC in HDAC1-GFP injected zygotes. Nevertheless, the dramatic reduction in H3K9ac was not accompanied with any changes in 5mC as well as 5hmC (Fig. 3.31a, b, c), suggesting that H3K9ac was not required for global active DNA demethylation in the paternal genome of mouse zygotes.

Results

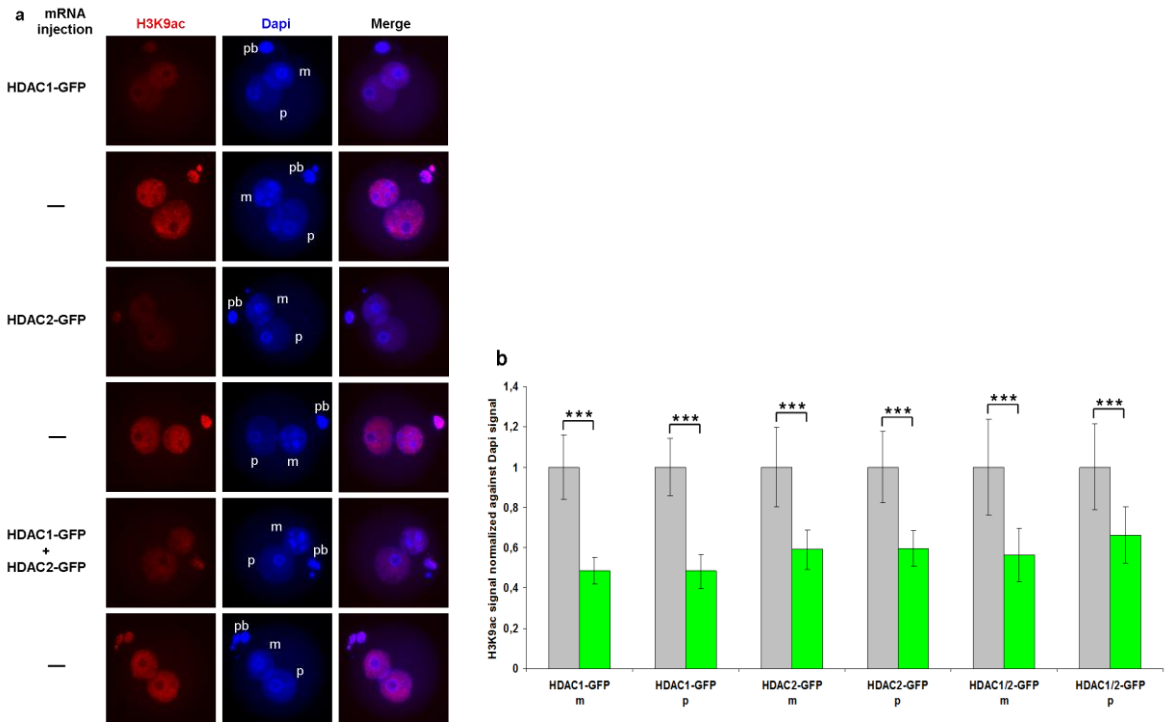


Fig. 3.30 Influences on H3K9ac in zygotes expressing HDAC1-GFP, HDAC2-GFP and their combination, respectively. **a**, Representative images of PN4/5 stage zygotes stained with antibodies against H3K9ac. H3K9ac, red; Dapi, blue; m, the maternal pronucleus; p, the paternal pronucleus; pb, polar body. **b**, Quantification of H3K9ac signal normalized against Dapi in both parental genomes of zygotes at PN4/5. Non-injected groups, grey; HDACs-GFP injected groups, green; The quantified values in control group were set to 1. Asterisks showed significant changes using Student's t-tests (***) ($P < 0.001$). Error bars indicated s.d.. For each group, at least 10 zygotes were analysed from at least two repeated experiments.

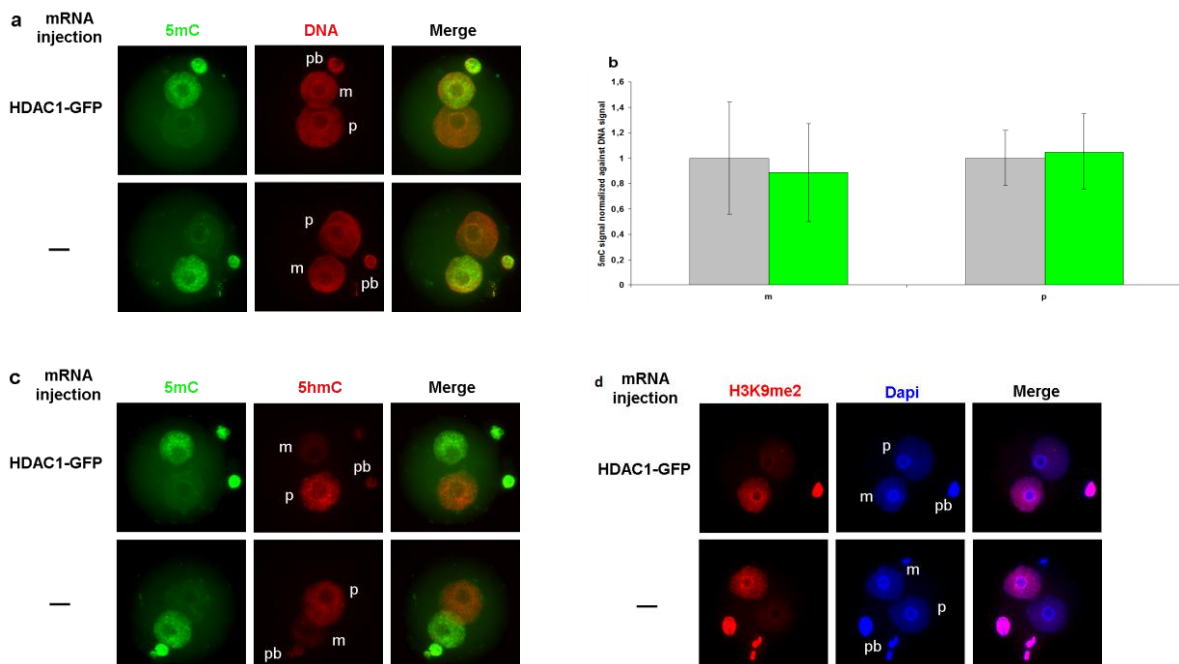


Fig. 3.31 Influences on 5mC and 5hmC in zygotes expressing HDAC1-GFP. **a**, Representative images of PN4/5 stage zygotes stained with antibodies against 5mC and DNA. 5mC, green; DNA, red; **b**, Quantification of

Results

5mC signal normalized against DNA signal in both parental genomes of zygotes at PN4/5. Non-injected group, grey; HDAC1-GFP injected group, green; The quantified values in control group were set to 1. Asterisks showed significant changes using Student's t-tests (***)= $P < 0.001$). Error bars indicated s.d.. **c**, Representative images of PN4/5 stage zygotes stained with antibodies against 5hmC and 5mC. 5hmC, red; 5mC, green. **d**, Representative images of PN4/5 stage zygotes stained with antibodies against H3K9me2. H3K9me2, red; Dapi, blue. m, the maternal pronucleus; p, the paternal pronucleus; pb, polar body. For each group, at least 10 zygotes were analysed from at least two repeated experiments.

3.6.2 Effect on H3K9me2 by co-injection of G9aCat-NLS-GFP and HDAC1-GFP

The efficient removal of H3K9ac by HDAC1-GFP means that more vacant K9 sites could appear across the chromatin and serve as the substrates for G9aCat-NLS-GFP. Based on this, subsequently, we performed the co-injection of G9aCat-NLS-GFP and HDAC1-GFP in order to modify the free K9 sites into the dimethylation form. Theoretically, more H3K9me2 signal would emerge in co-injected zygotes. However, unfortunately, the immunostaining showed rather comparable signal intensities of H3K9me2 between co-injected zygotes and G9aCat-NLS-GFP alone injected ones (Fig. 3.32), indicating that dimethyl groups were not successfully transferred to the deacetylated K9 sites.

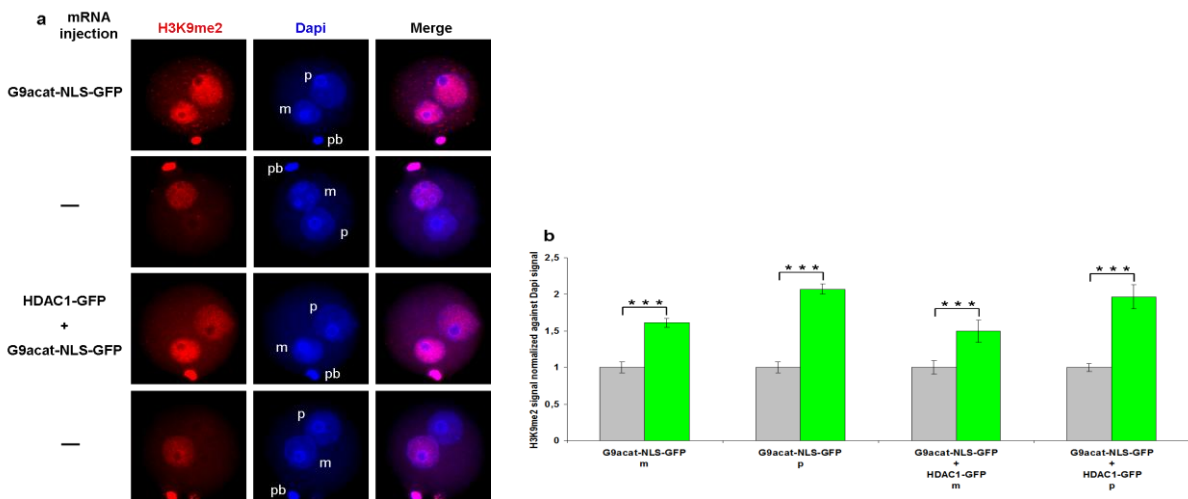


Fig. 3.32 Influences on H3K9me2 in zygotes expressing both HDAC1-GFP and G9aCat-NLS-GFP. a, Representative images of PN4/5 stage zygotes stained with antibodies against H3K9me2. H3K9me2, red; Dapi, blue. m, the maternal pronucleus; p, the paternal pronucleus; pb, polar body. **b**, Quantification of H3Kme2 signal normalized against Dapi signal in both parental genomes of zygotes at PN4/5. Non-injected groups, grey; injected groups, green; The quantified values in control group were set to 1. Asterisks showed significant changes using Student's t-tests (***)= $P < 0.001$). Error bars indicated s.d.. For each group, at least 10 zygotes were analysed from at least two repeated experiments.

4 Discussion

In mouse zygotes, reprogramming is triggered upon the fusion of oocyte and sperm, which is characterized by chromatin reorganization and DNA demethylation (Burton and Torres-Padilla, 2014; Reik et al., 2001; Wu and Zhang, 2010). Traditionally, on one hand, it has been viewed that DNA demethylation occurs only in the paternal genome in mouse based on immunofluorescence staining of 5mC (Mayer et al., 2000; Oswald et al., 2000), which is later proved to be a Tet3-related iterative oxidation to 5hmC, further to 5fC and 5caC (He et al., 2011; Inoue et al., 2011; Iqbal et al., 2011; Ito et al., 2011; Wossidlo et al., 2011). Most recently, it is clearly demonstrated on the molecular level that both the maternal and the paternal genomes undergo DNA demethylation in a combination manner of replication-dependent dilution and Tet3-based oxidation (Arand et al., 2015; Guo et al., 2014b; Shen et al., 2014). On the other hand, it is assumed that H3K9me2 could be the major player involving in maintenance of 5mC in the maternal genome, since it displays a rather dominant distribution in female pronucleus (Lepikhov and Walter, 2004; Liu et al., 2004; Santos et al., 2005) and a number of evidence demonstrates the interplay between H3K9me2 and 5mC across species (Bernatavichute et al., 2008; Jackson et al., 2004; Tamaru and Selker, 2001). Furthermore, recently Nakamura et al. have confirmed that H3K9me2, together with PGC7, indeed is responsible for preventing oxidation of 5mC in the maternal genome, as well as some loci in the paternal one (Nakamura et al., 2007; Nakamura et al., 2012). However, because of the existence of histone H3 variants, namely H3.1, H3.2 and H3.3 (Hake and Allis, 2006; Kamakaka and Biggins, 2005; Loyola and Almouzni, 2007), on each of which lysine 9 could be theoretically modified to be a dimethylated form, it is necessary to dissect the relation between H3K9me2 and histone H3 variants, which could further clarify the roles of histone H3 variants in embryonic reprogramming. According to the literature, H3K9me2 is regarded to be enriched on H3.1 or H3.2 but not H3.3 (Loyola and Almouzni, 2007), which raises the question that whether it is true in mouse zygotes and how the differences in H3K9me2 on histone H3 variants are caused or regulated. The exploration of this regulation pathway for H3K9me2 will definitely help us gain a better understanding of the distinctive chromatin structures and DNA methylation patterns between the maternal and the paternal pronuclei. Here, in this work, we show that it is primarily histone H3.1 and secondarily H3.2 that carry K9me2 to impede oxidation of 5mC into 5hmC in an H3T11phos dependent manner on a global level in the maternal genome of mouse zygotes. Furthermore, we reveal that H3.1 and H3.2, which are lack of H3K9me2 during replication, are responsible for the dilution-dependent passive DNA demethylation on a small scale in both parental genomes. Last but not least important, we conclude that H3.3 escapes from being dimethylated at K9 by the endogenous histone methyltransferases due to the presence of H3K9ac and the absence of H3T11phos, which ensures the proper occurrence of active DNA demethylation on a relatively global level in both male and female genomes of mouse zygotes. Taken together, the regulatory mechanism may also shed a light upon reprogramming in stem cells, induced pluripotent cells as well as somatic cell nuclear cloning.

4.1 Inefficient disruption in H3K9me2/me3/ac by H3.1/2/3-GFPK9R in both parental genomes of mouse zygotes

As early as 2004, Liu et al. have proposed a model that H3K9me2 and H3K9me3 are diluted in a replication-dependent manner during mouse zygotic stage (Liu et al., 2004), which is confirmed by our observation. However, our experiments by microinjection of H3.1/2/3-GFPK9R mRNAs demonstrate that it is not a simple dilution model but rather a complicated one involving remethylation activities for both H3K9me2 and H3K9me3, consistent with the previous data that *de novo* H3K9me2 has been detected in the paternal genome of mouse zygotes (Santos et al., 2005). As a specific histone methyltransferase for H3K9me2, G9a, could be a promising candidate for remethylation process. However, it is not the case in mouse zygote, because the application of Bix 01294 (a specific inhibitor against G9a) to mouse zygotes failed to bring about any changes in H3K9me2 (Supplementary Fig. 1), indicative of the presence of an active G9a suppressing mechanism, triggered by oocyte activation, which was proposed by Liu et al (Liu et al., 2004). Alternatively, it may be due to the absence of G9a in mouse zygotes, in line with our data and the published ones that G9a is undetectable on both protein and mRNA levels in mouse zygotic stage (Fig. 3.21) (Kageyama et al., 2007; Li et al., 2013). For the other potential histone methyltransferases involved in histone remethylation, Suv39h2, mainly responsible for H3K9me3, could be one of the players owing to the presence of its mRNA in mouse zygotes (Kageyama et al., 2007; Schuhmacher et al., 2015). Also indeed, when applying Chaetocin at a very low concentration in mouse zygotes, which is supposed to be specifically inhibit SU(VAR)3-9 (Greiner et al., 2005), we observe the severe changes in H3K9me3, reorganization of heterochromatin as well as nuclear topology (supplementary Fig. 2), in line with the published data (Zinner, 2007). How this dynamic turnover of demethylation (either active or passive) and remethylation at K9 on histone H3 variants is achieved and why remain to be investigated in the future.

Next, we dissect the distribution of H3K9me2 among histone H3 variants. All three histone H3-GFPK9R mutants cause slight decrease of H3K9me2 in the maternal pronucleus, while only K9R mutants of H3.2 and H3.3 lead to reduction in H3K9me2 in the paternal genomes, reflecting the differences in distribution of H3K9me2 on histone H3 variants between the female and male genomes. As for H3K9me3, it is enriched on H3.1 and H3.2 but not on H3.3 in the maternal genome. Generally speaking, as repressive marks, both H3K9me2 and H3K9me3 are mostly related to H3.1 and H3.2, which is in line with the literature that H3.1 and H3.2 are responsible for the formation of constitutive and facultative heterochromatin characterized by H3K9me2 and H3K9me3 (Hake and Allis, 2006; Jacob et al., 2014). Additionally, regarding H3.3, its link to repressive mark H3K9me2 shown by quantification is not so surprising, because some groups have claimed its passive role in specific local regions (Goldberg et al., 2010; Schwartz and Ahmad, 2006; Szenker et al., 2011), although typically it serves as an active mark (Hake and Allis, 2006; Loyola and Almouzni, 2007).

Despite the minor but significant reduction in H3K9me2, no obvious loss in 5mC is observed. On one hand, these two marks may not be overlapped with each other in some certain local regions. On the other hand, the loss in 5mC may be compensated to a small degree by *de novo* methylation occurring on unmethylated K4 of newly transcribed exogenous histone H3, based on the reports that unmethylated H3K4 could be well recognized by DNMT3A–DNMT3L complex both *in vivo* and *in vitro*, respectively, further leading to *de novo* methylation ((Hashimoto et al., 2010; Hu et al., 2009; Ooi et al., 2007; Otani et al.,

2009; Zhang et al., 2010). Notably, both Dnmt3A and Dnmt3L are located in the parental pronuclei in mouse zygotes (Gu et al., 2011; Hirasawa et al., 2008), which make this hypothesis theoretically possible.

Concerning the slight impacts on H3K9me2 as well as H3K9me3 by H3.1/2/3-GFPK9R mutants, it could be attributed to the rather low efficiency in randomly replacing old histone H3 carrying H3K9me2 by the K9R mutants in mouse zygotes, most probably because the old methylated histone H3 always exists in the form of a dimer with H4 in the cytoplasm and is prepared for the new assembly of a tetramer, further for an octamer before deposition into the chromatin during DNA replication (Tagami et al., 2004), leaving rather limited chance for newly synthesized monomer of histone H3K9R mutants to substitute for the old histone H3.

In contrast to H3K9me2/3, H3K9ac is progressively accumulated in both pronuclei through DNA replication. Nevertheless, no reduction in H3K9ac is caused by any of H3.1/2/3-GFPK9R mutants, indicating that the mutants fail to target to the H3K9ac-demanding areas, although they succeed to impair the other regions requiring H3K9me2 or me3 in an inefficient manner as shown above, which to some extent points out the possible role of K9 in determining the histone deposition into the certain chromatin regions. Also, this potential view is supported by our experiment that *in vitro* modified H3.3-GFPK9me2 protein loses the ability to be transported into both pronuclei in mouse zygotes. According to the literature, it has been demonstrated in some other species that pre-acetylation on K9 of histone H3 is essential for its incorporation into chromatin (Kuo et al., 1996; Sobel et al., 1995; Turner and O'Neill, 1995), suggesting that the rule seems to be evolutionarily conserved, at least in mice. Since K9ac is closely associated with H3.3 (Hake and Allis, 2006; Loyola and Almouzni, 2007), we speculate that this preacetylation step at K9 may be specific to H3.3 but not H3.1 and H3.2.

4.2 Phosphorylation on H3.1/2S10 and H3.1/2T11 serving as a double switch for H3K9me2 in the maternal genome of mouse zygotes

According to the literature, the crosstalks among these three neighboring sites, lysine 9 (K9), serine 10 (S10) and threonine 11 (T11), on histone H3 have been illustrated (Baek, 2011; Fischle, 2008; Sabbattini et al., 2014). Typically, it refers to the interaction between methylation on K9 and phosphorylation on either S10 or T11 or both. Since these modifications could be theoretically applied onto each of histone H3 variants (H3.1, H3.2 or H3.3) in a cell cycle-dependent or independent manner, the crosstalks among them become spatially and temporally dynamic. Furthermore, given the established link between H3K9me2 and 5mC in the maternal genome of mouse zygotes (Nakamura et al., 2012), whether H3S10phos and H3T11phos play any roles in this pathway is rather intriguing. Here, in our study, we demonstrate that H3.1/2S10phos and H3.1/2T11phos offer a protection for H3K9me2, further contributing to the maintenance of 5mC. In contrast, H3.3, which is not related to H3T11phos, is not responsible for the maintenance of 5mC in the maternal genome, implying that it may be involved in active DNA demethylation.

Regarding the protection of H3S10phos for H3K9me2, it is conceivable from the published data that S10phos on H3 could prevent K9 from being targeted by either antibodies or histone methyltransferases (Duan et al., 2008; Jeong et al., 2010). However, owing to the

dephosphorylation on S10 from G1 to S phase in mouse zygotes (Ribeiro-Mason et al., 2012; Teperek-Tkacz et al., 2010), the protection effect from S10phos on K9 is gradually becoming weak. Also, due to the same reason, it is not easy to evaluate the effects of H3.1/2/3-GFPS10A mutants on S10phos in mouse zygotes. It must be mentioned that the extent of dephosphorylation on S10 in mouse zygotes is observed to be variable depending on the antibodies based on our experiments and the published data (Ribeiro-Mason et al., 2012; Teperek-Tkacz et al., 2010). Additionally, the differences from H3.1, H3.2 and H3.3 in contribution to the shielding for H3K9me2 (30%, 30% and 15%, respectively) again confirm that H3.1 and H3.2 are highly enriched with H3K9me2. Besides, by further comparison with the amount of loss in 5mC by H3.1, H3.2 and H3.3 (15%, 15% and 0%), it clearly shows that the loss in H3K9me2 does not correspond to the equal amount of reduction in 5mC. Such discrepancy reflects that indeed some H3K9me2-rich regions are hardly overlapped by 5mC, which is consistent with the results aforementioned. However, we can not rule out the possibility that this observation can also potentially be due to different performance of H3K9me2 and 5mC antibodies.

As for H3T11phos, its dynamics in mouse zygotes has not been documented before. To our knowledge, in our study, it is the first time for description of this histone mark in mouse zygotes. Generally, concomitant with the disappearance of H3S10phos, H3T11phos is dramatically accumulated from DNA replication on (Supplementary Fig. 3), in which H3.1 and H3.2 are involved equally, while H3.3 is not phosphorylated. Moreover, the loss of H3K9me2 triggered by reduction in H3T11phos by either H3.1-GFPT11A or H3.2-GFPT11A clearly demonstrates a cross talk between these two histone marks, which is similar to an *in vitro* experiment that demethylation of K9me3 on the H3 peptide by KDM4A and KDM4C is blocked when T11 is phosphorylated (Lohse et al., 2013). However, another group has reported an opposite *in vitro* observation that the removal of H3K9me3 by KDM4C is accelerated by H3T11phos (Metzger et al., 2008). These two inverse results may be ascribed to the different reaction systems, for both experiments are performed *in vitro*. At least, we have shown this protection role of H3T11phos in H3K9me2, to a certain extent, suggesting the existence of active endogenous histone demethylases in mouse zygotes. Whether it is conserved or not in other species should be checked. Meanwhile, notably, H3.1-GFPT11A causes much more changes in H3K9me2 in both female and male pronuclei than H3.2-GFPT11A, indicating that H3.1 is the main carrier for H3K9me2. Subsequently, the further detection of both 5mC and 5hmC, with H3.1-GFPT11A injected group showing a more prominent abolishment of 5mC in the maternal genome compared to H3.2-GFPT11A injected group, strongly demonstrates that it is mainly H3.1T11phos that protects H3.1K9me2 from endogenous histone demethylase, further impeding the conversion of 5mC to 5hmC in the maternal genome. Rather interestingly, in the paternal genome, although no changes in 5mC are caused by either H3.1-GFPT11A or H3.2-GFPT11A, 5hmC levels appear to descend based on the signal intensities from IF-experiment, suggesting that it might be the case that T11A or other potential modifications interfere with the iterative oxidation of 5hmC to 5fC and 5caC. However, rather than blocking of the oxidation pathway, it seems that the other pathways may participate, for 5caC intensity in H3.1-GFPT11A expressing zygotes remains relatively equal compared to the control, although fC data are missing here. Notably, in H3.3-GFPT11A injected group, 5hmC seemed to be increased in both parental genomes to some

extent without influencing 5mC, similar to that in H3.3-GFPS10A injected group. Generally speaking, on the level of 5hmC, it appears to be fluctuating depending on histone H3 variants. One possible assumption behind is that another Tet-related pathway may be influenced either negatively or positively, in which, rather than phosphorylation, the O-linked N-acetylglucosamine transferase (OGT) mediated glycosylation on either serine 10 or threonine 11 may be interfered, since OGT is reported to interact with all Tets proteins and to be essential for mouse embryogenesis (Deplus et al., 2013; Shi et al., 2013; Vella et al., 2013). It is conceivable that competition between phosphorylation and glycosylation on H3T11 may determine the fate of downstream modifications such as H3K9me2 as well as 5mC. Besides, by comparing the efficiency between H3.1/2-GFPK9R and H3.1/2-GFPT11A in affecting H3K9me2 (minor versus dramatic), we assume that the crosstalk between H3K9me2 and H3T11phos may occur between the distinct copies of histone H3 within the same nucleosome or between the neighboring nucleosomes spatially close to each other.

In summary, it is phosphorylation on threonine (T) rather than on serine (S) of H3.1/2 that serves as a dominant protection layer for K9me2, which further prevents 5mC from demethylation in the maternal genome, of which H3.1 accounts for the most contribution. This is also the first evidence showing the roles of H3.1 and H3.2 in regulation of the dynamics of H3K9me2 and 5mC in mouse zygotes.

4.3 Artificial introduction of H3K9me2 on H3.1 and H3.2 fails to block global active DNA demethylation in the paternal genome of mouse zygotes

In the paternal genome, H3K9me2 is completely absent before replication and becomes rather sparse during replication (Lepikhov and Walter, 2004; Santos et al., 2005). Furthermore, recently, it shows that this small amount of H3K9me2 shields some loci of 5mC from being oxidized by Tet3 in the male pronucleus of mouse zygotes (Nakamura et al., 2012). Therefore, the lack of H3K9me2 on a large scale is considered as the main reason to explain why DNA demethylation could take place preferentially in the paternal genome of mouse zygotes. However, so far, no direct evidence has been available to support this idea. In our study, both constructs of G9a are employed, full length and catalytical domain only, in order to introduce H3K9me2 on a global level into the paternal genome. As expected, G9aCat-NLS-GFP could successfully introduce H3K9me2 into both pronuclei of mouse zygotes in a rather efficient manner. Here, the insertion of a nuclear localization sequence (NLS) from simian vacuolating virus 40 (SV40) into the construct helps G9aCat protein to reach both pronuclei in zygotes, since the deletion of NLS causes the problem of nuclear trafficking of the protein (Supplementary Fig. 8), consistent with the report that the NLS of G9a is located in its N-terminal part (Esteve et al., 2005). Despite the accumulation of G9aCat-GFP in cytoplasm, it has no influence on H3K9me2 in both pronuclei (Supplementary Fig. 4), suggesting that the occurrence of transfer of dimethyl group to the K9 site of histone H3 is not in cytoplasm, but inside nuclear. Surprisingly, in contrast to the high efficiency of G9aCat-NLS-GFP, G9aFL-GFP displays rather low activity for dimethylating K9 on histone H3, suggesting that G9a could be somehow negatively regulated via N-terminal domain in mouse zygotes, while its catalytical domain could easily escape from the potential inhibitors, which has also been proposed by Liu et al (Liu et al., 2004). Apart from the efficiency, the time point of mRNA

microinjection is also critical. In our experiments, it must be done within 1.5hpf, before the formation of both pronuclei in mouse zygotes. Otherwise, neither G9aCat-NLS-GFP nor G9aFL-GFP shows its methylation activity. The reason behind remains to be explored in the future. Additionally, regarding the specificity, besides performing H3K9me2, G9a is also shown to be responsible for methylation of H3K27 to a very low extent (Patnaik et al., 2004; Tachibana et al., 2001; Wu et al., 2011). Here, this side effect is not further checked, because H3K27 methylation and 5mC are only locally overlapped with each other according to the genome-wide mapping of these two marks in mES cells, implying that in mouse zygotes, at least, H3K27 methylation may not be a major player against oxidation of 5mC on a global level.

Despite dramatic increase in H3K9me2 in both pronuclei, only minor but significant growth in 5mC was obtained correspondingly. Notably, this small amount of 5mC rescued by the reacquisition of H3K9me2 in both parental genomes on one hand confirmed the protection role of H3K9me2 in 5mC and, on the other hand, may reflect the passive dilution mechanism in which the replication-dependent loss of H3K9me2 could lead to the exposure of 5mC to Tet3 dioxygenase, which could explain the recent findings that passive DNA demethylation occurs in both parental genomes and Tet3-based oxidation is related to DNA replication to some degree (Arand et al., 2015; Guo et al., 2014b; Shen et al., 2014). Furthermore, it can be easily inferred that it is the loss of H3K9me2, but not the absence of Dnmt1, that causes the reduction in 5mC in both parental genomes. Otherwise, no increase in 5mC would be acquired after rescue of H3K9me2. Subsequently, the hairpin bisulfite sequencing data on the repetitive elements, including Long Interspersed Elements (LINE1), Intracisternal A-Particle Element (IAP) and Major Satellites (mSat) presented similar patterns of 5mC between G9aCat-NLS-GFP and non-injected groups (Supplementary Fig. 5c), further confirming the immunostaining results that globally active DNA demethylation is not affected given the broad distribution of repetitive elements across the whole genome. In addition, according to the literature, Liu et al. have reported that the 5mC level stays constant despite of global introduction of H3K9me2 into the paternal pronucleus by applying cycloheximide to mouse zygotes (Liu et al., 2004). This result, however, it is not convincing, because, as an inhibitor of protein synthesis, cycloheximide could interfere with the activities of numerous proteins in mouse zygotes. At least, we observed that cycloheximide could impede DNA replication and DNA repair pathway in mouse zygotes, which is confirmed by EdU labeling and γ H2AX staining, respectively (Supplementary Fig. 5). As we know, both of these two factors, DNA replication and DNA repair pathway, could exert impact on either passive or active DNA demethylation. The advantage of our experiment is that we performed the detection of these modifications under a much cleaner background. Collectively, the artificial introduction of H3K9me2 into both genomes fails to globally block active DNA demethylation, although it is responsible for the arrest of a small amount of 5mC which should otherwise undergo Tet3-related passive demethylation during DNA replication.

Next, the concerned question is that which histone H3 variants are involved in the G9aCat-NLS-GFP-mediated H3K9me2 process in both parental genomes, since the anti-H3K9me2 antibody can not distinguish the epitopes among histone H3 variants, which only differ in four amino acids in the C-terminal domain (Hake and Allis, 2006; Kamakaka and Biggins, 2005). Also, based on the results above and the literature, we know that H3K9me2

has distinct distribution patterns across chromatin via their unique chaperones and is mostly enriched on H3.1 and H3.2 at least in the maternal genome (Burgess and Zhang, 2013; Filipescu et al., 2013). However, the detailed profiles of histone H3 variants in the paternal genome of mouse zygotes are not so clear. Hence, further exploration of the landscape of H3K9me2 in both parental genomes, especially in the paternal one, is really helpful to dissect the contribution of histone H3 variants to DNA demethylation. By taking advantage of the role of T11phos in protection of K9me2 on histone H3, it is conceivable that the introduction of H3K9me2 by G9aCat-NLS-GFP may be impaired by the T11A mutant of either H3.1-GFPT11A or H3.2-GFPT11A or H3.3-GFPT11A. Indeed, co-injection experiments prove that H3K9me2 driven by G9aCat-NLS-GFP is disrupted by T11A mutation either on H3.1 or on H3.2, but not on H3.3, suggesting that H3.1 and H3.2 are involved in the dilution-based passive DNA demethylation in both parental genomes and further implying that H3.3 may be the key player responsible for Tet3-based active DNA demethylation. In summary, H3.1 and H3.2, which lack H3K9me2 during replication, are involved in the dilution-dependent passive demethylation of 5mC in a small amount in both parental genomes.

4.4 Relation between H3.3 and active DNA demethylation in both parental genomes of mouse zygotes

Since neither H3.1 nor H3.2 is responsible for global active DNA demethylation, apparently H3.3 becomes the most promising one. Indeed, it has been suggested by many groups because the deposition of H3.3 coincides with active DNA demethylation in a similar temporal and spatial manner, namely both starting shortly after fertilization and preferentially occurring in male pronucleus of mouse zygotes (Okada et al., 2010; Torres-Padilla et al., 2006; van der Heijden et al., 2005; Wossidlo et al., 2010; Wu and Zhang, 2010). For H3.3, it is regarded to be highly correlated with H3K9 acetylation according to the literature (Ahmad and Henikoff, 2002; Loyola and Almouzni, 2007). Furthermore, in our study, the H3.3K9ac and H3K9me2 associated regions are shown to be differentially compartmented across the chromatin, because H3K9ac level is not disturbed by the dramatic increase of H3K9me2 via G9aCat-NLS-GFP in both pronuclei (Supplementary Fig. 6). Additionally, some evidence suggests that H3K9ac has a negative and strong correlation with DNA methylation (Bell et al., 2011; Wu et al., 2007; Zhang et al., 2012). Hence, it prompts us to investigate to what extent H3K9ac could be linked to active DNA demethylation in mouse zygotes. Unfortunately, however, the removal of H3K9ac from H3.3 by HDAC1-GFP does not show any effect on 5mC in both parental genomes, indicating that H3K9ac is not a prerequisite for active DNA methylation pathway.

Although acetylation at K9 of H3.3 is dispensible for Tet3-mediated oxidation process, it definitely could serve as a protector for the K9 site against G9aCat-NLS-GFP or endogenous histone methyltransferases to avoid being dimethylated in mouse zygotes. Therefore, the coinjection of HDAC1-GFP and G9aCat-NLS-GFP was designed to clear off the acetyl groups from K9 on H3.3, followed by the transfer of dimethyl groups to the target sites. This could probably block global active DNA demethylation. Again unfortunately, no change in H3K9me2 is observed in coinjection group compared to G9aCat-NLS-GFP alone injected one. For the reason behind, given the fact that the presence of T11phos shows the ability to protect H3K9me2, it is most probably due to the absence of T11phos on H3.3,

leading to the accessibility for endogenous histone demethylase to the K9 site. Based on this speculation, it has been assumed that K9 site has been successfully targeted by G9aCat-NLS-GFP, but immediately attacked by some endogenous histone demethylases. In the future, manipulation of T11 site into a phosphorylation form and the removal of acetyl group from K9 site will be a possible way to introduce K9me2 for blocking Tet3-related oxidation of 5mC, by which H3.3 could be definitely linked to active DNA demethylation. However, we can not fully rule out the possibility that other modifications or factors could interfere with G9aCat-NLS-GFP activity after the K9 site becomes vacant.

Lastly, given the facts that T11phos is present on H3.1 and absent on H3.3, whereas K9ac is unrelated to H3.1 but related to H3.3, we speculate that these two histone marks may be mutually exclusive. To test the possibility of this potential crosstalk between H3K9ac and H3T11phos, the mutation of lysine 9 to glutamine (K9Q) on H3.1 was performed, which could mimic the acetylation form at K9 to some extent. However, H3T11phos is not impaired by the H3.1-GFPK9Q mutant in mouse zygotes (Supplementary Fig. 7), which excludes the possibility of the interaction between H3T11phos and H3K9ac. As a result, H3K9ac may not be responsible for the missing of H3T11phos on H3.3.

Taken together, it is the presence of K9ac and the absence of T11phos on H3.3 that serve as the first and second protection mechanisms, respectively, for K9 site from being dimethylated by some potential histone methyltransferases, which ensures the proper occurrence of Tet3-based global active DNA demethylation in both parental genomes of mouse zygotes.

4.5 Conclusions

In this study, a clear picture describing the relations between histone H3 variants (H3.1, H3.2 and H3.3), H3K9 marks (me2, me3 and ac) and DNA modifications (5mC, 5hmC) in mouse zygotes is presented. On one hand, H3.1 and H3.2, which are highly enriched with H3K9me2, are responsible for the maintenance of 5mC in an H3T11phos dependent manner in the maternal genome, of which H3.1 is much more dominant. On the other hand, H3.1 and H3.2, which are losing H3K9me2 during replication, are involved in the dilution-dependent passive demethylation of 5mC in a small amount in both parental genomes. As for H3.3, it is positively and negatively correlated with K9ac and T11phos, respectively, through which it successfully escapes the capture from the endogenous histone methyltransferases, ensuring the active DNA demethylation to occur in both parental genomes in a proper way.

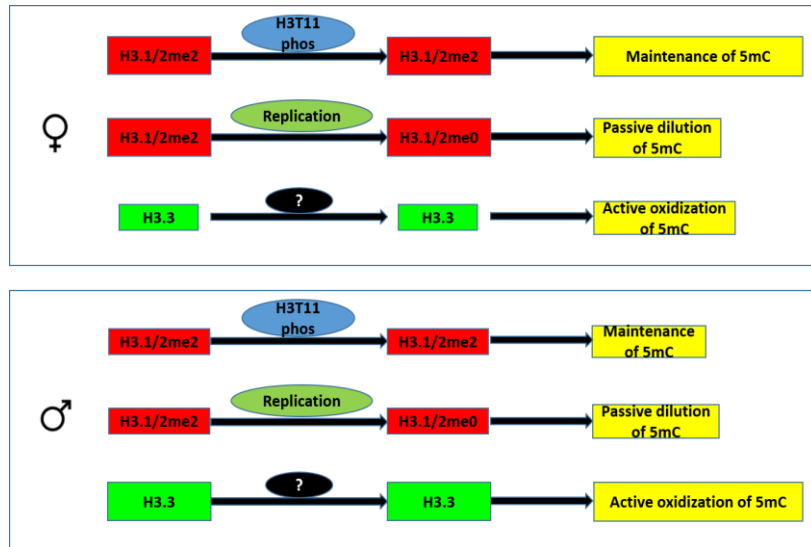


Fig. 4.1 The schematic of relations between histone H3 variants, H3K9 modifications and DNA methylation

4.6 Perspectives

In the future, still many open questions are remaining to be answered. Firstly, what are the upstream switches for H3T11phos and H3S10phos? In other words, why do these two histone marks display distinctive patterns among histone H3 variants in mouse zygotes? Secondly, to what extent is this novel “phospho switch” conserved across the species or across the cell types like stem cells, somatic cells or even cancer cells? Thirdly, whether the competition between phosphorylation and glycosylation on H3T11 exists or not should be further explored. And the enzyme, OGT, should also be paid attention to in terms of its potential role in DNA demethylation. Fourthly, to what extent, H3T11phos or H3S10phos could be linked to DNA repair pathway, for dephosphorylation at S10 and T11 has been observed upon DNA damage (Sen and De Benedetti, 2006; Shimada and Nakanishi, 2008; Shimada et al., 2008). Meanwhile, how the other histone variants participate in the DNA repair pathway in mouse zygotes is also a hotspot in the future. For example, gamma H2A.X, the phosphorylation form of H2A.X on serine139, shows the preferential localization in the paternal pronucleus of mouse zygotes (Wossidlo et al., 2010; Ziegler-Birling et al., 2009). Fifthly, whether the crosstalk between methylation and phosphorylation is a general mechanism or not on the chromatin should be investigated, such as H3K4me1/2/3 and H3T3phos, H3K27me1/2/3 and H2S28phos.

Zusammenfassung

Die epigenetische Reprogrammierung in der Mauszygote besteht aus der globalen Chromatinreorganisation sowie globalen Veränderungen der DNA Methylierung. Die Oxidation von 5-Methylcytosin (5mC) zu 5-Hydroxymethylcytosin (5hmC) und zu weiter oxidierten Basen durch die Tet dioxygenase 3 steht im paternalern und maternalen Genom in Korrelation mit dem Status der Methylierung von Lysin 9 an Histon 3 (H3K9me2/3). Es wurde gezeigt, dass die H3 Histonvarianten, H3.1, H3.2, H3.3, asymmetrisch und dynamisch in das Chromatin intergriert werden. Dies kann auf eine DNA-replikationsabhangige oder –unabhangige Weise geschehen. In dieser Arbeit wurde die dynamische Kontrolle von H3K9me2 und von DNA Modifikationen in Relation zum Phosphorylierungsstatus an H3S10 und H3T11 sowie der Histon H3 Varianten in der Mauszygote untersucht. Es konnte gezeigt werden, dass H3.1 und H3.2 das Hauptziel fur die Dimethylierung von Lysin 9 sind. Dieser Prozess ist abhangig vom Phosphorylierungsstatus von H3S10 und H3T11. H3K9me2 behindert die Oxidation von 5mC zu 5hmC im maternalen Genom der Mauszygote. Wahrend der Replikation wird K9me2 an beiden Histonvarianten (H3.1 und H3.2) reduziert was mit einer replikationsabhangigen passiven DNA Demethylierung in beiden parentalen Genomen einhergeht. Fur H3.3 wurde beobachtet, dass die Phase der aktiven DNA Demethylierung in beiden parentalen Genomen in Verbindung zu deutlichen und einzigartigen Dynamiken von K9ac und T11phos steht. Zusammenfassend lasst sich sagen, dass die Daten dieser Arbeit darauf hinweisen, dass ein Spektrum aus verschiedenen Histonvarianten und –modifikationen die aktive und passive Reprogrammierung in der Mauszygote kontrollieren.

Summary

In mouse zygotes, reprogramming involves chromatin reorganization and changes in the DNA modifications. The conversion of 5-methylcytosine (5mC) to 5-hydroxymethylcytosine (5hmC) and further oxidized forms by the Tet dioxygenase 3 (Tet3) in maternal and paternal genomes has been associated to the modification status of histone H3 at lysine 9 (H3K9me2/3). It has also been shown that histone H3 variants H3.1, H3.2, H3.3, are asymmetrically and dynamically deposited into chromatin in DNA replication dependent and independent manner in the mouse zygote. Here we investigate the dynamics of H3 variants during epigenetic reprogramming in the zygote, in particular the control of H3K9me2 in relation to the phosphorylation status at H3S10 and H3T11 and their impact on changes in DNA modifications in mouse zygotes. We find that H3.1 and H3.2 are the prime targets for K9me2 modification impeding the oxidation of 5mC into 5hmC in an H3T11phos dependent manner in the maternal genome of mouse zygotes. Upon replication, K9me2 on both H3.1 and H3.2 is reduced and paralleled by a replication-dependent passive DNA demethylation in both parental genomes. For H3.3 we observe that phases of active DNA demethylation in both parental genomes are linked to distinct and unique dynamics of K9ac and T11phosphorylation, respectively. In summary our data indicate that a differential variant specific modification spectrum controls active and passive reprogramming processes in mouse zygotes.

References

- Adenot, P. G., Campion, E., Legouy, E., Allis, C. D., Dimitrov, S., Renard, J. and Thompson, E. M.** (2000). Somatic linker histone H1 is present throughout mouse embryogenesis and is not replaced by variant H1 degrees. *J Cell Sci* **113** (Pt 16), 2897-907.
- Adenot, P. G., Mercier, Y., Renard, J. P. and Thompson, E. M.** (1997). Differential H4 acetylation of paternal and maternal chromatin precedes DNA replication and differential transcriptional activity in pronuclei of 1-cell mouse embryos. *Development* **124**, 4615-25.
- Ahmad, K. and Henikoff, S.** (2002). The histone variant H3.3 marks active chromatin by replication-independent nucleosome assembly. *Mol Cell* **9**, 1191-200.
- Akiyama, T., Suzuki, O., Matsuda, J. and Aoki, F.** (2011). Dynamic replacement of histone H3 variants reprograms epigenetic marks in early mouse embryos. *PLoS Genet* **7**, e1002279.
- Allan, J., Hartman, P. G., Crane-Robinson, C. and Aviles, F. X.** (1980). The structure of histone H1 and its location in chromatin. *Nature* **288**, 675-9.
- Ancelin, K., Lange, U. C., Hajkova, P., Schneider, R., Bannister, A. J., Kouzarides, T. and Surani, M. A.** (2006). Blimp1 associates with Prmt5 and directs histone arginine methylation in mouse germ cells. *Nat Cell Biol* **8**, 623-30.
- Arand, J., Wossidlo, M., Lepikhov, K., Peat, J. R., Reik, W. and Walter, J.** (2015). Selective impairment of methylation maintenance is the major cause of DNA methylation reprogramming in the early embryo. *Epigenetics Chromatin* **8**, 1.
- Arney, K. L., Bao, S., Bannister, A. J., Kouzarides, T. and Surani, M. A.** (2002). Histone methylation defines epigenetic asymmetry in the mouse zygote. *Int J Dev Biol* **46**, 317-20.
- Baek, S. H.** (2011). When signaling kinases meet histones and histone modifiers in the nucleus. *Mol Cell* **42**, 274-84.
- Barski, A., Cuddapah, S., Cui, K., Roh, T. Y., Schones, D. E., Wang, Z., Wei, G., Chepelev, I. and Zhao, K.** (2007). High-resolution profiling of histone methylations in the human genome. *Cell* **129**, 823-37.
- Bell, J. T., Pai, A. A., Pickrell, J. K., Gaffney, D. J., Pique-Regi, R., Degner, J. F., Gilad, Y. and Pritchard, J. K.** (2011). DNA methylation patterns associate with genetic and gene expression variation in HapMap cell lines. *Genome Biol* **12**, R10.
- Bernatavichute, Y. V., Zhang, X., Cokus, S., Pellegrini, M. and Jacobsen, S. E.** (2008). Genome-wide association of histone H3 lysine nine methylation with CHG DNA methylation in *Arabidopsis thaliana*. *PLoS One* **3**, e3156.
- Bernstein, B. E., Meissner, A. and Lander, E. S.** (2007). The mammalian epigenome. *Cell* **128**, 669-81.
- Boskovic, A., Bender, A., Gall, L., Ziegler-Birling, C., Beaujean, N. and Torres-Padilla, M. E.** (2012). Analysis of active chromatin modifications in early mammalian embryos reveals uncoupling of H2A.Z acetylation and H3K36 trimethylation from embryonic genome activation. *Epigenetics* **7**, 747-57.
- Burgess, R. J. and Zhang, Z.** (2013). Histone chaperones in nucleosome assembly and human disease. *Nat Struct Mol Biol* **20**, 14-22.
- Burton, A. and Torres-Padilla, M. E.** (2010). Epigenetic reprogramming and development: a unique heterochromatin organization in the preimplantation mouse embryo. *Brief Funct Genomics* **9**, 444-54.

References

- Burton, A. and Torres-Padilla, M. E.** (2014). Chromatin dynamics in the regulation of cell fate allocation during early embryogenesis. *Nat Rev Mol Cell Biol* **15**, 723-34.
- Butler, J. S. and Dent, S. Y.** (2012). Chromatin 'resetting' during transcription elongation: a central role for methylated H3K36. *Nat Struct Mol Biol* **19**, 863-4.
- Celeste, A., Petersen, S., Romanienko, P. J., Fernandez-Capetillo, O., Chen, H. T., Sedelnikova, O. A., Reina-San-Martin, B., Coppola, V., Meffre, E., Difilippantonio, M. J. et al.** (2002). Genomic instability in mice lacking histone H2AX. *Science* **296**, 922-7.
- Chadwick, B. P. and Willard, H. F.** (2001). A novel chromatin protein, distantly related to histone H2A, is largely excluded from the inactive X chromosome. *J Cell Biol* **152**, 375-84.
- Chang, C. C., Ma, Y., Jacobs, S., Tian, X. C., Yang, X. and Rasmussen, T. P.** (2005). A maternal store of macroH2A is removed from pronuclei prior to onset of somatic macroH2A expression in preimplantation embryos. *Dev Biol* **278**, 367-80.
- Cheng, J., Blum, R., Bowman, C., Hu, D., Shilatifard, A., Shen, S. and Dynlacht, B. D.** (2014). A role for H3K4 monomethylation in gene repression and partitioning of chromatin readers. *Mol Cell* **53**, 979-92.
- Cheung, P., Tanner, K. G., Cheung, W. L., Sassone-Corsi, P., Denu, J. M. and Allis, C. D.** (2000). Synergistic coupling of histone H3 phosphorylation and acetylation in response to epidermal growth factor stimulation. *Mol Cell* **5**, 905-15.
- Chin, H. G., Pradhan, M., Esteve, P. O., Patnaik, D., Evans, T. C., Jr. and Pradhan, S.** (2005). Sequence specificity and role of proximal amino acids of the histone H3 tail on catalysis of murine G9A lysine 9 histone H3 methyltransferase. *Biochemistry* **44**, 12998-3006.
- Cosgrove, M. S., Boeke, J. D. and Wolberger, C.** (2004). Regulated nucleosome mobility and the histone code. *Nat Struct Mol Biol* **11**, 1037-43.
- Costanzi, C. and Pehrson, J. R.** (2001). MACROH2A2, a new member of the MARCOH2A core histone family. *J Biol Chem* **276**, 21776-84.
- Craig, J. M., Earnshaw, W. C. and Vagnarelli, P.** (1999). Mammalian centromeres: DNA sequence, protein composition, and role in cell cycle progression. *Exp Cell Res* **246**, 249-62.
- Daujat, S., Weiss, T., Mohn, F., Lange, U. C., Ziegler-Birling, C., Zeissler, U., Lappe, M., Schubeler, D., Torres-Padilla, M. E. and Schneider, R.** (2009). H3K64 trimethylation marks heterochromatin and is dynamically remodeled during developmental reprogramming. *Nat Struct Mol Biol* **16**, 777-81.
- Daujat, S., Zeissler, U., Waldmann, T., Happel, N. and Schneider, R.** (2005). HP1 binds specifically to Lys26-methylated histone H1.4, whereas simultaneous Ser27 phosphorylation blocks HP1 binding. *J Biol Chem* **280**, 38090-5.
- Demidov, D., Hesse, S., Tewes, A., Rutten, T., Fuchs, J., Ashtiyani, R. K., Lein, S., Fischer, A., Reuter, G. and Houben, A.** (2009). Aurora1 phosphorylation activity on histone H3 and its cross-talk with other post-translational histone modifications in Arabidopsis. *Plant J* **59**, 221-30.
- Deplus, R., Delatte, B., Schwinn, M. K., Defrance, M., Mendez, J., Murphy, N., Dawson, M. A., Volkmar, M., Putmans, P., Calonne, E. et al.** (2013). TET2 and TET3 regulate GlcNAcylation and H3K4 methylation through OGT and SET1/COMPASS. *EMBO J* **32**, 645-55.

References

- Derijck, A. A., van der Heijden, G. W., Giele, M., Philippens, M. E., van Bavel, C. C. and de Boer, P.** (2006). gammaH2AX signalling during sperm chromatin remodelling in the mouse zygote. *DNA Repair (Amst)* **5**, 959-71.
- Dhayalan, A., Rajavelu, A., Rathert, P., Tamas, R., Jurkowska, R. Z., Ragozin, S. and Jeltsch, A.** (2010). The Dnmt3a PWWP domain reads histone 3 lysine 36 trimethylation and guides DNA methylation. *J Biol Chem* **285**, 26114-20.
- Di Cerbo, V., Mohn, F., Ryan, D. P., Montellier, E., Kacem, S., Tropberger, P., Kallis, E., Holzner, M., Hoerner, L., Feldmann, A. et al.** (2014). Acetylation of histone H3 at lysine 64 regulates nucleosome dynamics and facilitates transcription. *Elife* **3**, e01632.
- Dinant, C., Houtsmuller, A. B. and Vermeulen, W.** (2008). Chromatin structure and DNA damage repair. *Epigenetics Chromatin* **1**, 9.
- Esteve, P. O., Patnaik, D., Chin, H. G., Benner, J., Teitell, M. A. and Pradhan, S.** (2005). Functional analysis of the N- and C-terminus of mammalian G9a histone H3 methyltransferase. *Nucleic Acids Res* **33**, 3211-23.
- Faast, R., Thonglairoam, V., Schulz, T. C., Beall, J., Wells, J. R., Taylor, H., Matthaei, K., Rathjen, P. D., Tremethick, D. J. and Lyons, I.** (2001). Histone variant H2A.Z is required for early mammalian development. *Curr Biol* **11**, 1183-7.
- Filipescu, D., Szenker, E. and Almouzni, G.** (2013). Developmental roles of histone H3 variants and their chaperones. *Trends Genet* **29**, 630-40.
- Fischle, W.** (2008). Talk is cheap--cross-talk in establishment, maintenance, and readout of chromatin modifications. *Genes Dev* **22**, 3375-82.
- Fouse, S. D., Shen, Y., Pellegrini, M., Cole, S., Meissner, A., Van Neste, L., Jaenisch, R. and Fan, G.** (2008). Promoter CpG methylation contributes to ES cell gene regulation in parallel with Oct4/Nanog, PcG complex, and histone H3 K4/K27 trimethylation. *Cell Stem Cell* **2**, 160-9.
- Gao, S., Chung, Y. G., Parseghian, M. H., King, G. J., Adashi, E. Y. and Latham, K. E.** (2004). Rapid H1 linker histone transitions following fertilization or somatic cell nuclear transfer: evidence for a uniform developmental program in mice. *Dev Biol* **266**, 62-75.
- Goldberg, A. D., Banaszynski, L. A., Noh, K. M., Lewis, P. W., Elsaesser, S. J., Stadler, S., Dewell, S., Law, M., Guo, X., Li, X. et al.** (2010). Distinct factors control histone variant H3.3 localization at specific genomic regions. *Cell* **140**, 678-91.
- Govin, J., Escoffier, E., Rousseaux, S., Kuhn, L., Ferro, M., Thevenon, J., Catena, R., Davidson, I., Garin, J., Khochbin, S. et al.** (2007). Pericentric heterochromatin reprogramming by new histone variants during mouse spermiogenesis. *J Cell Biol* **176**, 283-94.
- Greiner, D., Bonaldi, T., Eskeland, R., Roemer, E. and Imhof, A.** (2005). Identification of a specific inhibitor of the histone methyltransferase SU(VAR)3-9. *Nat Chem Biol* **1**, 143-5.
- Gu, T. P., Guo, F., Yang, H., Wu, H. P., Xu, G. F., Liu, W., Xie, Z. G., Shi, L., He, X., Jin, S. G. et al.** (2011). The role of Tet3 DNA dioxygenase in epigenetic reprogramming by oocytes. *Nature* **477**, 606-10.
- Guccione, E., Bassi, C., Casadio, F., Martinato, F., Cesaroni, M., Schuchlantz, H., Luscher, B. and Amati, B.** (2007). Methylation of histone H3R2 by PRMT6 and H3K4 by an MLL complex are mutually exclusive. *Nature* **449**, 933-7.

References

- Guenther, M. G., Levine, S. S., Boyer, L. A., Jaenisch, R. and Young, R. A.** (2007). A chromatin landmark and transcription initiation at most promoters in human cells. *Cell* **130**, 77-88.
- Guo, F., Li, X., Liang, D., Li, T., Zhu, P., Guo, H., Wu, X., Wen, L., Gu, T. P., Hu, B. et al.** (2014a). Active and Passive Demethylation of Male and Female Pronuclear DNA in the Mammalian Zygote. *Cell Stem Cell*.
- Guo, F., Li, X., Liang, D., Li, T., Zhu, P., Guo, H., Wu, X., Wen, L., Gu, T. P., Hu, B. et al.** (2014b). Active and passive demethylation of male and female pronuclear DNA in the Mammalian zygote. *Cell Stem Cell* **15**, 447-58.
- Hake, S. B. and Allis, C. D.** (2006). Histone H3 variants and their potential role in indexing mammalian genomes: the "H3 barcode hypothesis". *Proc Natl Acad Sci U S A* **103**, 6428-35.
- Hake, S. B., Garcia, B. A., Kauer, M., Baker, S. P., Shabanowitz, J., Hunt, D. F. and Allis, C. D.** (2005). Serine 31 phosphorylation of histone variant H3.3 is specific to regions bordering centromeres in metaphase chromosomes. *Proc Natl Acad Sci U S A* **102**, 6344-9.
- Harshman, S. W., Young, N. L., Parthun, M. R. and Freitas, M. A.** (2013). H1 histones: current perspectives and challenges. *Nucleic Acids Res* **41**, 9593-609.
- Hartman, P. G., Chapman, G. E., Moss, T. and Bradbury, E. M.** (1977). Studies on the role and mode of operation of the very-lysine-rich histone H1 in eukaryote chromatin. The three structural regions of the histone H1 molecule. *Eur J Biochem* **77**, 45-51.
- Hashimoto, H., Vertino, P. M. and Cheng, X.** (2010). Molecular coupling of DNA methylation and histone methylation. *Epigenomics* **2**, 657-69.
- Hayashi-Takanaka, Y., Yamagata, K., Wakayama, T., Stasevich, T. J., Kainuma, T., Tsurimoto, T., Tachibana, M., Shinkai, Y., Kurumizaka, H., Nozaki, N. et al.** (2011). Tracking epigenetic histone modifications in single cells using Fab-based live endogenous modification labeling. *Nucleic Acids Res* **39**, 6475-88.
- He, Y. F., Li, B. Z., Li, Z., Liu, P., Wang, Y., Tang, Q., Ding, J., Jia, Y., Chen, Z., Li, L. et al.** (2011). Tet-mediated formation of 5-carboxylcytosine and its excision by TDG in mammalian DNA. *Science* **333**, 1303-7.
- Hergeth, S. P., Dunder, M., Tropberger, P., Zee, B. M., Garcia, B. A., Daujat, S. and Schneider, R.** (2011). Isoform-specific phosphorylation of human linker histone H1.4 in mitosis by the kinase Aurora B. *J Cell Sci* **124**, 1623-8.
- Hirasawa, R., Chiba, H., Kaneda, M., Tajima, S., Li, E., Jaenisch, R. and Sasaki, H.** (2008). Maternal and zygotic Dnmt1 are necessary and sufficient for the maintenance of DNA methylation imprints during preimplantation development. *Genes Dev* **22**, 1607-16.
- Hirota, T., Lipp, J. J., Toh, B. H. and Peters, J. M.** (2005). Histone H3 serine 10 phosphorylation by Aurora B causes HP1 dissociation from heterochromatin. *Nature* **438**, 1176-80.
- Howman, E. V., Fowler, K. J., Newson, A. J., Redward, S., MacDonald, A. C., Kalitsis, P. and Choo, K. H.** (2000). Early disruption of centromeric chromatin organization in centromere protein A (Cenpa) null mice. *Proc Natl Acad Sci U S A* **97**, 1148-53.
- Huang, Y., Pastor, W. A., Shen, Y., Tahiliani, M., Liu, D. R. and Rao, A.** (2010). The Behaviour of 5-Hydroxymethylcytosine in Bisulfite Sequencing. *Plos one* **5**, e8888.

- Hu, J. L., Zhou, B. O., Zhang, R. R., Zhang, K. L., Zhou, J. Q. and Xu, G. L.** (2009). The N-terminus of histone H3 is required for de novo DNA methylation in chromatin. *Proc Natl Acad Sci U S A* **106**, 22187-92.
- Inoue, A., Shen, L., Dai, Q., He, C. and Zhang, Y.** (2011). Generation and replication-dependent dilution of 5fC and 5caC during mouse preimplantation development. *Cell Res* **21**, 1670-6.
- Inoue, A. and Zhang, Y.** (2014). Nucleosome assembly is required for nuclear pore complex assembly in mouse zygotes. *Nat Struct Mol Biol* **21**, 609-16.
- Iqbal, K., Jin, S. G., Pfeifer, G. P. and Szabo, P. E.** (2011). Reprogramming of the paternal genome upon fertilization involves genome-wide oxidation of 5-methylcytosine. *Proc Natl Acad Sci U S A* **108**, 3642-7.
- Ishibashi, T., Li, A., Eirin-Lopez, J. M., Zhao, M., Missiaen, K., Abbott, D. W., Meistrich, M., Hendzel, M. J. and Ausio, J.** (2010). H2A.Bbd: an X-chromosome-encoded histone involved in mammalian spermiogenesis. *Nucleic Acids Res* **38**, 1780-9.
- Ito, S., Shen, L., Dai, Q., Wu, S. C., Collins, L. B., Swenberg, J. A., He, C. and Zhang, Y.** (2011). Tet proteins can convert 5-methylcytosine to 5-formylcytosine and 5-carboxylcytosine. *Science* **333**, 1300-3.
- Jack, A. P., Bussemer, S., Hahn, M., Punzeler, S., Snyder, M., Wells, M., Csankovszki, G., Solovei, I., Schotta, G. and Hake, S. B.** (2013). H3K56me3 is a novel, conserved heterochromatic mark that largely but not completely overlaps with H3K9me3 in both regulation and localization. *PLoS One* **8**, e51765.
- Jackson, J. P., Johnson, L., Jasencakova, Z., Zhang, X., PerezBurgos, L., Singh, P. B., Cheng, X., Schubert, I., Jenuwein, T. and Jacobsen, S. E.** (2004). Dimethylation of histone H3 lysine 9 is a critical mark for DNA methylation and gene silencing in *Arabidopsis thaliana*. *Chromosoma* **112**, 308-15.
- Jackson, J. P., Lindroth, A. M., Cao, X. and Jacobsen, S. E.** (2002). Control of CpNpG DNA methylation by the KRYPTONITE histone H3 methyltransferase. *Nature* **416**, 556-60.
- Jacob, Y., Bergamin, E., Donoghue, M. T., Mongeon, V., LeBlanc, C., Voigt, P., Underwood, C. J., Brunzelle, J. S., Michaels, S. D., Reinberg, D. et al.** (2014). Selective methylation of histone H3 variant H3.1 regulates heterochromatin replication. *Science* **343**, 1249-53.
- Joo, H. Y., Zhai, L., Yang, C., Nie, S., Erdjument-Bromage, H., Tempst, P., Chang, C. and Wang, H.** (2007). Regulation of cell cycle progression and gene expression by H2A deubiquitination. *Nature* **449**, 1068-72.
- Kafer, G. R., Lehnert, S. A., Kaye, P. L. and Moser, R. J.** (2008). Differential expression of H2A and H3 variant histones in mouse preimplantation embryos and R1 ES cells. *Reproduction, Fertility and Development* **20**, 58-58.
- Kageyama, S., Sonehara, H., Nagata, M. and Aoki, F.** (2007). Expression of Histone Methylases and Demethylases during Preimplantation Development in Mice. *Journal of Mammalian Ova Research* **24**, 126-131.
- Kamakaka, R. T. and Biggins, S.** (2005). Histone variants: deviants? *Genes Dev* **19**, 295-310.

- Kamieniarz, K., Izzo, A., Dundr, M., Tropberger, P., Ozretic, L., Kirfel, J., Scheer, E., Tropel, P., Wisniewski, J. R., Tora, L. et al.** (2012). A dual role of linker histone H1.4 Lys 34 acetylation in transcriptional activation. *Genes Dev* **26**, 797-802.
- Kim, J. M., Liu, H., Tazaki, M., Nagata, M. and Aoki, F.** (2003). Changes in histone acetylation during mouse oocyte meiosis. *J Cell Biol* **162**, 37-46.
- Kirmizis, A., Santos-Rosa, H., Penkett, C. J., Singer, M. A., Vermeulen, M., Mann, M., Bahler, J., Green, R. D. and Kouzarides, T.** (2007). Arginine methylation at histone H3R2 controls deposition of H3K4 trimethylation. *Nature* **449**, 928-32.
- Kourmouli, N., Jeppesen, P., Mahadevhaiah, S., Burgoyne, P., Wu, R., Gilbert, D. M., Bongiorno, S., Prantera, G., Fanti, L., Pimpinelli, S. et al.** (2004). Heterochromatin and trimethylated lysine 20 of histone H4 in animals. *J Cell Sci* **117**, 2491-501.
- Kuo, M. H., Brownell, J. E., Sobel, R. E., Ranalli, T. A., Cook, R. G., Edmondson, D. G., Roth, S. Y. and Allis, C. D.** (1996). Transcription-linked acetylation by Gcn5p of histones H3 and H4 at specific lysines. *Nature* **383**, 269-72.
- Kurdistani, S. K., Tavazoie, S. and Grunstein, M.** (2004). Mapping global histone acetylation patterns to gene expression. *Cell* **117**, 721-33.
- Lange, U. C., Siebert, S., Wossidlo, M., Weiss, T., Ziegler-Birling, C., Walter, J., Torres-Padilla, M. E., Daujat, S. and Schneider, R.** (2013). Dissecting the role of H3K64me3 in mouse pericentromeric heterochromatin. *Nat Commun* **4**, 2233.
- Lehnertz, B., Ueda, Y., Derijck, A. A., Braunschweig, U., Perez-Burgos, L., Kubicek, S., Chen, T., Li, E., Jenuwein, T. and Peters, A. H.** (2003). Suv39h-mediated histone H3 lysine 9 methylation directs DNA methylation to major satellite repeats at pericentric heterochromatin. *Curr Biol* **13**, 1192-200.
- Lennox, R. W. and Cohen, L. H.** (1983). The histone H1 complements of dividing and nondividing cells of the mouse. *J Biol Chem* **258**, 262-8.
- Lennox, R. W. and Cohen, L. H.** (1984). The alterations in H1 histone complement during mouse spermatogenesis and their significance for H1 subtype function. *Dev Biol* **103**, 80-4.
- Lepikhov, K. and Walter, J.** (2004). Differential dynamics of histone H3 methylation at positions K4 and K9 in the mouse zygote. *BMC Dev Biol* **4**, 12.
- Li, B., Tang, N., Chen, S., Li, X., Huang, X., Wang, X. and Sun, F.** (2013). G9a co-localized with histone H3 lysine 9 monomethylation but not dimethylation in a nuclear membrane-dependent manner during mouse preimplantation embryo development. *J Assist Reprod Genet* **30**, 441-8.
- Lin, C. J., Conti, M. and Ramalho-Santos, M.** (2013). Histone variant H3.3 maintains a decondensed chromatin state essential for mouse preimplantation development. *Development* **140**, 3624-34.
- Liokatis, S., Stutzer, A., Elsasser, S. J., Theillet, F. X., Klingberg, R., van Rossum, B., Schwarzer, D., Allis, C. D., Fischle, W. and Selenko, P.** (2012). Phosphorylation of histone H3 Ser10 establishes a hierarchy for subsequent intramolecular modification events. *Nat Struct Mol Biol* **19**, 819-23.
- Liu, H., Kim, J. M. and Aoki, F.** (2004). Regulation of histone H3 lysine 9 methylation in oocytes and early pre-implantation embryos. *Development* **131**, 2269-80.

References

- Lo, W. S., Duggan, L., Emre, N. C., Belotserkovskya, R., Lane, W. S., Shiekhattar, R. and Berger, S. L.** (2001). Snf1--a histone kinase that works in concert with the histone acetyltransferase Gcn5 to regulate transcription. *Science* **293**, 1142-6.
- Lo, W. S., Trievel, R. C., Rojas, J. R., Duggan, L., Hsu, J. Y., Allis, C. D., Marmorstein, R. and Berger, S. L.** (2000). Phosphorylation of serine 10 in histone H3 is functionally linked in vitro and in vivo to Gcn5-mediated acetylation at lysine 14. *Mol Cell* **5**, 917-26.
- Lohse, B., Helgstrand, C., Kristensen, J. B., Leurs, U., Cloos, P. A., Kristensen, J. L. and Clausen, R. P.** (2013). Posttranslational modifications of the histone 3 tail and their impact on the activity of histone lysine demethylases in vitro. *PLoS One* **8**, e67653.
- Loyola, A. and Almouzni, G.** (2007). Marking histone H3 variants: how, when and why? *Trends Biochem Sci* **32**, 425-33.
- Luger, K., Mader, A. W., Richmond, R. K., Sargent, D. F. and Richmond, T. J.** (1997). Crystal structure of the nucleosome core particle at 2.8 Å resolution. *Nature* **389**, 251-60.
- Madabushi, A., Hwang, B. J., Jin, J. and Lu, A. L.** (2013). Histone deacetylase SIRT1 modulates and deacetylates DNA base excision repair enzyme thymine DNA glycosylase. *Biochem J* **456**, 89-98.
- Margaritis, T., Oreal, V., Brabers, N., Maestroni, L., Vitaliano-Prunier, A., Benschop, J. J., van Hooff, S., van Leenen, D., Dargemont, C., Geli, V. et al.** (2012). Two distinct repressive mechanisms for histone 3 lysine 4 methylation through promoting 3'-end antisense transcription. *PLoS Genet* **8**, e1002952.
- Marzluff, W. F., Gongidi, P., Woods, K. R., Jin, J. and Maltais, L. J.** (2002). The human and mouse replication-dependent histone genes. *Genomics* **80**, 487-98.
- Marzluff, W. F., Wagner, E. J. and Duronio, R. J.** (2008). Metabolism and regulation of canonical histone mRNAs: life without a poly(A) tail. *Nat Rev Genet* **9**, 843-54.
- Matsuda, R., Hori, T., Kitamura, H., Takeuchi, K., Fukagawa, T. and Harata, M.** (2010). Identification and characterization of the two isoforms of the vertebrate H2A.Z histone variant. *Nucleic Acids Res* **38**, 4263-73.
- Mayer, W., Niveleau, A., Walter, J., Fundele, R. and Haaf, T.** (2000). Demethylation of the zygotic paternal genome. *Nature* **403**, 501-2.
- Metzger, E., Imhof, A., Patel, D., Kahl, P., Hoffmeyer, K., Friedrichs, N., Muller, J. M., Greschik, H., Kirfel, J., Ji, S. et al.** (2010). Phosphorylation of histone H3T6 by PKCβ(I) controls demethylation at histone H3K4. *Nature* **464**, 792-6.
- Metzger, E., Yin, N., Wissmann, M., Kunowska, N., Fischer, K., Friedrichs, N., Patnaik, D., Higgins, J. M., Potier, N., Scheidtmann, K. H. et al.** (2008). Phosphorylation of histone H3 at threonine 11 establishes a novel chromatin mark for transcriptional regulation. *Nat Cell Biol* **10**, 53-60.
- Migliori, V., Muller, J., Phalke, S., Low, D., Bezzi, M., Mok, W. C., Sahu, S. K., Gunaratne, J., Capasso, P., Bassi, C. et al.** (2012). Symmetric dimethylation of H3R2 is a newly identified histone mark that supports euchromatin maintenance. *Nat Struct Mol Biol* **19**, 136-44.
- Morris, S. A., Rao, B., Garcia, B. A., Hake, S. B., Diaz, R. L., Shabanowitz, J., Hunt, D. F., Allis, C. D., Lieb, J. D. and Strahl, B. D.** (2007). Identification of histone H3 lysine 36 acetylation as a highly conserved histone modification. *J Biol Chem* **282**, 7632-40.

References

- Nagy, A., Gertsenstein, M. and Vintersten, K.** (2003). Manipulating the mouse embryo: a laboratory manual *Cold Spring Harbor Laboratory Press*.
- Nakagawa, T., Kajitani, T., Togo, S., Masuko, N., Ohdan, H., Hishikawa, Y., Koji, T., Matsuyama, T., Ikura, T., Muramatsu, M. et al.** (2008). Deubiquitylation of histone H2A activates transcriptional initiation via trans-histone cross-talk with H3K4 di- and trimethylation. *Genes Dev* **22**, 37-49.
- Nakamura, T., Arai, Y., Umehara, H., Masuhara, M., Kimura, T., Taniguchi, H., Sekimoto, T., Ikawa, M., Yoneda, Y., Okabe, M. et al.** (2007). PGC7/Stella protects against DNA demethylation in early embryogenesis. *Nat Cell Biol* **9**, 64-71.
- Nakamura, T., Liu, Y. J., Nakashima, H., Umehara, H., Inoue, K., Matoba, S., Tachibana, M., Ogura, A., Shinkai, Y. and Nakano, T.** (2012). PGC7 binds histone H3K9me2 to protect against conversion of 5mC to 5hmC in early embryos. *Nature* **486**, 415-9.
- Nashun, B., Yukawa, M., Liu, H., Akiyama, T. and Aoki, F.** (2010). Changes in the nuclear deposition of histone H2A variants during pre-implantation development in mice. *Development* **137**, 3785-94.
- Ng, S. S., Kavanagh, K. L., McDonough, M. A., Butler, D., Pilka, E. S., Lienard, B. M., Bray, J. E., Savitsky, P., Gileadi, O., von Delft, F. et al.** (2007). Crystal structures of histone demethylase JMJD2A reveal basis for substrate specificity. *Nature* **448**, 87-91.
- Okada, Y., Yamagata, K., Hong, K., Wakayama, T. and Zhang, Y.** (2010). A role for the elongator complex in zygotic paternal genome demethylation. *Nature* **463**, 554-8.
- Ooga, M., Inoue, A., Kageyama, S., Akiyama, T., Nagata, M. and Aoki, F.** (2008). Changes in H3K79 methylation during preimplantation development in mice. *Biol Reprod* **78**, 413-24.
- Ooi, S. K., Qiu, C., Bernstein, E., Li, K., Jia, D., Yang, Z., Erdjument-Bromage, H., Tempst, P., Lin, S. P., Allis, C. D. et al.** (2007). DNMT3L connects unmethylated lysine 4 of histone H3 to de novo methylation of DNA. *Nature* **448**, 714-7.
- Oswald, J., Engemann, S., Lane, N., Mayer, W., Olek, A., Fundele, R., Dean, W., Reik, W. and Walter, J.** (2000). Active demethylation of the paternal genome in the mouse zygote. *Curr Biol* **10**, 475-8.
- Otani, J., Nankumo, T., Arita, K., Inamoto, S., Ariyoshi, M. and Shirakawa, M.** (2009). Structural basis for recognition of H3K4 methylation status by the DNA methyltransferase 3A ATRX-DNMT3-DNMT3L domain. *EMBO Rep* **10**, 1235-41.
- Patnaik, D., Chin, H. G., Esteve, P. O., Benner, J., Jacobsen, S. E. and Pradhan, S.** (2004). Substrate specificity and kinetic mechanism of mammalian G9a histone H3 methyltransferase. *J Biol Chem* **279**, 53248-58.
- Pehrson, J. R. and Fried, V. A.** (1992). MacroH2A, a core histone containing a large nonhistone region. *Science* **257**, 1398-400.
- Pfaffeneder, T., Spada, F., Wagner, M., Brandmayr, C., Laube, S. K., Eisen, D., Truss, M., Steinbacher, J., Hackner, B., Kotljarova, O. et al.** (2014). Tet oxidizes thymine to 5-hydroxymethyluracil in mouse embryonic stem cell DNA. *Nat Chem Biol* **10**, 574-81.
- Probst, A. V., Santos, F., Reik, W., Almouzni, G. and Dean, W.** (2007). Structural differences in centromeric heterochromatin are spatially reconciled on fertilisation in the mouse zygote. *Chromosoma* **116**, 403-15.

- Rasmussen, T. P., Huang, T., Mastrangelo, M. A., Loring, J., Panning, B. and Jaenisch, R.** (1999). Messenger RNAs encoding mouse histone macroH2A1 isoforms are expressed at similar levels in male and female cells and result from alternative splicing. *Nucleic Acids Res* **27**, 3685-9.
- Reik, W., Dean, W. and Walter, J.** (2001). Epigenetic reprogramming in mammalian development. *Science* **293**, 1089-93.
- Ribeiro-Mason, K., Boulesteix, C., Fleurot, R., Aguirre-Lavin, T., Adenot, P., Gall, L., Debey, P. and Beaujean, N.** (2012). H3S10 phosphorylation marks constitutive heterochromatin during interphase in early mouse embryos until the 4-cell stage. *J Reprod Dev* **58**, 467-75.
- Sabbattini, P., Sjoberg, M., Nikic, S., Frangini, A., Holmqvist, P. H., Kunowska, N., Carroll, T., Brookes, E., Arthur, S. J., Pombo, A. et al.** (2014). An H3K9/S10 methylphospho switch modulates Polycomb and Pol II binding at repressed genes during differentiation. *Mol Biol Cell* **25**, 904-15.
- Santenard, A., Ziegler-Birling, C., Koch, M., Tora, L., Bannister, A. J. and Torres-Padilla, M. E.** (2010). Heterochromatin formation in the mouse embryo requires critical residues of the histone variant H3.3. *Nat Cell Biol* **12**, 853-62.
- Santos, F., Peat, J., Burgess, H., Rada, C., Reik, W. and Dean, W.** (2013). Active demethylation in mouse zygotes involves cytosine deamination and base excision repair. *Epigenetics Chromatin* **6**, 39.
- Santos, F., Peters, A. H., Otte, A. P., Reik, W. and Dean, W.** (2005). Dynamic chromatin modifications characterise the first cell cycle in mouse embryos. *Dev Biol* **280**, 225-36.
- Sarcinella, E., Zuzarte, P. C., Lau, P. N., Draker, R. and Cheung, P.** (2007). Monoubiquitylation of H2A.Z distinguishes its association with euchromatin or facultative heterochromatin. *Mol Cell Biol* **27**, 6457-68.
- Sarmiento, O. F., Digilio, L. C., Wang, Y., Perlin, J., Herr, J. C., Allis, C. D. and Coonrod, S. A.** (2004). Dynamic alterations of specific histone modifications during early murine development. *J Cell Sci* **117**, 4449-59.
- Schuhmacher, M. K., Kudithipudi, S., Kusevic, D., Weirich, S. and Jeltsch, A.** (2015). Activity and specificity of the human SUV39H2 protein lysine methyltransferase. *Biochim Biophys Acta* **1849**, 55-63.
- Schwartz, B. E. and Ahmad, K.** (2006). 2. Chromatin assembly with H3 histones: full throttle down multiple pathways. *Curr Top Dev Biol* **74**, 31-55.
- Sen, S. P. and De Benedetti, A.** (2006). TLK1B promotes repair of UV-damaged DNA through chromatin remodeling by Asf1. *BMC Mol Biol* **7**, 37.
- Seyedin, S. M. and Kistler, W. S.** (1979). H1 histone subfractions of mammalian testes. 2. Organ specificity in mice and rabbits. *Biochemistry* **18**, 1376-9.
- Shen, L., Inoue, A., He, J., Liu, Y., Lu, F. and Zhang, Y.** (2014). Tet3 and DNA replication mediate demethylation of both the maternal and paternal genomes in mouse zygotes. *Cell Stem Cell* **15**, 459-70.
- Shi, F. T., Kim, H., Lu, W., He, Q., Liu, D., Goodell, M. A., Wan, M. and Songyang, Z.** (2013). Ten-eleven translocation 1 (Tet1) is regulated by O-linked N-acetylglucosamine transferase (Ogt) for target gene repression in mouse embryonic stem cells. *J Biol Chem* **288**, 20776-84.

- Shimada, M. and Nakanishi, M.** (2008). Checkpoints meet the transcription at a novel histone milestone (H3-T11). *Cell Cycle* **7**, 1555-9.
- Shimada, M., Niida, H., Zineldeen, D. H., Tagami, H., Tanaka, M., Saito, H. and Nakanishi, M.** (2008). Chk1 is a histone H3 threonine 11 kinase that regulates DNA damage-induced transcriptional repression. *Cell* **132**, 221-32.
- Sirotkin, A. M., Edelman, W., Cheng, G., Klein-Szanto, A., Kucherlapati, R. and Skoultschi, A. I.** (1995). Mice develop normally without the H1(0) linker histone. *Proc Natl Acad Sci U S A* **92**, 6434-8.
- Smallwood, S. A., Tomizawa, S., Krueger, F., Ruf, N., Carli, N., Segonds-Pichon, A., Sato, S., Hata, K., Andrews, S. R. and Kelsey, G.** (2011). Dynamic CpG island methylation landscape in oocytes and preimplantation embryos. *Nat Genet* **43**, 811-4.
- Smith, Z. D., Chan, M. M., Mikkelsen, T. S., Gu, H., Gnirke, A., Regev, A. and Meissner, A.** (2012). A unique regulatory phase of DNA methylation in the early mammalian embryo. *Nature* **484**, 339-44.
- Sobel, R. E., Cook, R. G., Perry, C. A., Annunziato, A. T. and Allis, C. D.** (1995). Conservation of deposition-related acetylation sites in newly synthesized histones H3 and H4. *Proc Natl Acad Sci U S A* **92**, 1237-41.
- Soboleva, T. A., Nekrasov, M., Pahwa, A., Williams, R., Huttley, G. A. and Tremethick, D. J.** (2012). A unique H2A histone variant occupies the transcriptional start site of active genes. *Nat Struct Mol Biol* **19**, 25-30.
- Soppe, W. J., Jasencakova, Z., Houben, A., Kakutani, T., Meister, A., Huang, M. S., Jacobsen, S. E., Schubert, I. and Fransz, P. F.** (2002). DNA methylation controls histone H3 lysine 9 methylation and heterochromatin assembly in Arabidopsis. *EMBO J* **21**, 6549-59.
- Stein, P., Worrad, D. M., Belyaev, N. D., Turner, B. M. and Schultz, R. M.** (1997). Stage-dependent redistributions of acetylated histones in nuclei of the early preimplantation mouse embryo. *Mol Reprod Dev* **47**, 421-9.
- Strahl, B. D. and Allis, C. D.** (2000). The language of covalent histone modifications. *Nature* **403**, 41-5.
- Szenker, E., Ray-Gallet, D. and Almouzni, G.** (2011). The double face of the histone variant H3.3. *Cell Res* **21**, 421-34.
- Tachibana, M., Sugimoto, K., Fukushima, T. and Shinkai, Y.** (2001). Set domain-containing protein, G9a, is a novel lysine-preferring mammalian histone methyltransferase with hyperactivity and specific selectivity to lysines 9 and 27 of histone H3. *J Biol Chem* **276**, 25309-17.
- Tachiwana, H., Osakabe, A., Kimura, H. and Kurumizaka, H.** (2008). Nucleosome formation with the testis-specific histone H3 variant, H3t, by human nucleosome assembly proteins in vitro. *Nucleic Acids Res* **36**, 2208-18.
- Tagami, H., Ray-Gallet, D., Almouzni, G. and Nakatani, Y.** (2004). Histone H3.1 and H3.3 complexes mediate nucleosome assembly pathways dependent or independent of DNA synthesis. *Cell* **116**, 51-61.
- Tahiliani, M., Koh, K. P., Shen, Y., Pastor, W. A., Bandukwala, H., Brudno, Y., Agarwal, S., Iyer, L. M., Liu, D. R., Aravind, L. et al.** (2009). Conversion of 5-methylcytosine to 5-hydroxymethylcytosine in mammalian DNA by MLL partner TET1. *Science* **324**, 930-5.

References

- Tamaru, H. and Selker, E. U.** (2001). A histone H3 methyltransferase controls DNA methylation in *Neurospora crassa*. *Nature* **414**, 277-83.
- Tanaka, M., Kihara, M., Hennebold, J. D., Eppig, J. J., Viveiros, M. M., Emery, B. R., Carrell, D. T., Kirkman, N. J., Meczekalski, B., Zhou, J. et al.** (2005). H1FOO is coupled to the initiation of oocytic growth. *Biol Reprod* **72**, 135-42.
- Teperek-Tkacz, M., Meglicki, M., Pasternak, M., Kubiak, J. Z. and Borsuk, E.** (2010). Phosphorylation of histone H3 serine 10 in early mouse embryos: active phosphorylation at late S phase and differential effects of ZM447439 on first two embryonic mitoses. *Cell Cycle* **9**, 4674-87.
- Torres-Padilla, M. E., Bannister, A. J., Hurd, P. J., Kouzarides, T. and Zernicka-Goetz, M.** (2006). Dynamic distribution of the replacement histone variant H3.3 in the mouse oocyte and preimplantation embryos. *Int J Dev Biol* **50**, 455-61.
- Turner, B. M. and O'Neill, L. P.** (1995). Histone acetylation in chromatin and chromosomes. *Semin Cell Biol* **6**, 229-36.
- van der Heijden, G. W., Derijck, A. A., Ramos, L., Giele, M., van der Vlag, J. and de Boer, P.** (2006). Transmission of modified nucleosomes from the mouse male germline to the zygote and subsequent remodeling of paternal chromatin. *Dev Biol* **298**, 458-69.
- van der Heijden, G. W., Dieker, J. W., Derijck, A. A., Muller, S., Berden, J. H., Braat, D. D., van der Vlag, J. and de Boer, P.** (2005). Asymmetry in histone H3 variants and lysine methylation between paternal and maternal chromatin of the early mouse zygote. *Mech Dev* **122**, 1008-22.
- Van Hooser, A. A., Mancini, M. A., Allis, C. D., Sullivan, K. F. and Brinkley, B. R.** (1999). The mammalian centromere: structural domains and the attenuation of chromatin modeling. *FASEB J* **13 Suppl 2**, S216-20.
- Vella, P., Scelfo, A., Jammula, S., Chiacchiera, F., Williams, K., Cuomo, A., Roberto, A., Christensen, J., Bonaldi, T., Helin, K. et al.** (2013). Tet proteins connect the O-linked N-acetylglucosamine transferase Ogt to chromatin in embryonic stem cells. *Mol Cell* **49**, 645-56.
- Vempati, R. K., Jayani, R. S., Notani, D., Sengupta, A., Galande, S. and Haldar, D.** (2010). p300-mediated acetylation of histone H3 lysine 56 functions in DNA damage response in mammals. *J Biol Chem* **285**, 28553-64.
- Villar-Garea, A. and Imhof, A.** (2008). Fine mapping of posttranslational modifications of the linker histone H1 from *Drosophila melanogaster*. *PLoS One* **3**, e1553.
- Waddington, C.** (1942). The epigenotype. *Endeavour* **1**, 18-20.
- Wagner, E. J. and Carpenter, P. B.** (2012). Understanding the language of Lys36 methylation at histone H3. *Nat Rev Mol Cell Biol* **13**, 115-26.
- Watanabe, S., Radman-Livaja, M., Rando, O. J. and Peterson, C. L.** (2013). A histone acetylation switch regulates H2A.Z deposition by the SWR-C remodeling enzyme. *Science* **340**, 195-9.
- Weake, V. M. and Workman, J. L.** (2008). Histone ubiquitination: triggering gene activity. *Mol Cell* **29**, 653-63.
- Weiss, T., Hergeth, S., Zeissler, U., Izzo, A., Tropberger, P., Zee, B. M., Dundr, M., Garcia, B. A., Daujat, S. and Schneider, R.** (2010). Histone H1 variant-specific lysine methylation by G9a/KMT1C and Glp1/KMT1D. *Epigenetics Chromatin* **3**, 7.

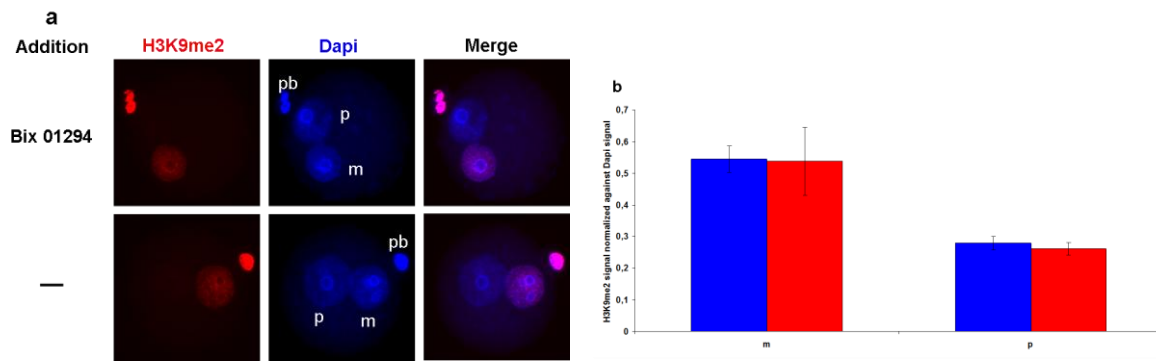
References

- West, M. H. and Bonner, W. M.** (1980). Histone 2A, a heteromorphous family of eight protein species. *Biochemistry* **19**, 3238-45.
- Wilmot, I., Schnieke, A. E., McWhir, J., Kind, A. J. and Campbell, K. H.** (1997). Viable offspring derived from fetal and adult mammalian cells. *Nature* **385**, 810-3.
- Wongtawan, T., Taylor, J. E., Lawson, K. A., Wilmot, I. and Pennings, S.** (2011). Histone H4K20me3 and HP1alpha are late heterochromatin markers in development, but present in undifferentiated embryonic stem cells. *J Cell Sci* **124**, 1878-90.
- Wossidlo, M., Arand, J., Sebastiano, V., Lepikhov, K., Boiani, M., Reinhardt, R., Scholer, H. and Walter, J.** (2010). Dynamic link of DNA demethylation, DNA strand breaks and repair in mouse zygotes. *EMBO J* **29**, 1877-88.
- Wossidlo, M., Nakamura, T., Lepikhov, K., Marques, C. J., Zakhartchenko, V., Boiani, M., Arand, J., Nakano, T., Reik, W. and Walter, J.** (2011). 5-Hydroxymethylcytosine in the mammalian zygote is linked with epigenetic reprogramming. *Nat Commun* **2**, 241.
- Wu, C. and Morris, J. R.** (2001). Genes, genetics, and epigenetics: a correspondence. *Science* **293**, 1103-5.
- Wu, F., Caron, C., De Robertis, C., Khochbin, S. and Rousseaux, S.** (2008). Testis-specific histone variants H2AL1/2 rapidly disappear from paternal heterochromatin after fertilization. *J Reprod Dev* **54**, 413-7.
- Wu, H., Chen, X., Xiong, J., Li, Y., Li, H., Ding, X., Liu, S., Chen, S., Gao, S. and Zhu, B.** (2011). Histone methyltransferase G9a contributes to H3K27 methylation in vivo. *Cell Res* **21**, 365-7.
- Wu, J., Wang, S. H., Potter, D., Liu, J. C., Smith, L. T., Wu, Y. Z., Huang, T. H. and Plass, C.** (2007). Diverse histone modifications on histone 3 lysine 9 and their relation to DNA methylation in specifying gene silencing. *BMC Genomics* **8**, 131.
- Wu, S. C. and Zhang, Y.** (2010). Active DNA demethylation: many roads lead to Rome. *Nat Rev Mol Cell Biol* **11**, 607-20.
- Wyrick, J. J. and Parra, M. A.** (2009). The role of histone H2A and H2B post-translational modifications in transcription: a genomic perspective. *Biochim Biophys Acta* **1789**, 37-44.
- Xu, Y., Ayrapetov, M. K., Xu, C., Gursoy-Yuzugullu, O., Hu, Y. and Price, B. D.** (2012). Histone H2A.Z controls a critical chromatin remodeling step required for DNA double-strand break repair. *Mol Cell* **48**, 723-33.
- Yuan, C. C., Matthews, A. G., Jin, Y., Chen, C. F., Chapman, B. A., Ohsumi, T. K., Glass, K. C., Kutateladze, T. G., Borowsky, M. L., Struhl, K. et al.** (2012). Histone H3R2 symmetric dimethylation and histone H3K4 trimethylation are tightly correlated in eukaryotic genomes. *Cell Rep* **1**, 83-90.
- Yuan, J., Pu, M., Zhang, Z. and Lou, Z.** (2009). Histone H3-K56 acetylation is important for genomic stability in mammals. *Cell Cycle* **8**, 1747-53.
- Yuan, W., Xu, M., Huang, C., Liu, N., Chen, S. and Zhu, B.** (2011). H3K36 methylation antagonizes PRC2-mediated H3K27 methylation. *J Biol Chem* **286**, 7983-9.
- Zhang, K. and Tang, H.** (2003). Analysis of core histones by liquid chromatography-mass spectrometry and peptide mapping. *J Chromatogr B Analyt Technol Biomed Life Sci* **783**, 173-9.

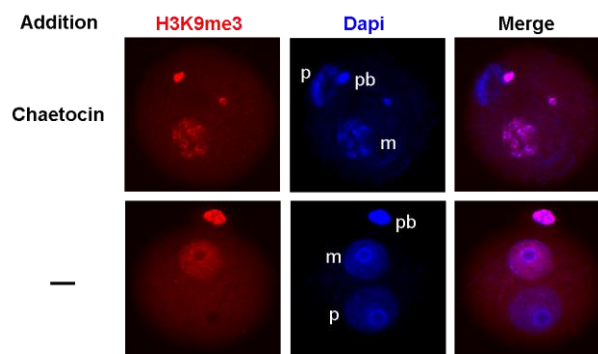
References

- Zhang, L., Eugeni, E. E., Parthun, M. R. and Freitas, M. A.** (2003). Identification of novel histone post-translational modifications by peptide mass fingerprinting. *Chromosoma* **112**, 77-86.
- Zhang, Y., Griffin, K., Mondal, N. and Parvin, J. D.** (2004). Phosphorylation of histone H2A inhibits transcription on chromatin templates. *J Biol Chem* **279**, 21866-72.
- Zhang, Y., Jurkowska, R., Soeroes, S., Rajavelu, A., Dhayalan, A., Bock, I., Rathert, P., Brandt, O., Reinhardt, R., Fischle, W. et al.** (2010). Chromatin methylation activity of Dnmt3a and Dnmt3a/3L is guided by interaction of the ADD domain with the histone H3 tail. *Nucleic Acids Res* **38**, 4246-53.
- Zhang, Z., Liu, J., Kaur, M. and Krantz, I. D.** (2012). Characterization of DNA methylation and its association with other biological systems in lymphoblastoid cell lines. *Genomics* **99**, 209-19.
- Zhou, B. R., Feng, H., Kato, H., Dai, L., Yang, Y., Zhou, Y. and Bai, Y.** (2013). Structural insights into the histone H1-nucleosome complex. *Proc Natl Acad Sci U S A* **110**, 19390-5.
- Zhou, V. W., Goren, A. and Bernstein, B. E.** (2011). Charting histone modifications and the functional organization of mammalian genomes. *Nat Rev Genet* **12**, 7-18.
- Ziegler-Birling, C., Helmrich, A., Tora, L. and Torres-Padilla, M. E.** (2009). Distribution of p53 binding protein 1 (53BP1) and phosphorylated H2A.X during mouse preimplantation development in the absence of DNA damage. *Int J Dev Biol* **53**, 1003-11.
- Zierhut, C., Jenness, C., Kimura, H. and Funabiki, H.** (2014). Nucleosomal regulation of chromatin composition and nuclear assembly revealed by histone depletion. *Nat Struct Mol Biol* **21**, 617-25.
- Zilberman, D., Coleman-Derr, D., Ballinger, T. and Henikoff, S.** (2008). Histone H2A.Z and DNA methylation are mutually antagonistic chromatin marks. *Nature* **456**, 125-9.
- Zinner, R.** (2007). Histone lysine methylation in the context of nuclear architecture *PhD dissertation (Ludwig Maximilian University of Munich)*, 86-88.

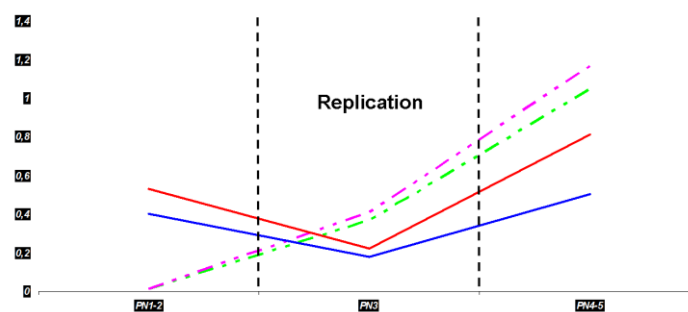
Appendices



Supplementary Fig. 1 Influence on H3K9me2 by BIX 01294. a, Representative images of treated- and untreated zygotes stained with antibodies against H3K9me2. H3K9me2, red; Dapi, blue; m, the maternal pronucleus; p, the paternal pronucleus; pb, polar body. **b**, Quantification of H3K9me2 signal normalized against Dapi signal in both parental genomes of zygotes at PN4/5. Non-treated group, blue; treated group, red; Error bars indicated s.d.. For each group, at least 10 zygotes were analysed from at least two repeated experiments.

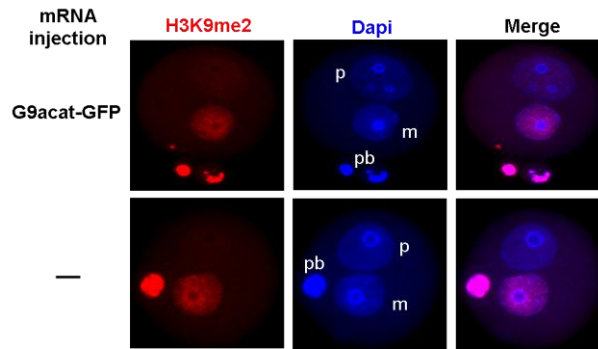


Supplementary Fig. 2 Influences on H3K9me3 and nuclear topology by Chaetocin treatment in mouse zygotes. Representative images of PN4/5 stage zygotes stained with antibodies against H3K9me3. H3K9me3, red; Dapi, blue. m, the maternal pronucleus; p, the paternal pronucleus; pb, polar body. For each group, at least 10 zygotes were analysed from at least two repeated experiments.

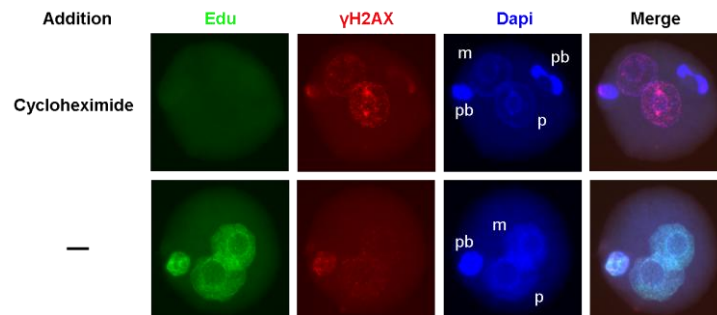


Supplementary Fig. 3 Quantification of H3S10phos and H3T11phos in mouse zygotes. Quantification of H3S10phos and H3T11phos signals normalized against Dapi signals in both parental genomes of zygotes in different PN stages. Solid lines, H3S10phos; dashed lines, H3T11phos; red and pink, the paternal pronuclei; blue and green, the maternal pronuclei. For each group, at least 10 zygotes were analysed from at least two repeated experiments.

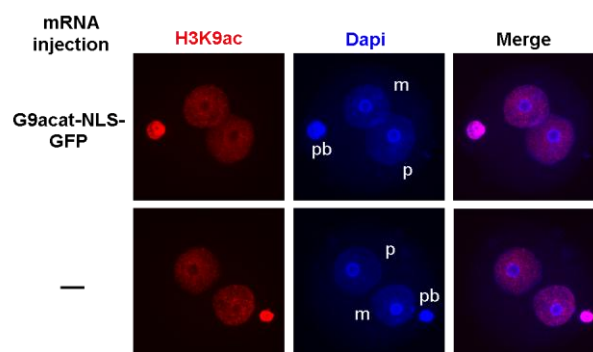
Appendices



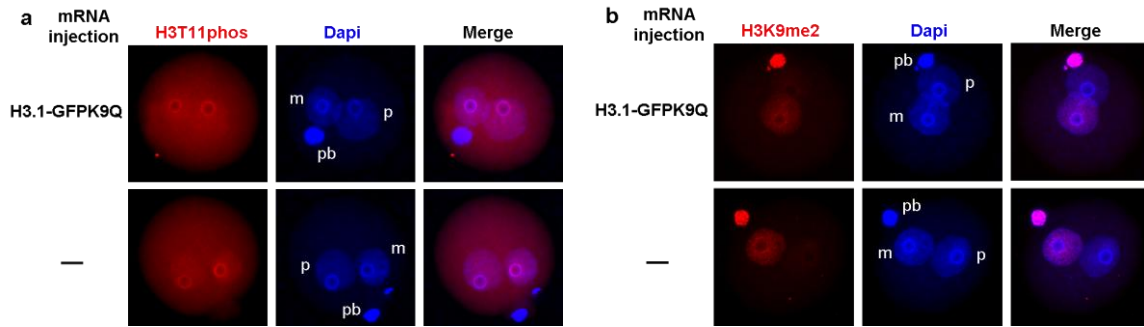
Supplementary Fig. 4 No influence on H3K9me2 in zygotes by microinjection of G9aCat-GFP. Representative images of PN4/5 stage zygotes stained with antibodies against H3K9me2. H3K9me2, red; Dapi, blue; m, the maternal pronucleus; p, the paternal pronucleus; pb, polar body. For each group, at least 10 zygotes were analysed from at least two repeated experiments.



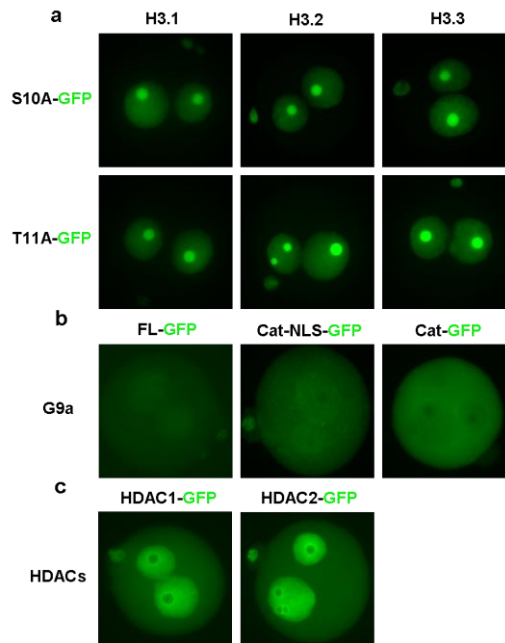
Supplementary Fig. 5 Influences on DNA replication and DNA repair by cycloheximide treatment in mouse zygotes. Representative images of PN4/5 stage zygotes labeled with Edu and stained with antibodies against gamma-H2AX. Edu, green; gamma-H2AX, red; Dapi, blue. m, the maternal pronucleus; p, the paternal pronucleus; pb, polar body. For each group, at least 10 zygotes were analysed from at least two repeated experiments.



Supplementary Fig. 6 No Influence on H3K9ac in zygotes by microinjection of G9aCat-NLS-GFP. Representative images of PN4/5 stage zygotes stained with antibodies against H3K9ac. H3K9ac, red; Dapi, blue. m, the maternal pronucleus; p, the paternal pronucleus; pb, polar body. For each group, at least 10 zygotes were analysed from at least two repeated experiments.



Supplementary Fig. 7 Impacts on H3T11phos and H3K9me2 in zygotes by microinjection of H3.1-GFPK9Q. **a.** Representative images of PN4/5 stage zygotes stained with antibodies against H3T11phos. **b.** Representative images of PN4/5 stage zygotes stained with antibodies against H3TK9me2. H3T11phos or H3K9me2, red; Dapi, blue. m, the maternal pronucleus; p, the paternal pronucleus; pb, polar body. For each group, at least 10 zygotes were analysed from at least two repeated experiments.



Supplementary Fig. 8 Nuclear localization of the injected constructs fused with GFP. **a.** Representative images of PN4/5 stage zygotes microinjected with H3.1/2/3-GFPS10A and H3.1/2/3-GFPT11A, respectively. **b.** Representative images of PN4/5 stage zygotes microinjected with G9aFL-GFP, G9aCat-NLS-GFP and G9aCat-GFP, respectively. **c.** Representative images of PN4/5 stage zygotes microinjected with HDAC1-GFP and HDAC2-GFP, respectively. For each group, at least 10 zygotes were analysed from at least two repeated experiments.

Abbreviations

Abbreviations

APS (10%)	Ammonium persulfate
BSA	Bovine serum albumin
bp	Base pair
DAPI	4',6-diamidino-2-phenylindole
DAB	Diaminobenzidin
Dnmt	DNA methyltransferase
dNTPs	Deoxyribonucleotide triphosphates
°C	Degree Celsius
DMSO	Dimethyl sulfoxide
5% DMDCS	Dimethyldichlorosilane
DTT	Dithiothreitol
EDTA	Ethylenediaminetetraacetic acid
EdU	5-ethynyl-2'-deoxyuridine
5caC	5-Carboxyl-Cytosine
5fC	5-Formyl-Cytosine
5hmC	5-Hydroxymethyl-Cytosine
5mC	5-Methyl-Cytosine
g	Gram
Glycerol	Carl Roth, Karlsruhe, Germany
h	Hour
hCG	Human chorionic gonadotropin
HDACs	Histone deacetylase
HMT	Histone methyltransferase
HP1	Heterochromatin protein 1
hpf	Hours post fertilization
IAP	Intracisternal A-particle element
IF	Immunofluorescence
IPTG	Isopropyl β -D-1-thiogalactopyranoside
IVF	<i>In vitro</i> fertilization
IVT	<i>In vitro</i> transcription
L	Liter
LINE1	Long interspersed element
μ g	Microgram
mg	Milligram
min	Minute
μ l	Microliter
ml	Milliliter
M	Molar
μ M	Micromolar
mM	Millimolar
mRNA	Messenger RNA
mSat	Major satellite
ng	Nanogram
%	Percentage
PCR	Polymerase chain reaction
PMSG	Pregnant mare's serum gonadotropin
RT	Room temperature
RT	Reverse transcription

Abbreviations

SDS	Sodium dodecyl sulfate
TEMED	Tetramethylethylenediamine

Curriculum Vitae

Name: Jie Lan

Nationality: Chinese

Gender: Male

Birth date: Oct. 13, 1984

Birth place: Hohhot, Inner Mongolia, People's Republic of China

E-mail: lanjie1013@hotmail.com **Telephone:** +49 17627813040, +86 13754095826

Current Address: Scheidter Straße 110, 66125, Saarbrücken, Germany



EDUCATION

09. 2010-present, Saarland University, Sarrbruecken, Saarland, Germany, **Ph.D candidate.**

Major: Epigenetics (Histone modifications and DNA methylation in mouse embryos)

First Supervisor: Prof. Dr. Jörn Walter

Second Supervisor: Prof. Dr. Uli Müller

Thesis topic: Epigenetic reprogramming involving histone H3 variants, histone modifications and DNA methylation in mouse zygotes

09. 2007-07. 2010, Northwest A&F University, Yangling, Shaanxi, China, **Master of Science**

Major: Developmental Biology (Animal cloning and transgene).

Supervisor: Prof. Dr. Yong Zhang

Major courses: Developmental Biology, Molecular Biology, Advanced Biochemistry, Molecular Genetics, Cell Biology, Reproductive Endocrinology, Embryo Engineering, Histology and Embryology, Scientific English, etc.

Thesis topic: Methylation profiles of pluripotency-related genes in bovine *in vitro* fertilized embryos, nuclear transferred embryos and mature gametes

09. 2003-07. 2007, Northwest A&F University, Yangling, Shaanxi, China, **Bachelor of Science.**

Major: Biology Science (Animal direction)

Supervisor: Associate Prof. Dr. Xiao e Zhao

Major courses: Physiology, Anatomy, Histology and Embryology, Biochemistry, Molecular Biology, Cell Biology, Gene Engineering, Genetics, Immunology, Protein and enzyme engineering, Bioinformatics, Organic Chemistry, Zoology, Botany, Microbiology, Fermentation engineering, English, etc.

Thesis topic: Study on mouse oviductal epithelial primary cell culture and its purification

PROGRAMME INVOLVED DURING MY PhD RESEARCH

SPP 1356 - 'Pluripotency and Cellular Reprogramming'

DATA TO BE PUBLISHED

◇ **Jie Lan**, Konstantin Lepikhov, Pascal Giehr, Jörn Walter. The manuscript (done, in preparation for submission very soon)

PUBLICATIONS

◇ Konstantin Lepikhov, Julia Arand, Sarah Fuchs, **Jie Lan**, Mark Wossidlo, and Jörn Walter. DNA methylation reprogramming in preimplantation development. *Epigenetic Mechanisms in Cellular Reprogramming*, 2014, **Springer**, ISBN 978-3-642-31973-0. (**Book Chapter**)

◇ **Lan Jie**, Hua Song, He Xiao-ning et al. Methylation patterns in 5' terminal regions of pluripotency-related genes in mature gametes of bovine. *Zygotes*, 2011; 19 (2): 165-9. (**Research article**)

◇ **Lan Jie**, Song Yong-li, Hua Song et al. cDNA Cloning of Goat DNA Methyltransferase 1, Screening of shRNA Vectors and Influences to Development of Nuclear Transfer Embryos. *Agricultural Sciences in China*, 2010; 9 (7): 1035–1040. (**Research article**)

◇ **Lan Jie**, Hua Song, Zhang Hai-ling et al. Methylation patterns in 5' terminal regions of pluripotency-related genes in bovine in vitro fertilized and cloned embryos. *J Genet Genomics*, 2010; 37 (5): 297-304. (**Research article**)

◇ **Lan Jie**, Hua Song, He Xiao-ning et al. DNA methyltransferases and methyl-binding proteins of mammals. *Acta Biochim Biophys Sin (Shanghai)*, 2010; 42 (4): 243-52. (**Review**)

◇ Xiao-Ying He, Yue-Mao Zheng, **Jie Lan**, Yue-Hong Wu, Jing Yan, Xiao-Ning He, Tuo Zhang, Yu-Long He, Yan-Ling Zheng, Yong Zhang. Recombinant adenovirus-mediated human telomerase reverse transcriptase gene can stimulate cell proliferation and maintain primitive characteristics in bovine mammary gland epithelial cells. *Development, Growth & Differentiation*, 2011; 53 (3): 312–322. (**Research article**)

PRESENTATIONS

DFG Meeting SPP1356, 3rd PhD / post doc Workshop, Würzburg, Germany **2011**.

Topic: The possible role of H3.3K9me2 in regulating DNA demethylation in the mouse zygotes.

POSTER PRESENTATIONS

International Symposium on Reprogrammed Stem Cells at the Berlin-Brandenburg Academy of Science and Humanities, Berlin, 20 – 22, March, **2014**.

Topic: Dissecting the relationships between histone H3 variants, H3K9 modifications and DNA methylation in mouse zygotes.

PARTICIPATION IN INTERNATIONAL SYMPOSIUMS

◇ The 5th Weissenburg Symposium Biriciana, Epigenetics—a Different Way of Looking at Genetics, Weissenburg, Bayern, 15-17, September, 2014

◇ International Symposium on Reprogrammed Stem Cells at the Berlin-Brandenburg Academy of Science and Humanities, Berlin, 20 – 22, March, 2014

Curriculum Vitae

- ◇ The 6th Internal Progress Meeting, Veitshöchheim, Würzburg, 20-21, June, 2013
- ◇ The 5th Internal Progress Meeting, Veitshöchheim, Würzburg, 03-4, July, 2012
- ◇ The 4th Internal Progress Meeting, Veitshöchheim, Würzburg, 05-06, July, 2011